THE APPLICATION OF NUCLEAR MAGNETIC RESONANCE IN THE STRUCTURAL ELUCIDATION OF NATURAL PRODUCTS

Margie M. Nair

BSc(Hon) (Unisa)

Dissertation submitted in

fulfillment of the requirements

for degree of

MASTER OF SCIENCE

in the Department of Chemistry

UNIVERSITY OF CAPE TOWN

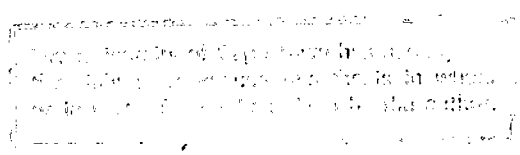

September 1994

Two roads diverged in a wood

and I- I took the one less traveled by,

and that has made all the difference.

Robert Frost

Acknowledgements

Special thanks to:

My supervisor, Professor Jackson for his unremitting support, faith and patience but mostly for his confidence in my work for which I am most grateful.

Mr Campbell and Professor Bull of the Department of Chemistry for their kind donation of samples.

Dr Lajos Radics of Varian in Darmstadt, Germany for his constructive criticism of our approach to inverse detection experiments.

My parents for divine guidance.

Conference contributions

Poster entitled "*Structural elucidation of cucurbitacin derivatives via multipulse NMR techniques*" presented at the XVIth **International Conference on Magnetic Resonance in Biological Systems** in The Netherlands on 17 August 1994.

Abstract

Multipulse Nuclear Magnetic Resonance (NMR) techniques were investigated via structural assignment of various natural products. The natural products chosen for investigation of 2D NMR spectroscopy as a structural tool were the opium alkaloids codeine and papaverine, the diterpenoid alkaloids delphinine and aconitine and the triterpenoid derivatives of cucurbitaceae. One dimensional NMR spectroscopy viz ^{1}H, ^{13}C and Distortionless Enhancement by Polarisation Transfer (DEPT) spectroscopy was initially applied to obtain a level of indication of the complexity of the structural problem solving. Various multipulse techniques were chosen depending on the sample quantity available, the sensitivity of the technique, the information provided and its applicabilty in the field of natural products. Both homonuclear scalar and dipolar correlation as well as short and long range heteronuclear correlation was investigated. The homonuclear Correlation Spectroscopy (COSY) experiment which revealed scalar ^{1}H-^{1}H scalar correlations was adequate for the structural assignment. The Heteronuclear Multiple Quantum Coherence (HMQC) experiment offered greater sensitivity on small sample quantities whilst the long range Heteronuclear Correlation (HETCOR) and Heteronuclear Multiple Bond Coherence (HMBC) experiments were essential for complete assignment of the quaternary groups. The stereochemical designation of some of the compounds was confirmed using the Rotating Frame Overhauser Enhancement Spectroscopy (ROESY) experiment which proved to be a more applicable pulse sequence for the natural products under investigation. The ^{1}H and ^{13}C assignments of these derivatives and the experimental approach used to obtain this data was compared to that present in the literature. The results indicate that apart from offering tremendous versatility depending on the special attributes of the compound, two dimensional NMR techniques are imperative for the unambiguous structural assignment of natural products.

CONTENTS

CHAPTER THREE

CHAPTER FOUR

CHAPTER FIVE

Symbols and Abbreviations

Abbreviations

NMR	Nuclear Magnetic Resonance
COSY	COrrelation SpectroscopY
TOCSY	TOtal Correlation SpectroscopY
HMQC	Heteronuclear Multiple Quantum Coherence
HMBC	Heteronuclear Multiple Bond Coherence
nOe	nuclear Overhauser effect
NOESY	Nuclear Overhauser Enhancement SpectroscopY
ROESY	Rotating frame Overhauser Enhancement SpectroscopY
HETCOR	HETeronuclear CORrelation
DEPT	Distortionless Enhancement by Polarisation Transfer
BIRD	BIlinear Rotation Decoupling
SFORD	Single Frequency Off Resonance Decoupling

Symbols

δ	Chemical Shift
$^{i}J_{AB}$	i Bond coupling constant between nuclei A and B.
δ_H	^{1}H Chemical shift
δ_C	^{13}C Chemical shift
τ	interval
τ_M	mixing period
τ_C	motional correlation time
ω_0	frequency of zero quantum transition
ω_2	frequency of double quantum transition
t_1	first time domain
t_2	second time domain

F1	first frequency domain
F2	second frequency domain
ω	angular Larmor frequency
v	Larmor frequency
d	doublet
dd	double doublet
s	singlet
m	multiplet
dt	doublet of triplets
t	triplet
o	ortho
m	meta
p	para
q	quaternary

List of Figures, Structural Diagrams and Tables.

List of Figures

Structural Diagrams

List of Tables

CHAPTER ONE

1. OVERVIEW OF NUCLEAR MAGNETIC RESONANCE

1.1 INTRODUCTION TO NMR.

1.1.1 Applications of NMR

Nuclear Magnetic Resonance is one of the most powerful spectroscopic tools available to the chemist for the structural elucidation of organic molecules. Improved sensitivity and rapid advancements in two dimensional NMR spectroscopy has provided unique insights into the **structural, stereochemical** and **conformational** details of molecules. A research chemist who has isolated an unknown product will need to elucidate its structure and stereochemistry. A one dimensional spectrum may serve to confirm the presence of chemical groups via characteristic chemical shifts i.e it may provide some knowledge of its identity. Two dimensional NMR spectroscopy includes **homonuclear** correlation (interactions between protons via scalar or dipolar coupling) and **heteronuclear** correlation (scalar coupling transmitted via proton and X nucleus). This correlation spectroscopy reveals both short range (one bond) and long range (two to three bond) coupling depending on the pulse sequence chosen. In conclusion to the process of structural elucidation the stereochemistry of the compound can then be determined via nuclear Overhauser enhancement (nOe) spectroscopy since dipolar interaction occurs through space in a molecule.

a) **In the biological field**

Bell and Sadler[1] have reported on the effect of dietary changes on the composition of blood plasma. Using NMR spectroscopy, insight has been gained into the nature of stored body fats (adipose tissue) and on those that circulate in the blood (lipoproteins). In this study *in vivo* ^{13}C NMR revealed that dietary changes do lead to changes in the

composition of stored fats and *in vitro* ^{1}H NMR showed that similiar changes occur in circulating fats.

Dramatic improvements in multidimensional NMR techniques for conformational studies of biological macromolecules has been reported.[2] The complexities of analysing spectra of macromolecules include spectral overlap and poor sensitivity due to low sample quantity. The incorporation of higher field strengths together with the emergence of multidimensional NMR techniques has led to major breakthroughs in conformational studies of proteins, peptides and carbohydrates.

b) **In the chemical industry**

NMR has use in quantitative analysis where integral ratios reveal the chemical constituents of a sample. Allerhand and Maple[3] have reported on the quantitative analysis of complex mixtures using high resolution NMR . The integrated intensities of ^{13}C resonances were used for the determination of the proportions of gasoline components in a mixture. Suppression of the Overhauser effect which is due to broadband decoupling of protons makes ^{13}C quantitative analysis feasible. This can be achieved via gated decoupling.

c) **In solution chemistry**

NMR allows for the determination of association/binding constants necessary to establish metal ligand relationships in complex equilibria. Nuclear spins exhibit a temperature dependence which in turn allows for the investigation of its relaxation properties. Thus molecular motion can be studied via NMR.

1.2 BASIC PRINCIPLES OF NMR SPECTROSCOPY

The basic principles of NMR spectroscopy have been reviewed in several excellent publications[4,5] and only a brief outline will be provided here. An NMR spectrum is

usually obtained by accumulation of free induction decays (**fid**) after a radiofrequency pulse is applied. In this single pulse spectra (Fig.1) the time between pulses allow for the spins to relax back to equilibrium. Maximum intensity of the signal is accomplished with a ninety degree pulse for a single scan experiment provided a suitable delay period of at least $5*T_1$ is chosen..

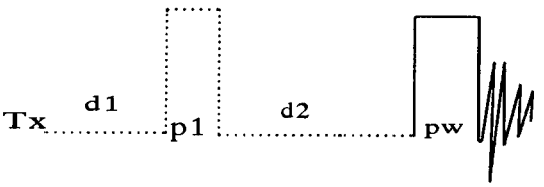

Figure1 Proton 1D pulse sequence

In all descriptions of NMR the atomic nucleus is placed in a static magnetic field. This magnetic moment then precesses with a **Lamor frequency** v about the direction of this field. Nuclei with a spin quantum number of I= *1/2* will precess either about the direction of the magnetic field or in the opposite direction. Nuclei which spin parallel to the magnetic field vector represent the state with the lower potential energy.
The difference in population of these two spin states is given by the **Boltzmann distribution equation**

$$N_2/N_1 = \exp(-\Delta E/kT) \sim 1-\Delta E/kT \quad \text{(i)}$$

where k is the Boltzmann constant and T is the absolute temperature and N_1 and N_2 represent the spin populations of the ground and excited states respectively. The

difference in energy between the ground and the excited states is relatively small and is represented by ΔE.

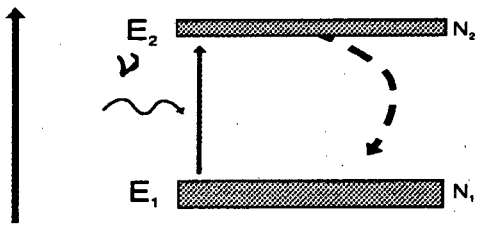

Figure2 Nuclear Zeeman levels

The state with the lower potential energy E_1 will be more populated. Irradiation at the Lamor resonance frequency v promotes spins between the E_1 and the E_2 energy level. Spin lattice relaxation tends to reestablish the Boltzmann population.

The Boltzmann distribution (Fig.2). predicts that the tendency of nuclei to align with the magnetic field and to drop into the lowest energy level is opposed by thermal motions which tend to equalize the population in the two levels. The near equality of population in the two levels is an important factor in determining the intensity of the NMR signal. The difference in energy between the two levels is zero in the absence of a polarizing field. When the sample is placed in a magnetic field, redistribution of population occurs via an interaction of the nuclei with their surrounding lattice. This is characterised by the lifetime T_1 and is called the *spin-lattice relaxation time*.

Consider the equilibrium magnetisation M_o that builds up along the direction of the magnetic field defined as the Z axis.

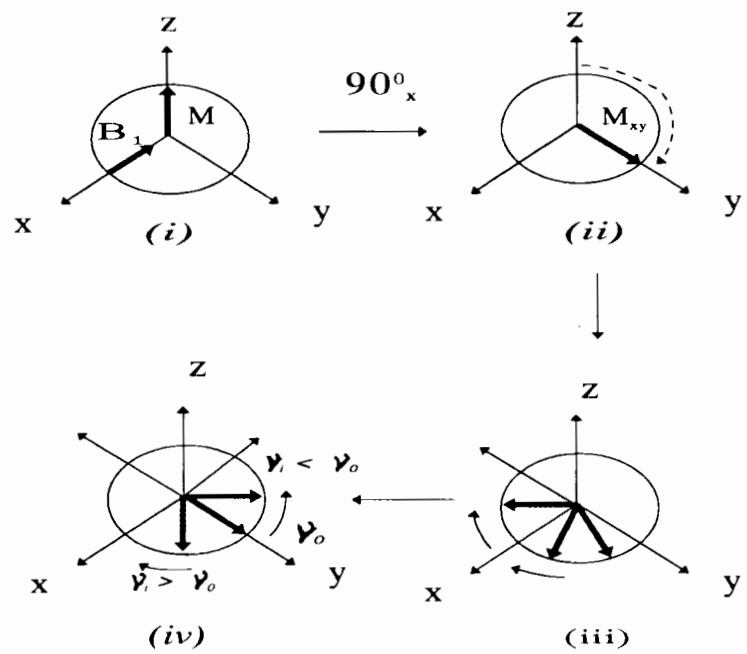

Figure3 Bloch vector diagram

(i) Macroscopic magnetisation M in the laboratory frame parallel to the external field B_O. (ii) Transverse magnetisation M_{xy} along the positive y axis after a 90°$_x$ pulse. (iii) Lamor precession of components of vector M in the laboratory frame and (iv) in the rotating frame.

A radiofrequency (rf) alternating field represented by vector B_1 rotates with Lamor frequency v at resonance and perpendicular to the magnetic field vector (Fig.3). The **rotating frame coordinate system** rotates about the Z axis which is aligned with the B_o field, at the carrier frequency of the radiofrequency pulse. In the frame both the sample magnetisation (z axis) and the B_1 field vector (x axis) are static. Thus B_1 will act upon the sample magnetisation forcing it away from the Z axis. The flip angle will depend

on the duration and power of B_1 . A 90° pulse will point M along the positive Y axis. Thus the **longitudinal magnetisation** along Z is converted into **transverse magnetisation** along Y. The nuclear magnetic moments and the resultant transverse magnetisation still precess with Lamor frequency v_0 about the Z axis in the xy plane. In the rotating frame the transverse magnetisation with reference frequency v_0 stands whilst components with $v_i > v_0$ or $v_i < v_0$ will rotate clockwise and anticlockwise respectively and a signal with $v_i=v_0$ is static in the rotating frame. This transverse magnetisation will induce a current in the receiver coil of the spectrometer and a signal is generated. This signal will decay with time as its magnetisation relaxes back to equilibrium. If one detects the component of sample magnetisation in the Y direction, an experimentally decreasing sinusoidal signal will be observed. This is the so-called free induction decay (fid). Each component of the transverse magnetisation will be characterised by its Lamor frequency, phase shift and lifetime. The position of the signal in the FT NMR spectrum corresponds to the individual Lamor frequency. The lifetime of the transverse magnetisation will determine the signal width. Each fid is a time dependent function. The conventional NMR spectrum is a plot of signal intensity versus frequency. The conversion of the time dependency to frequency dependency is accomplished by the mathematical technique of **Fourier transformation**.[6]

1.3 PRINCIPLES OF TWO DIMENSIONAL NMR SPECTROSCOPY

2D NMR spectroscopy is a rapidly developing field and the varied techniques available make it an appreciated tool for structural elucidation studies. A comprehensive description of the theoretical aspects of the various 2D techniques is available in the literature.[7,8,9] For 1D NMR spectroscopy the common feature of all experiments is the

time sequence i.e. Preparation - Evolution - Detection . The basic 1D FT NMR technique operates with a fixed evolution period t_1 and the receiver signal is a function only of the detection time t_2. In the 2D experiment (Fig.4) a varying evolution time provides the second variable t_1 by introducing periodic changes of signal phase or intensity. Since the signal is now a function of two time variables ($S(t_1,t_2)$) upon fourier transformation a two dimensional spectrum will be obtained.

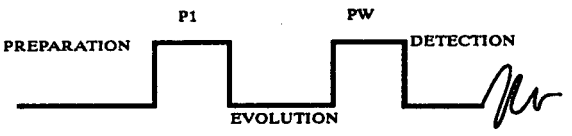

Figure4 Basic 2D pulse sequence

The variety of information contained in the different 2D experiments is a result of the changes that the spin system undergoes during the evolution period. The entire set of conditions and physical events to which the spin system is subjected to during the experiment e.g. decoupling or pulsing is termed the **pulse sequence.** In the basic 2D experiment mixing of resonance frequencies among mutually interacting spins produce crosspeaks. Essentially a cross peak is a result of **magnetisation transfer** from one spin to the interacting counterspin. Correlated two dimensional spectroscopy displays peaks which correspond to both single transitions (diagonal peaks) and to the correlations of different transitions (cross peaks).

Homonuclear pulse sequences follow the behaviour of like nuclear spins during t_1 and t_2. In the **heteronuclear** experiments one nuclei is followed during t_2 and the other indirectly through t_1.

The pulse sequence is usually preceded by the **preparation period** which allows the spin systems to relax back into its steady state. This is usually terminated by a pulse. This also defines the initial state for the subsequent evolution period. The spin system can be subjected to different conditions during the evolution period which determines the information provided along the F1 axis.

A **mixing period** consisting of a pulse (e.g. NOESY pulse sequence) or a series of pulses may follow the evolution period and in the NOESY experiment it is selected such that a maximum amount of nOe buildup occurs during the time period specified.

Phase cycling[10] is of paramount importance in multi-pulse NMR to reduce **artifacts.** The most common artifact in most 2D NMR experiments is the axial peaks which arise from transfer of longitudinal magnetisation by the mixing pulse into detectable transverse magnetisation. Phase cycles serve to detect a desired transfer and simultaneously to suppress undesired magnetisation. Phase sensitive spectra in contrast to absolute value mode spectra provide sign information as well as the additional advantages of a smaller line width and differing lineshapes. In order to understand the concept of phase cycling, the mechanism of **quadrature detection** must be explained first. Quadrature detection involves the use of two phase sensitive receivers where signal phases differ by 90° i.e the sine or cosine component may be detected. Separate digitisation of the signals occur and these are treated as real and imaginary parts of a complex spectrum. On Fourier transformation addition of both spectra produces frequency discrimination. An improved signal to noise ratio is a noticeable advantage. However, since the phases and amplitudes of the signals from both channels may not be perfect, artifacts will appear to a

certain extent. These artifacts can be reduced by balancing the channels and this is achieved via phase cycling. States *et al*[11] describe a procedure for obtaining a phase sensitive 2D NOESY spectrum using a 2D hypercomplex method. Phase sensitive spectra require an amplitude modulation of the signal in t_1. The 2D Hypercomplex method as opposed to the TPPI(time-proportional phase incrementation) method[12] generates two data sets for each t_1 value i.e they are separated during acquisition. The imaginary part of the experiment exhibits two peaks with phase twisted lineshapes. This is **sine modulated** $S_s(t_1,t_2)$ and the peaks have opposing intensities. The real part of the spectrum obtained by the second experiment produces two peaks of phase twisted lineshape but of the same sign. This is **cosine modulated** $S_c(t_1,t_2)$. By applying a similiar processing procedure to both $S_c(t_1,t_2)$ and $S_s(t_1,t_2)$ a spectrum with absorption mode peaks is obtained. Since sine is an odd function and cosine an even function this implies that in the frequency domain the sign of the two components can be distinguished. If the two spectra are combined, one of the peaks will cancel and the other is reinforced. All phase sensitive spectra submitted in this report were obtained using the 2D hypercomplex method of **States,Haberkorn and Ruben.**[11]

1.3.1 THE COSY PULSE SEQUENCE

The first two dimensional experiment was proposed by Jeener in which a simple sequence of two 90° pulses was applied to a proton spin system. A detailed analysis of this pulse sequence was investigated by Aue et al.[14]

Bax and Freeman[14] investigated various methods of simplifying the spectrum to enable ready assignment and to emphasize **cross peaks** relative to the **diagonal peaks.** A detailed description of the COSY experiment is available in the literature.[15,16] The COSY pulse sequence exploits the **J coupling** of nuclei i.e it is a tool for determining the coupling of spins. To determine the molecular structure of a compound the COSY

experiment is sometimes effective for resolving complex coupling patterns and for assigning these couplings which are as a result of the interaction of nuclei of different frequencies. Coupling values can provide conformational informational via the Karplus equation since the magnitude of the scalar coupling is a measure of the torsion angle about single and double bonds. Thus it provides information about the spatial structure of the molecule. In this two dimensional experiment **correlated spins** are identified by matching diagonal and cross peaks.

Consider the **A** doublet of an **AX** i.e. **two spin system** in the proton NMR spectrum. The **first 90°x pulse** rotates both doublet magnetisation vectors to the y′ axis. Due to the **AX** coupling, the doublet components of transverse magnetisation precess away from each other in the x′y′ plane. Both vectors dephase relative to the rotating frame due to chemical shift δ**A** of the observed nucleus **A**. The **second 90°x pulse (mixing pulse)** rotates the δ**A** dependent y′ components of the doublet magnetization to the ±Z axis.

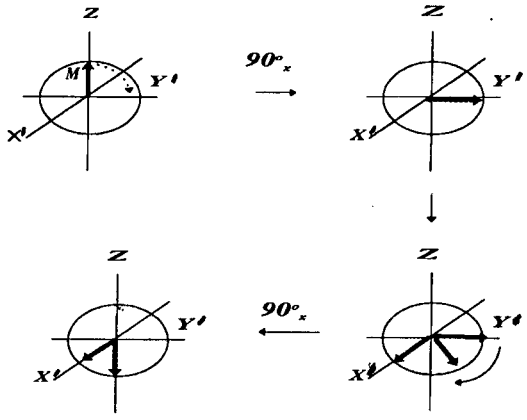

Figure5 Bloch vector diagram for COSY

Doublet magnetisation components of **X** protons are treated correspondingly. In conclusion the mixing pulse transfers δ**A** dependent magnetisation to nucleus **X** and

δX dependent magnetisation to nucleus **A**. The extent of this magnetisation exchange depends on the evolution time t_1 which is varied. The fid stored for each single experiment thus includes **A** and **X** signals which are both modulated by proton shielding δX and δA of the coupling nucleus. Two Fourier transforms in the t_2 and t_1 domains generate four signal maxima for an **AX** two spin system with chemical shift δA and δX. As both frequency domains are proton chemical shifts, the two dimensional COSY matrix is quadratic. Diagonal signals arise from the magnetisation experiencing the same modulation during t1 and t2. If the magnetisation evolves with a different frequency during t2 compared to t1 then this gives rise to cross peaks.

There are many variations to the COSY experiment and a phase sensitive pulse sequence is also available. The COSY-45[17] experiment is a variation of the COSY pulse sequence which involves varying the length of the second pulse. A COSY-45 experiment requires the application of a pulse of 90° followed by a second 45° pulse. The experiment emphasizes cross peaks intensity relative to the diagonal peak intensity . Since no additional information is contained in the diagonal and since large diagonal peaks may obscure cross peaks between nuclei with very similiar chemical shifts, this is often desirable. In the case of severe spectral overlap of the individual spin systems, which is common with some natural products, spectral analysis may be hampered. Relayed and multiple quantum coherence experiment may be of assistance. A RELAY-COSY[18] experiment enables determination of coupling information across a bonding chain e.g. an AMX system where the scalar interactions of two to three bonds need to be investigated i.e from A to X via M.

The problem of signal overlap may also be overcome via a double, triple or multiple quantum filtered COSY experiment.[19] Spectral simplification arises because multiple quantum coherences can only be generated in coupled systems. In the double quantum filtered experiment (DQCOSY), singlets are eliminated whilst for triple quantum filtered experiments two spin systems are also eliminated.

Improved determination of scalar coupling can be achieved by application of the **TOCSY**[20,21] experiment. TOCSY implies **total correlation spectroscopy.** The transfer of coherence takes place in the presence of an extended period of rf irradiation i.e. spin lock field in the rotating frame. This results in a net magnetisation transfer among scalar coupled homonuclear spins. The advantage of this phase sensitive spectrum is the enhanced resolution and sensitivity compared to the COSY experiment. The method is superior to the COSY experiment in that depending on the length of the mixing period the level of connectivity can be manipulated i.e. direct connectivities or relay connectivities using relay transfer can be obtained. Using the MLEV-17[20] composite pulse cycle, an AMX system will yield magnetization transfer from spin A to spin M during the first part of the mixing period and can be relayed to spin X during the second period.

1.3.2 INDIRECT DETECTION AND THE HMQC EXPERIMENT

The detection of a nucleus with a higher magnetogyric ratio in a heteronuclear shift correlation experiment offers higher sensitivity than the conventional experiment in which the less sensitive nucleus is detected. This is the indirect detection experiment. The exploitation of this gain in sensitivity is dependent on the dynamic range of the spectrometer and on the **cancellation** of unwanted signals. Indirect detection does have great applicability in studies of biological and chemical systems where observation of rare nuclei e.g. ^{13}C and ^{15}N is time consuming or difficult because of the low natural abundance and low NMR sensitivity of these nuclei.

Since the magnetogyric ratio of ^{1}H is somewhat four times larger than that of ^{13}C this implies that for an equivalent number of nuclei, the signal intensity will be four times larger.

A 2D version of the indirect detection experiment is the **HMQC** experiment. HMQC implies **heteronuclear multiple quantum coherence.** The original report on the

HMQC experiment [22] describes the correlation of single quantum transitions of one spin species to the forbidden heteronuclear multiple quantum transitions. The heteronuclear multiple quantum coherence can be converted into single quantum coherence. This leads to the indirect detection of the second species since these transitions have common energy levels with the heteronuclear multiple quantum transitions. Since these heteronuclear multiple quantum transitions are developed and observed through the first spin species with the larger magnetic moment, the sensitivity of these experiments is much improved. The pulse sequence of Muller attracted much interest and this has resulted in various modifications which have been proposed and applied.[23,24,25]
The essence of the ^{13}C HMQC experiment is the cancellation of signals from protons attached to ^{12}C since only signals from protons attached to ^{13}C contribute to a heteronuclear chemical shift correlation experiment. The **BIRD** pulse sequence (Bilinear rotation decoupling)[26] is used as part of the HMQC sequence to optimize cancellation of ^{12}C protons.

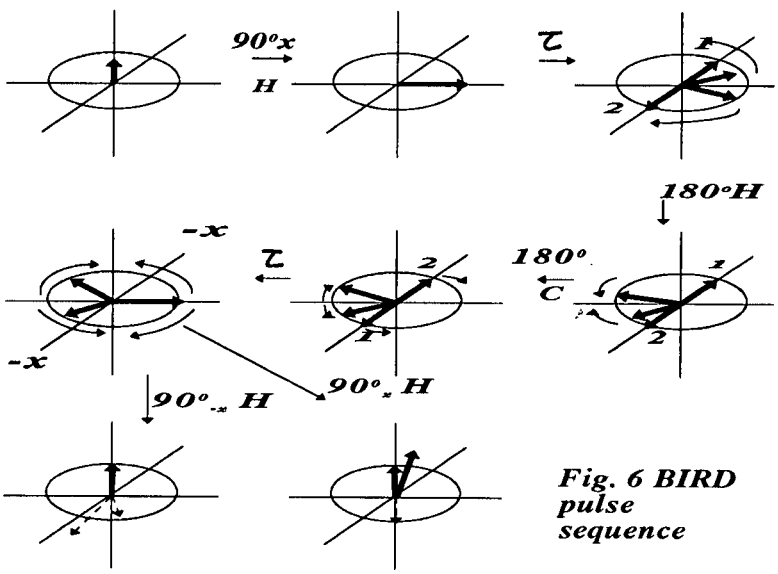

Fig. 6 BIRD pulse sequence

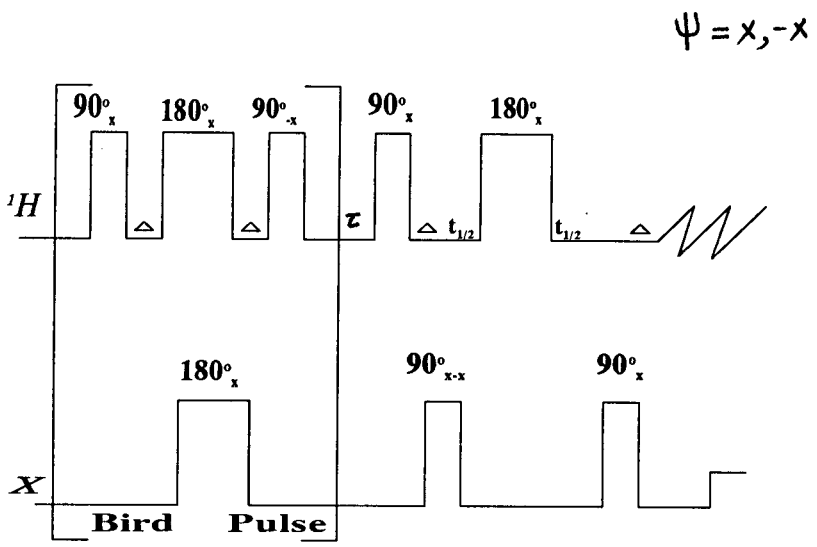

Figure7 HMQC using the BIRD pulse

In the BIRD pulse sequence (Fig.6), three pulses on the proton channel and one on the X channel inverts the Z magnetization of protons bound to ^{12}C while the Z magnetization of protons bound to ^{13}C are unaffected. The initial 90°x proton pulse is followed by an interval τ ($\tau=1/2{}^1J_{CH}$) during which the components of magnetization from coupling to the directly attached proton develop a net 180° phase inversion whilst those for longer range couplings dephase to a much smaller extent. A variable waiting period τ allows the ^{12}C bound protons to relax back to equilibrium. This waiting period is adjusted such that further execution of the pulse sequence will render ^{12}C bound protons at a null. After two waiting periods separated by a 180° proton and 180° ^{13}C pulse and followed by a

final 90°x-x pulse, the actual HMQC experiment begins. The ease of the adjustment of the waiting period adjustment is influenced by the variable relaxation time of protons. **Phase cycling** allows for the removal of undesired signals. This improves cancellation of the unwanted signals from ^{12}C bound protons. The pulse sequence most convenient for practical use proceeds as follows (Fig.7).

The first proton (180°) pulse is accompanied by a 180° pulse ($90°_x+90°_x$) on the ^{13}C nuclei. This occurs at a time equal to *1/2* J_{XH}. The resultant signal will focus on the y axis. The ^{13}C nuclei are not pulsed on the second scan with the result that the protons are focussed on the -y axis. With an inverted receiver phase the signal is now positive and the protons bound to ^{13}C produce a net positive signal. Protons bound to ^{12}C are eliminated. In the 2D experiment an evolution time is introduced between the two X nucleus 90° pulses. The rate of precession of the ^{13}C nuclei during this time will provide the ^{13}C chemical shift. A modulation of the intensity of the ^{13}C bound protons and a subsequent fourier transformation of that modulation yields the ^{13}C chemical shift. There are many variations to the HMQC experiment and these include the HMQC-RELAY[25] experiment as well as the HMQC-TOCSY experiment. Also the heteronuclear multiple bond coherence experiment (HMBC)[27] can be used to provide assignment information for nonprotonated carbons.This pulse sequence as described by Bax and Summers[27] enables the determination of two to three bond ^{1}H-^{13}C connectivity information and can be used as an alternative to the long range HETCOR experiment.

1.3.3 The nOe Experiment

Dipolar coupling is the interaction of the magnetic moments of two spins through space. The nOe measurement is an indirect means of extracting information about dipolar coupling and this is related to **internuclear distances** and molecular motion.[28] Dipolar coupling is responsible for phenomenon of relaxation in solution and it also generates **cross relaxation** in solution[29]. Cross relaxation is the mutual relaxation between

spatially neighbouring nuclei. This intramolecular cross relaxation gives rise to the nuclear Overhauser enhancement(nOe) effect. This is the variation in intensity of the signal as a result of the disturbance of the population of another nucleus. The nOe effect is dependent on the distance between cross relaxing nuclei and thus allows the determination of intramolecular interatomic distances. This is vital information for the determination of three dimensional structures.[30,31] The nOe effect in 2D NMR spectroscopy allows for the quantitative measurement of distances for larger molecules. In 2D NMR spectroscopy the dipolar coupling is effective during the mixing period τ_m. In order to understand the nOe effect one must consider the **relaxation pathways** available in a multispin system. Consider the relaxation pathways for a **homonuclear AX system** which is not scalar coupled. The two spin 1/2 nuclei I and S have equal γ but their chemical shifts differ. The nuclei will be present in the states $\alpha\alpha,\alpha\beta,\beta\alpha,\beta\beta$ which implies the system has four energy levels.

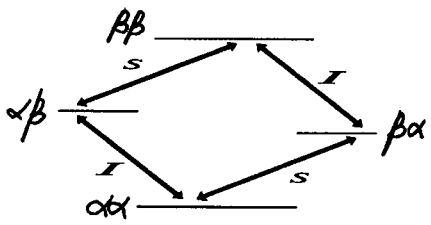

Figure8 Relaxation pathways for a homonuclear AX system

Any difference in energy between the two states $\alpha\beta$ and $\beta\alpha$ is considered to be negligible. Since we assume no J coupling the two transitions of nucleus I and S have equal energy. The state $\alpha\alpha$ is of lower energy and therefore contains an excess of

nuclei. ββ will be deficient by an equal amount. Consider the relaxation as a result of saturation of spin S. Only deviations from Boltzmann equilibrium are shown (Fig 9).

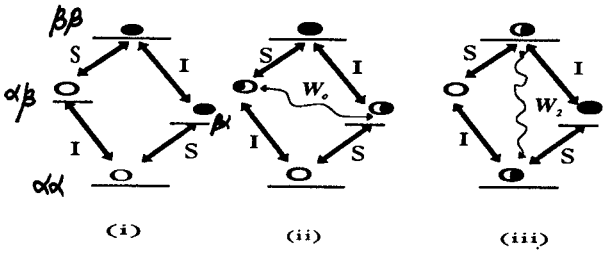

Figure9 Relaxation pathways after polarisation of spin I

The first state (i) corresponds to the Boltzmann equilibrium of spin I and saturation of spin S. The rate constants for the various processes is designated by W. Of interest are the zero quantum transitions W_0 and the double quantum transitions W_2 since for single quantum transitions saturating S does not affect the intensity of the spin I. If the zero quantum transition W_0 (ii) is effective, the populations of the two middle levels equalize i.e W_0 acts so as to transfer population from the state βα to the state αβ. There is a corresponding change in the population of the I spin and thus W_0 relaxation enables magnetization transfer through dipolar coupling resulting in the decrease in the intensity of signals due to spin I. If the double quantum transition W_2 (iii) is effective the upper and lower levels equalize. There is magnetization transfer from the state bb to the state aa and if the W_2 relaxation pathway dominates then there is an increase in the intensity of the signal due to I. For a longer correlation time τ_c cross relaxation occurs via low frequency transitions of W_0 since molecular rotation in the external field is not rapid. A

faster molecular reorientation is achieved via a shorter correlation time. The cross relaxation rate is given by W_2-W_0 and can be either positive or negative i.e if W_2-$W_0 > 0$ then the nOe is positive.

The two dimensional nOe experiment allows for the detection of nOe without the need to apply a saturating field. For macromolecules, interpretation of equilibrium nOe becomes difficult as the number of spins increases. The cross relaxation may be less specific and less useful. One dimensional nOe experiments have limited practical use for large molecules due to long accumulation times and the poor selectivity in irradiation.
The 2D NOESY (nuclear Overhauser enhancement spectroscopy)[32,33] experiment provides proton-proton Overhauser effects in large molecules.
A typical NOESY experiment consists of a sequence of three nonselective 90° pulses (Fig.10). The transverse magnetizations is prepared by the first 90° pulse. During the evolution period, t_1, the various magnetizations components acquire precession frequency information. This is the frequency labelling period. The mixing period τ_m occurs between the second and the third pulse where the magnetizations is longitudinal. During this period selective homonuclear nOe are built up by cross relaxation through mutual dipolar interactions. The remaining transverse components are destroyed by a magnetic field gradient pulses. The third 90° pulse concludes this pulse sequence by rotating the longitudinal magnetizations into the xy plane for detection. The cross peaks obtained indicate exchange of magnetizations which is a result of dipole-dipole cross relaxation during the mixing time. The time development of nOe in the NOESY spectrum can be investigated using different mixing times τ_m.

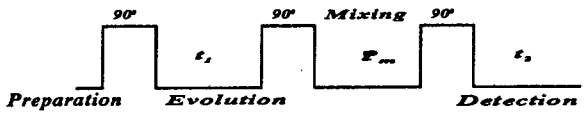

Figure10 Pulse sequence for 2D NOESY experiment

In conventional NOESY spectroscopy , positive nOe is expected for small rapidly tumbling molecules while negative nOe[34] is expected for large slowly tumbling molecules. Medium sized molecules have correlation times that result in small or no nOe enhancements. The NOESY experiment is an indispensable tool in the assignment of proteins and peptides.[35,36,37]

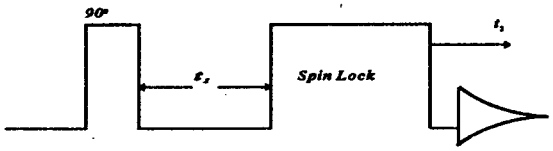

Figure11 Pulse sequence for 2D ROESY experiment

The ROESY (rotating frame Overhauser spectroscopy) experiment[38,39,40] detects cross relaxation between **spin locked transverse** magnetization (Fig.11). The ROESY experiment is suitable for molecules that have a motional correlation time τ_c, near the condition $\omega\tau_c=1$, where ω is the angular Larmor frequency. The rotating frame nOe increases for increasing values of τ_c and under spin locked conditions it is always positive. The dynamics of cross relaxation between transverse magnetization result in positive nOe enhancements for all correlation times and thus molecules which yield no enhancements with conventional NOESY spectroscopy can be studied using the ROESY pulse sequence.

In the ROESY pulse sequence a weak spin lock rf field is switched on during the mixing time. During this period projections of the magnetization vectors present at the end of t_1 onto the vector of the effective rf field remain spin locked. Spin exchange then occurs among the spin locked components of different nuclei. The spectral density functions cause the effect to be positive for all values of τ_c.

1.3.4 Application of multipulse NMR techniques in the field of natural products.

The structure of natural products that are obtained from plants are now widely elucidated using spectroscopic analysis of the isolated compounds. The rapid developments in the field of 2D NMR spectroscopy has been of significant advantage to the natural product chemist. The complexity of natural products have resulted in the imperative use of 2D techniques in order to unambiguously assign one dimensional ^{1}H and ^{13}C spectra. Prior methods to assign the structure of natural product derivatives relied mostly upon chemical shift information as well as the use of a selection of compounds to enable assignment via comparison.

In the spectroscopic context, natural products provide a valuable means of evaluating the various 2D NMR techniques. The combination of homonuclear and heteronuclear correlation techniques is a good means of spectroscopic assignment. The variations in the 2D pulse sequences allowed for comparison of these techniques with respect to the information provided, the complexity of these techniques, and their applicability.

The various homonuclear correlation techniques for instance allowed for scalar or dipolar correlation i.e short or long range ^{1}H-^{1}H correlation (COSY, TOCSY) or the use of proximate relationships via through space couplings (ROESY, NOESY). The sensitivity of the technique, the time required for acquisition and the usefulness of the information provided are all important considerations in evaluating a technique.

The various heteronuclear pulse sequences which emphasize the ^{1}H-^{13}C correlation via one bond coupling or long range two to three bond coupling were also evaluated. These techniques include the HETCOR and HMQC pulse sequences. The time factor is important in evaluating heteronuclear techniques, primarily due to the need for significantly larger amounts of samples than for the homonuclear approach. The quantities of natural products available for analysis are in general very limited.

The natural products chosen for the evaluation of 2D multipulse NMR techniques range from opium alkaloids to the relatively complex cucurbitacin derivatives. The opium alkaloids that were structurally assigned include codeine and papaverine. The diterpenoid alkaloid, delphinine was fully assigned and these assignments were used to assist in the assignment of aconitine, a related compound. The cucurbitacin derivatives were the most structurally complex of the natural products chosen and the assignments of cucurbitacin A 2,16,19 triacetate were used to demonstrate the effectiveness of multipulse NMR techniques in structural assignment as well as to assign related compounds.

CHAPTER TWO

2.1 THE OPIUM ALKALOIDS

2.1.1 INTRODUCTION

Opium, the sun dried latex of the unripe seed-capsules of the Indian poppy *Papaver somniferum*[41] is a brown, resinous looking substance with a characteristic smell and bitter taste. Opium possesses its medicinal properties only when produced under favourable conditions of soil and climate of tropical and subtropical countries. The action of opium depends on the quality of its many alkaloids, the quality being measured by its morphine and codeine content. Opium is dried, powdered and standardised to a definite content of morphine for use in medicine.

In small doses opium produces a state of excitement whilst in larger doses (medicinal) the stage of gentle excitement is followed by deep sleep and in larger more poisonous doses, coma or death may occur. Opium poisoning may be treated with aqueous solutions of potassium permanganate which destroys the alkaloids of opium.[41]

Apart from morphine, the chief alkaloids of opium are codeine and papaverine. Papaverine is a benzylisoquinoline derivative whilst codeine is a morphine type derivative.

In the series of opium alkaloids, papaverine in its general effect, stands between morphine and codeine. In comparatively small doses it induces sleep but in larger doses reflex irritability is increased. It has a paralysing action on the smooth muscles of the intestines and the blood vessels.[42]

Codeine (morphine methyl ether) is obtained as a methylated derivative of morphine. It is similar to morphine in its general effect but its toxicity and depressant action is less marked. It stimulates the spinal cord and the lower parts of the brain in man,[43] inducing sleep in small doses whilst in larger doses restlessness and increased reflex excitability

and possibly hallucinations occur.[44] In the form of codeine phosphate, it is widely prescribed in medicine for the relief of cough whilst in combination with aspirin, it is prescribed for the relief of headaches and rheumatic pains. It tends to have a constipating effect on the intestinal system.[45]

Stermitz and Rapoport[46] have reported a biosynthetic pathway for the formation of opium alkaloids which involves O-demethylation. In *Papaver somniferum*, thebaine is the first octahydrophenanthrene alkaloid formed and is converted via O-demethylation steps into codeine and finally to morphine. Much attention has been focussed on the interrelationship of these opium alkaloids.[47] The isoquinoline alkaloid papaverine may be obtained from laudanosoline which is a key intermediate for the biogenesis of a large group of isoquinoline alkaloids. Battersby and Harper[48] have reported on the biosynthesis of radioactive papaverine which was obtained when tyrosine-2-C^{14} was fed to opium poppies.

Papaverine and Codeine derivatives are present in many widely available pharmaceutical products and these opium derivatives were chosen to demonstrate some of the applications of multipulse NMR techniques in the structural determination of these products.

2.1.2 CODEINE

2.1.2.1 Assignment of the ^{1}H and ^{13}C spectrum

The IUPAC name for Codeine is **7,8 didehydro-4,5α-epoxy-3-methoxy-17-methyl morphinan-6α-ol**

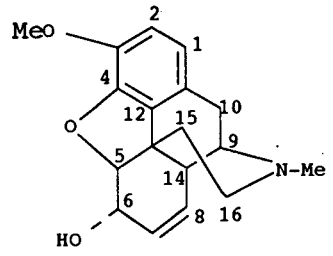

Structure [I] Codeine

The compound has a total of **18 carbons** and the edited DEPT spectrum (Appendix A) confirms that the compound has two methyl groups, eight methine groups and three methylene groups. Five quaternary carbon atoms are present.

The ^{1}H (Figure 12) and ^{13}C (Figure 13) spectra of codeine were assigned with the aid of the following multipulse sequences:

(i) COSY (ii) HMQC (iii) long range HETCOR (iv) HMBC (All spectra in Appendix A).

The most readily assigned groups in the ^{1}H spectrum are the doublets of the aromatic protons H_1 and H_2 which are observed in the proton spectrum at δ 6.44 and δ 6.64 respectively. The large ortho effect of the C_3 methoxyl substituent presumably resulted in the upfield resonance of H_2 proton. H_1 and H_2 can be distinguished from the olefinic protons of H_7 and H_8 whose multiplets are observed at δ 5.66 and δ 5.25 respectively, the more highly structured multiplicity arising from coupling to neighbouring protons.

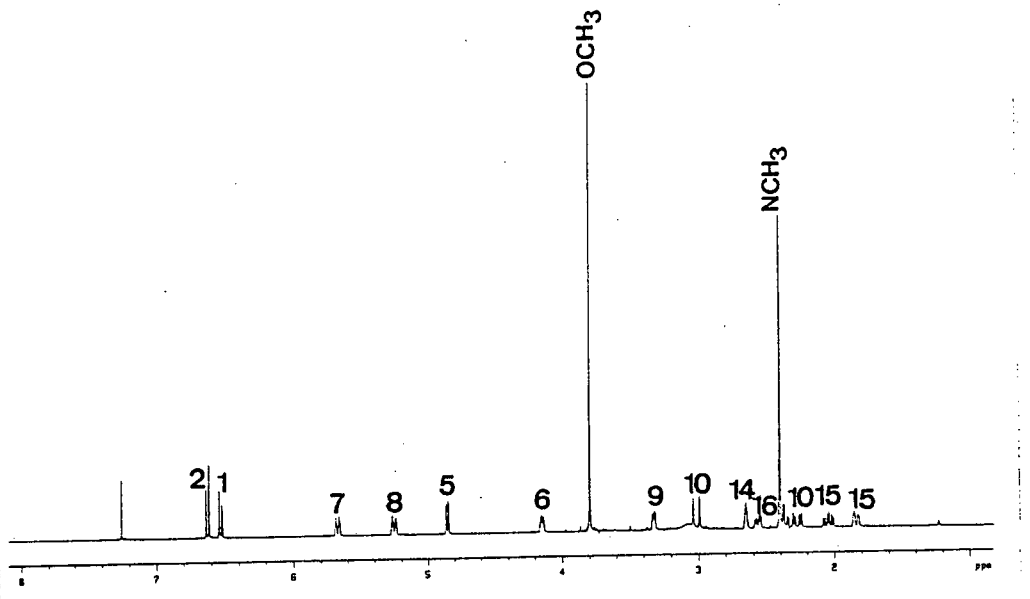

Figure 12 ^{1}H spectrum of codeine

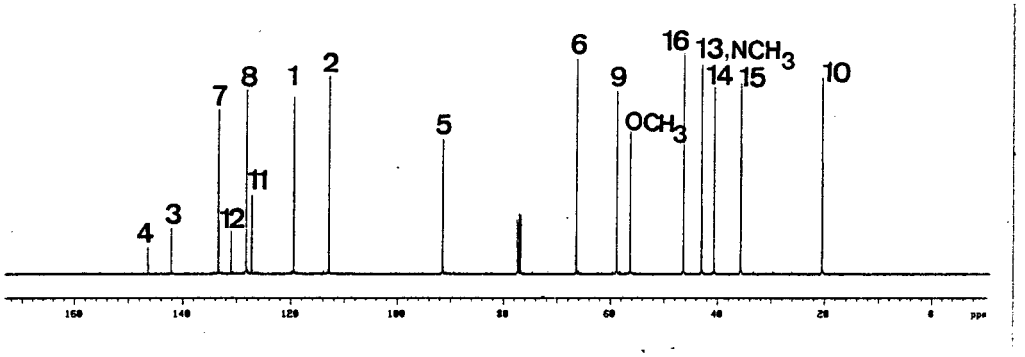

Figure 13 ^{13}C spectrum of codeine

The quaternary carbon atoms C_3,C_4,C_{11} and C_{12} can be relatively easily assigned as they correlate with either H_1 and H_2. The HMBC spectrum (figure 14) reveals the following

correlations i.e H_1 to C_3 and C_{12} , H_2 to C_{11} and C_4. C_4 and C_{12} appear are deshielded due to the influence of the oxygen atom.

The HMQC spectrum assigns C_1 and C_2 to the resonances at δ 119.48 and δ 112.93 respectively. Thus the remaining quaternary carbon atoms in the ^{13}C spectrum at δ 42.96 must be C_{13}. A C_{11} correlation to $H_{10\alpha\beta}$ is observed in the long range HETCOR spectrum thereby assigning the resonances at δ 2.29,dd and δ 3.02,d as $H_{10\alpha\beta}$. Further evidence is the $H_{10\alpha\beta}$ correlation in the COSY spectrum and the HMQC spectrum which assigns the ^{13}C resonance of C_{10} as δ 20.45. The long range HETCOR shows a correlation of H_{10} to a methine carbon presumably C_9. The HMQC reveals that the ^1H resonance of H_9 should be at δ 3.33. The COSY spectrum reveals a correlation between H_{10} and the H_9 methine proton at δ 3.33ppm thus confirming the observation in the long range HETCOR. The double doublet at δ 4.85 was assigned to the H_5 methine proton as this is shifted downfield by the presence of the C_5-O moeity. The COSY spectrum reveals a correlation of H_5 to the proton at δ 4.15 and this was assigned to the H_6 resonance as it is its nearest neighbour. The remaining methine proton H_{14} must therefore be assigned to the resonance at δ 2.66 and this is confirmed by a C_9-H_{14} correlation in the long range HETCOR. The ambiguity in assigning the resonances of H_7 and H_8 whose multiplets are observed at δ 5.66 and 5.25ppm was overcome with the aid of the HMBC spectrum which revealed a H_5 to C_7 correlation. Other noteworthy correlations were a C_6-H_8 correlation in the long range HETCOR as well as a H_6-H_8 correlation in the COSY spectrum.

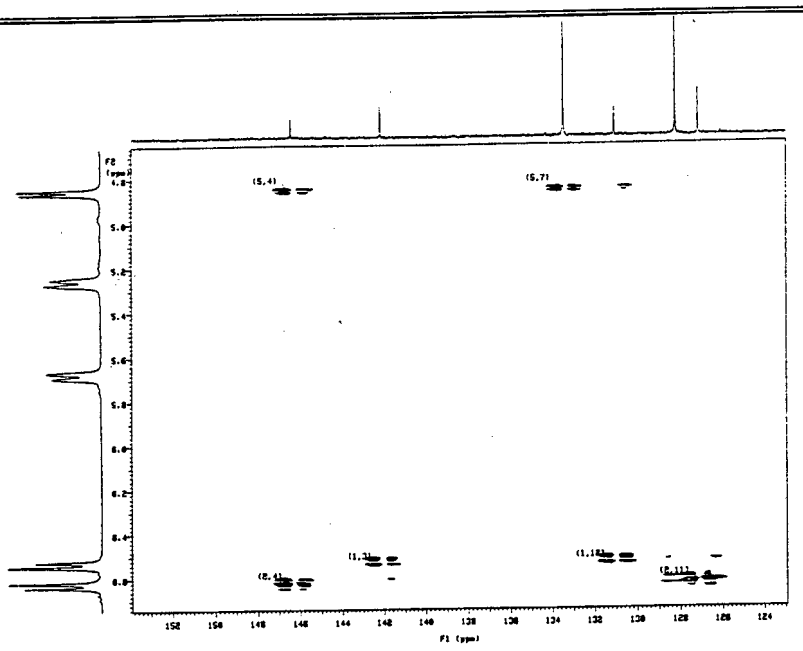

Figure 14 HMBC spectrum of codeine

The methylene groups $H_{15\alpha\beta}$ and $H_{16\alpha\beta}$ assignments was not an easy task but were assigned by considering their correlation to C_{13} and C_9. C_9-H_{16} correlation is observed in the long range HETCOR thereby assigning the double doublet at δ 2.36 and the triplet at δ 2.57 as $H_{16\alpha\beta}$ resonances in the ^1H spectrum. The deshielding influence of the nitrogen atom is also a important consideration for this argument. C_{13} correlates to both H_{15} and H_{16} in the long range HETCOR thereby assigning the resonances at δ 2.05 and δ 1.84 as that of $H_{15\alpha\beta}$ in the ^1H spectrum. The methoxy group is assigned to the singlet at δ 3.79 and the hydroxy group to the broad resonance at δ 3.08. The final sets of assignments appear in Table 1 and Table 2.

2.1.2.2 TABULATION OF RESULTS

Table 1 ^{1}H chemical shifts and assignments of Codeine

ATOM	δ_H(ppm)	δ_H(ppm) **Lit.**[52]	Multiplicity
H_1	6.53	6.57	d
H_2	6.63	6.66	d
H_5	4.86	4.90	dd
H_6	4.15	4.19	m
H_7	5.68	5.71	m
H_8	5.26	5.30	m
H_9	3.33	3.35	m
H_{10}	2.28,3.02	2.30(α),3.07(β)	dd,d
H_{14}	2.66	2.67	m
H_{15}	2.05,1.84	2.07(ax),1.88(eq)	m,dt
H_{16}	2.36,2.57	2.40(ax),2.60(eq)	dd,t
N-CH_3	2.40	2.45	s
O-CH_3	3.79	3.84	s
-OH	3.08	3.00	s

Table 2 ^{13}C assignments of Codeine

ATOM	δ_C(ppm)	δ_C(ppm) **Lit.**[52]
C_1	119.48	119.39
C_2	112.93	112.81
C_3	142.13	142.12
C_4	146.41	146.17
C_5	91.45	91.15
C_6	66.46	66.18
C_7	133.43	133.39
C_8	128.21	127.83
C_9	58.85	58.76
C_{10}	20.45	20.38
C_{11}	127.18	126.71
C_{12}	131.05	131.10
C_{13}	42.97	42.90
C_{14}	40.69	40.33
C_{15}	35.72	35.40
C_{16}	46.41	46.28
N-CH_3	43.03	42.76
O-CH_3	56.32	56.18

2.1.2.3 Comparison with literature assignments

Batterham *et al*[49] have studied the NMR spectra of codeine and its derivatives and the proton patterns on ring A,B,C were analysed by first order methods.

Ring C provides the ideal system for observation of long range, allylic, homoallylic and four bond couplings.

In codeine, the C_6 hydroxyl group is known to be equatorially oriented. The H_{14} proton thus displays a shielded chemical shift as it is axially oriented compared to other isocodeine derivatives in which the hydroxyl group is axially oriented. A *cis* diaxial relationship thus exists between the H_6 and H_{14} protons and this leads to homoallylic coupling. H_6 and H_8 allylic coupling is also possible. The signal from the H_6 proton is thus split into eight peaks since there is also vicinal coupling to H_5 and H_7. An allylic coupling is observed between the protons H_7 and H_{14} and this is also evident in the isocodeine series as noted by Battersham *et al*[49].

The H_7 proton, was as might be expected, more deshielded than the H_8 proton due to its proximity to the hydroxyl group.

The quaternary carbon atoms were assigned in this report with the aid of the long range HETCOR and the HMBC spectra. Wehrli[50] assigned the quaternary carbons of codeine using spin lattice relaxation data. The relaxation times were determined for solutions in $CDCl_3$ via the inverse recovery method. C_4 and C_{12} were expected to exhibit the longest T_1 values due to the absence of α CH systems. C_{12} is more shielded than C_4 due to the proximity of the methylene protons of C_{15}. C_{11} should have the fastest relaxation time relative to other aromatic carbons since three α proton atoms contribute to its relaxation. C_{13} was found to exhibit the shortest T_1 due to the relaxation effects of four α protons. Alternatively, Terrui *et al*[51] have assigned the quaternary carbons of codeine using their relative intensities i.e it was noted that $C_{11} > C_{12} \sim C_3 > C_4$.

Chazin and Colebrook[52] evaluated the diagnostic potential of spin lattice relaxation measurements on the morphine alkaloid, to provide information on the primary molecular structure and relative stereochemistry of some natural alkaloids. This was achieved via calculation of relaxation pathways from model structures, relaxation rate measurements and nOe enhancements. These authors were able to distinguish between the methylene protons of C_{15} and C_{16}. Their method of differentiating diastereotopic methylene protons was based on the relaxation pathways among these methylene protons. Since axial protons can be distinguished from equatorial protons by the number of intermediate vicinal pathways then this implies that when a proton of one of these two diastereotopic protons is saturated, the observation of nOe enhancement of both vicinal protons identifies the saturated resonance as that of the equatorial methylene proton. However, if the axial proton is saturated then only one of the vicinal protons will be significantly enhanced. This is due to inefficient cross relaxation as a result of large axial/axial interproton distances on adjacent carbon atoms. They concluded that ring D is in a boat conformation.

Carroll *et al*[53] have reported on the carbon-13 nuclear magnetic resonance spectra of morphine alkaloids. C_{10} and C_{15} were distinguished by the fact that C_{15} possessed more α and β substituents and fewer γ substituents than C_{10} and thus appeared downfield. They indicated that C_{10} was at an unusually high field due to the combined γ effects from C_8, C_{16}, and N-CH_3.

The authors mentioned above have used elegant theoretical arguments to effect a complete assignment of the ^1H and ^{13}C spectra of Codeine. The assignments presented here are in agreement with their assignments. However, the assignments presented here follow directly from observed internuclear correlations without the need for arguments based on relative chemical shifts and relaxation rates.

2.1.3 PAPAVERINE

2.1.3.1 THE ASSIGNMENT OF PAPAVERINE

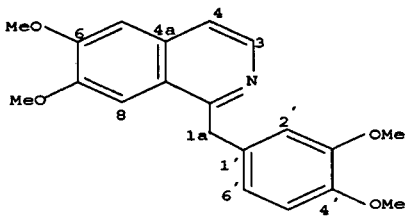

Structure [II] Papaverine

The IUPAC name for papaverine is **1-(3',4'-DIMETHOXYBENZYL)-6,7 DIMETHOXY ~ ISOQUINOLINE**. The nomenclature follows the numbering along the isoquinoline backbone and then the numerical arrangement is extended to the dimethoxybenzyl ring. The compound has **twenty carbon atoms**. Spectral analysis for protonated carbons via an edited DEPT spectrum (Appendix A) confirmed that the compound has four methyl groups, a single methylene group and seven methine groups. Thus eight quaternary carbon atoms are present.

The ^{1}H (Figure 15) and ^{13}C spectrum (Figure 16) of papaverine was assigned with the aid of the following 2D experiments viz COSY, HMQC,HMBC and long range HETCOR (Appendix A). The least complicated assignment is that of the H_3 proton (δ 8.24), it being deshielded due to the influence of the neighbouring nitrogen atom. The H_3 resonance is a doublet and this indicates coupling to probably the H_4 proton which is its nearest neighbour. This is confirmed via the COSY spectrum which reveals a homonuclear correlation between the H_3 proton and the doublet present at δ 7.20. The HETCOR spectrum analysis indicates that the ^{13}C resonance of C_4 is 118.62ppm and furthermore the long range HETCOR reveals a C_4-H_3 correlation. The COSY spectrum

indicates a coupling between the H_4 proton and the proton at δ 6.80 and this is probably four bond correlation with the H_5 proton. The HETCOR analysis reveals that the C_5 carbon atom appears at δ 105.88ppm. Analysis of the long range HETCOR indicates a three bond coupling of the H_4 proton to the C_5 carbon atom at δ 105.88.

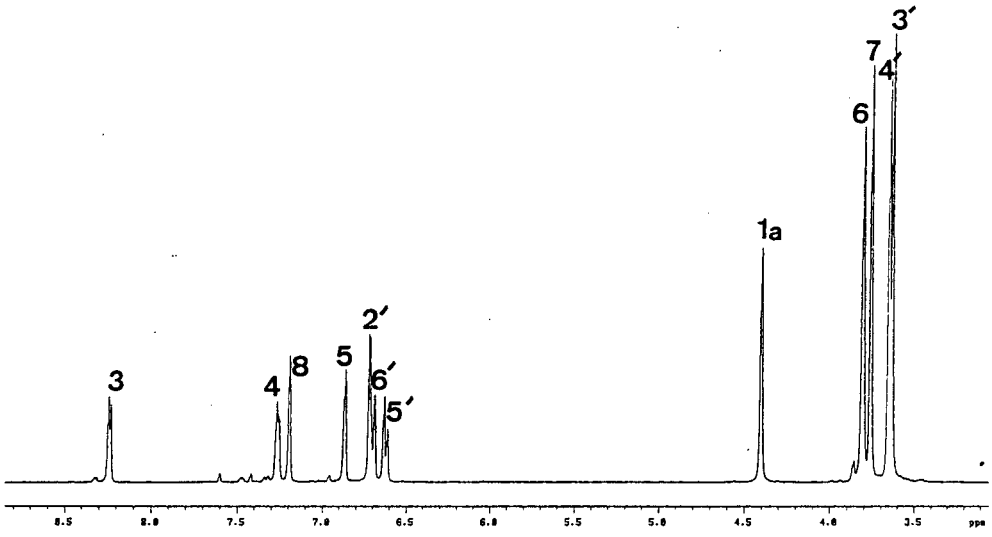

Figure 15 ^{1}H spectrum of papaverine

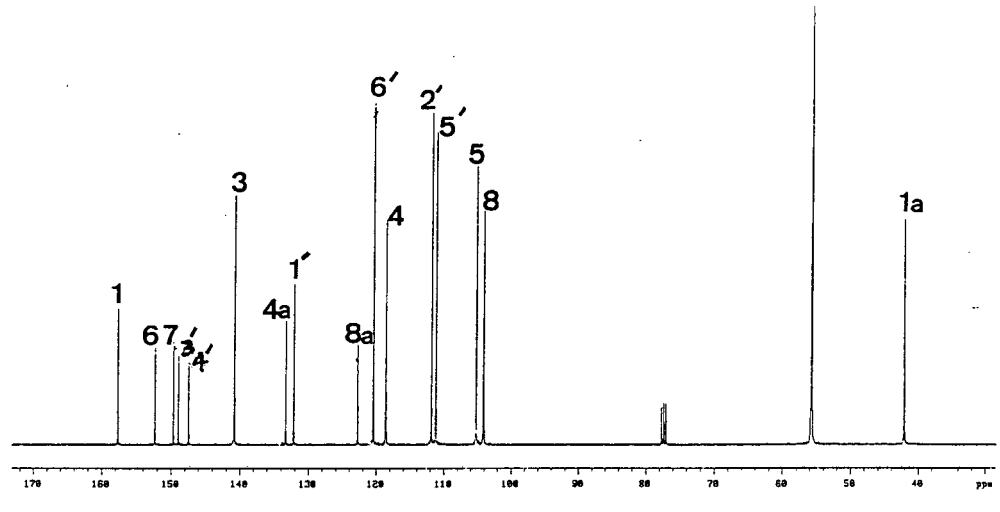

Figure 16 ^{13}C spectrum of papaverine

H_8 and H_2' should produce singlets as they have no neighbouring protons. The singlet in the ^1H spectrum at δ 7.14 was assigned to the H_8 proton on the basis of the influence of the C_7 methoxy group as it is likely to produce a downfield shift of this ^1H resonance. This argument is confirmed by the assignment of the methoxy group at δ 3.70 as 7-OMe by ^1H-^1H correlation to H_8 in the COSY spectrum.

The COSY spectrum (Figure 17) produces interesting correlations between the methoxy groups (7-OMe, 6-OMe, 3'-OMe, 4'-OMe) and their nearest methine neighbours. There is strong overlap of resonances of the methoxy groups in both the ^1H and the ^{13}C spectrum and these groups can best be assigned with the aid of the COSY and the long range HETCOR spectrum. The assignment of the quaternary carbons also assist in the assignment of the methoxy groups. Thus if the H_2' proton singlet resonates at δ 6.72 then a correlation to 3'-OMe in the COSY spectrum confirms this argument. The methoxy groups at δ 3.70ppm and δ 3.74ppm were assigned to 7-OMe and 6-OMe respectively since 7-OMe correlates with the H_8 proton in the COSY spectrum. 6-OMe shows correlation with H_5. The doublet at δ 6.63 was assigned to H_5' since it shows correlation to the remaining methoxy group viz C_4'-OMe. The CH_2 moeity resonates at δ 4.39 in the ^1H spectrum.

Papaverine has eight quaternary carbons and these were assigned with the aid of an HMBC spectrum (Figure 18) and a long range HETCOR spectrum.
The H_3 proton coupling to the quaternary carbon at δ 157.66 assigns this carbon as C_1. This carbon atom is also most likely to be shifted to low field due to the influence of the neighbouring nitrogen atom. A three bond coupling between the H_3 proton and C_{4a} in the long range HETCOR assigns the resonance at δ 133.3 as C_{4a}.

Quaternary carbon atom C_{8a} at δ 122.79 correlates via three bond coupling to H_4 in the long range HETCOR and three bond correlation to H_5 as noted in the HMBC spectrum as well. C_{8a} also correlates to the methylene proton H_{1a} in the long range HETCOR via three bond coupling.. Three bond correlation of the methylene group H_{1a} to C_6' is evident in the long range HETCOR as well as two bond correlation to C_1' and C_1 (δ 157.66).

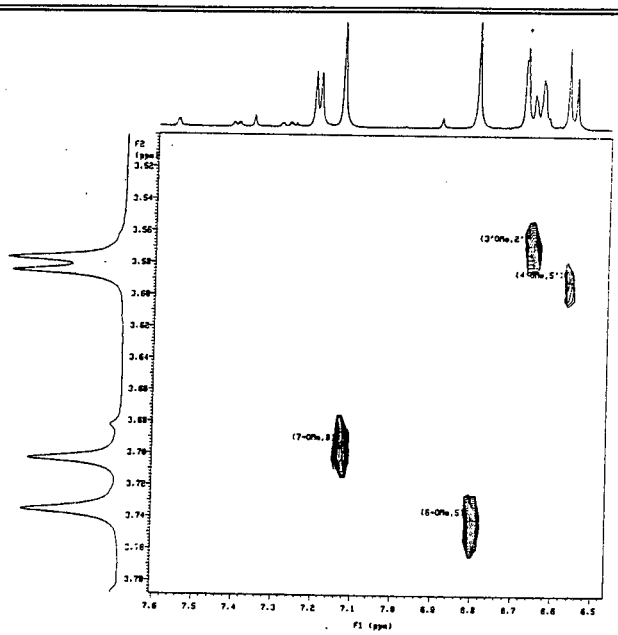

Figure 17 Expanded COSY spectrum of papaverine.

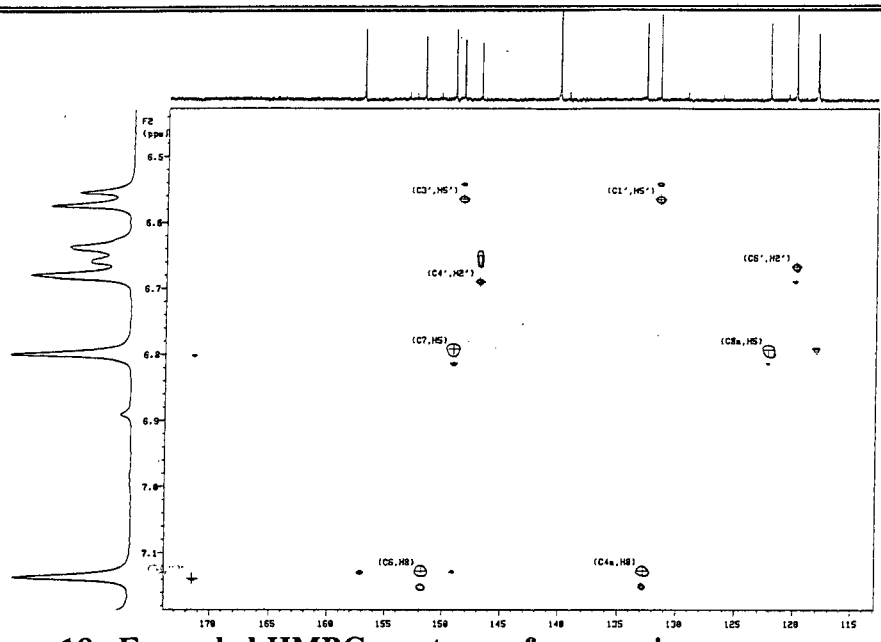

Figure 18 Expanded HMBC spectrum of papaverine

In the HMBC spectrum C_6' correlates with H_2'. The quaternary C_1' correlates via two bond coupling to H_6' in the long range HETCOR and is assigned to the ^{13}C resonance at δ 132.16. C_1' also correlates to H_5' in the HMBC spectrum.

The remaining quaternary carbon atoms are linked to methoxy groups and have been assigned as follows. C_6 has been assigned to the ^{13}C resonance at δ 152.32 since it correlates to H_8 in the HMBC spectrum and C_7 to the resonance at δ 149.68 since it correlates to H_5. The assignment of C_3' and C_4' at δ 147.46 and δ 148.96 is derived from the long range HETCOR and HMBC spectra where three bond coupling of C_3' to H_5' and C_4' to H_2' is noted.

The final set of assignments are given in Table 3 and 4.

2.1.3.2 Tabulation of results

Table 3 ^{1}H Assignments of Papaverine

ATOM	δ_H(ppm)	δ_H(ppm)Lit.[56]	Multiplicity
1a	4.35	4.55	s
3	8.18	8.38	d
4	7.21	7.40	d
5	6.80	7.03	s
8	7.14	7.35	s
2′	6.68#	6.74	s
5′	6.57#	6.78	d
6′	6.65#	6.81	d
3′-OMe	3.58	3.78	s
4′-OMe	3.59	3.82	s
6′-OMe	3.74	3.99	s
7′-OMe	3.70	3.91	s

Differ from literature assignments

Table 4 ^{13}C Assignments of Papaverine

Atom	δ_C	δ_C(ppm)Lit.[56]
1	157.66	157.5
1a	42.07	41.9
3	140.82	140.7
4	118.62	118.4
4a	133.33	133.1
5	105.18	105.0
6	152.32	152.1
7	149.68	149.5
8	104.08	103.9
8a	122.79	122.6
1′	132.16	132.0
2′	111.87	111.7
3′	147.46#	148.8
4′	148.96#	147.3
5′	111.95	111.0
6′	120.47	120.2
6-OMe	55.8	55.5
7-OMe	55.8	55.5
3′-OMe	55.8	55.5
4′-OMe	55.8	55.5

Differ from literature assignments

2.1.3.3 Comparison with literature assignments

Marsoioli et al[54] have reported on the ^{13}C spectral analysis of some isoquinoline alkaloids. For spectral interpretation Marsoili[54] utilized substituent shielding effects and ^{13}C-^{1}H long range couplings. SFORD(single frequency off resonance decoupling) and coupled ^{13}C NMR spectra were recorded for papaverine. The ^{13}C NMR values reported in Table 4 are in good agreement with that proposed by Marsoili[54].

Rae and Simmonds[55] have utilized relaxation methods to determine the stereochemistry about the C_1-CH_2 bond. It was assumed that the relaxation rate of H_8 in papaverine should be quite sensitive to the distances between this hydrogen and the methylene hydrogen and this should permit the estimation of these distances. This depended on the determination of the contribution of the 7 methoxy hydrogen to H_8 relaxation. The value of the torsional angle C_{8a}-C_1-CH_2-C was reported to be between 70 to 92°.

Rae[55] also reassigned H_5 and H_8 on the basis of a NOESY spectrum. In the NOESY spectrum the two singlets δ 7.036 and δ 7.331, as reported by Rae[55], were assigned to H_5 and H_8. The first singlet showed a cross peak with the resonance of H_4 and was assigned to H_5 and the less shielded resonance showed a cross peak with the CH_2 resonance and was assigned to H_8. Cross peaks between H_5 and H_8 also permitted the assignment of two of the methoxy groups.

Janssen *et al*[56] have assigned the ^{1}H and ^{13}C spectra of some isoquinoline alkaloids. Their assignments were aided by model compounds and lanthanide -induced chemical shifts. The assignments of H_2', H_5',H_6' (ring C) are not in agreement with the values submitted in this report although ^{13}C values are in good agreement. The long range HETCOR and HMBC spectra may serve to eliminate some discrepancies that have arisen. The resonance at δ 6.68ppm has been assigned to H_2' whilst Janssen[56] report the assignment as H_6'. In the long range HETCOR a cross peak is observed between C_3'-H_2' (2 bond). If the resonance was assigned to H_6' as Janssen[56] suggests then a C_3'-H_6'

correlation is present (4 bond). If the ^1H resonance at 6.56ppm which is assigned as H_5' is assigned to H_2' according to Janssen then the cross peak in the long range HETCOR which assigns C_4'-H_5' (2 bond) must be reassigned to C_4'-H_2' (3 bond). Also if the resonance at δ 6.65ppm is reassigned from H_6' to H_5' then the C_1'-H_6' correlation (2 bond) must be replaced by C_1'-H_5' correlation (3 bond). Additional arguments for the H_2' and H_5' assignments are the correlation to H_3' and H_4' methoxy groups respectively in the COSY spectrum (see Figure 18). In the proton spectrum H_6' and H_5' are present as unsymmetrical doublets and H_2' is a singlet which further justifies the above discrepancies with Janssen assignments.

CHAPTER THREE

3.1. THE DITERPENOID ALKALOIDS: DELPHININE AND ACONITINE

3.1.1 Introduction

The genera Aconitum and Delphinium belong to the sub-order *Ranunculaceae.* There is a close parallel in the nuclear and peripheral structure and as well as in the reactions of delphinine and aconitine. **Delphinine** is extracted from the seeds of *Delphinium staphisagria L., Ranunculaceae*[57]. It is a toxic alkaloid with an orthorhombic structure and is practically insoluble in water. It is one of the most complex members of the Aconite-Delphinium-Garrya group. It possesses six rings , a tertiary nitrogen with a N-methyl group, an acetoxy, benzoxy and tertiary hydroxy group and four methoxy groups. Delphinine poisoning leads to respiratory paralysis and there is concomitant cardiac and vasomotor damage. It also produces an irritant action on the skin[58].

Aconitine is the active principle of the aconite root, *Aconitium napellus L.*[59] and is used sometimes as a homeopathic remedy. It also produces an intense tingling sensation on contact with the skin. The root is highly poisonous and is seldom used in medicine today although it may appear in the form of a liniment. The action of aconitine resembles that of delphinine. Administration of large doses via the mouth produces numbness and a burning sensation. This may lead to convulsions, respiratory paralysis and it may have a direct toxic action on the heart[60]. Aconitine contains four methoxy groups and three hydroxy groups.

These diterpenoid alkaloids were chosen to demonstrate the applications of multipulse NMR techniques since their complex structure with many characteristic substituents can assist in demonstrating the applicability of these techniques. Furthermore, their pharmacological action is of interest to medical science and structural elucidation of these molecules may contribute to research in this field.

In this report the ^{1}H (Figure19) and ^{13}C (Figure 20) spectra of delphinine were assigned with the aid of various 2D multipulse NMR sequences and the ^{13}C substituent effect was then considered in the assignment of aconitine. The stereochemistry of the ring A methoxy of delphinine is also discussed.

3.1.2 Assignment of ^{1}H and ^{13}C spectrum of Delphinine

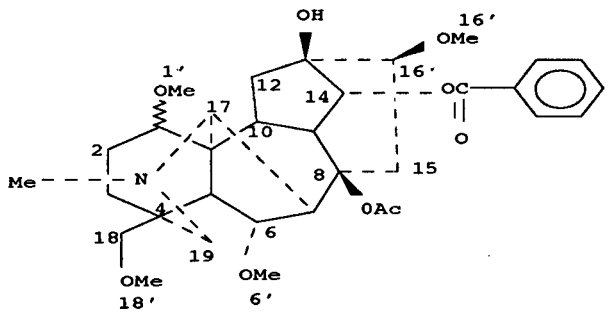

Structure [III] Delphinine

The IUPAC name for delphinine is **1,6,19 trimethoxy-4-(methoxymethyl)-16-methyl aconitane-8,10,11-triol 8 acetate 10 benzoate.**

The compound has 33 carbon atoms. An edited DEPT analysis for protonated carbons confirmed that there are six CH_3 groups and six CH_2 groups as well as fourteen CH groups. Seven quaternary carbon atoms are present. The 2D spectra recorded to assist in the assignment of the ^{1}H and ^{13}C spectra include COSY, HETCOR, long range HETCOR, HMQC and ROESY. (Appendix B)

The proton that is most readily assigned is H_{14} since it is the most deshielded proton due to the influence of the oxygen atom. A doublet is observed at δ 4.9 in the ^{1}H spectrum and this splitting pattern is due to coupling to H_9. This is confirmed by analysis of the COSY spectrum in which H_{14} shows correlation to H_9 at δ 2.89. Another observation in

the COSY spectrum is the correlation between H_9 and a multiplet presumably H_{10} (δ 2.09).

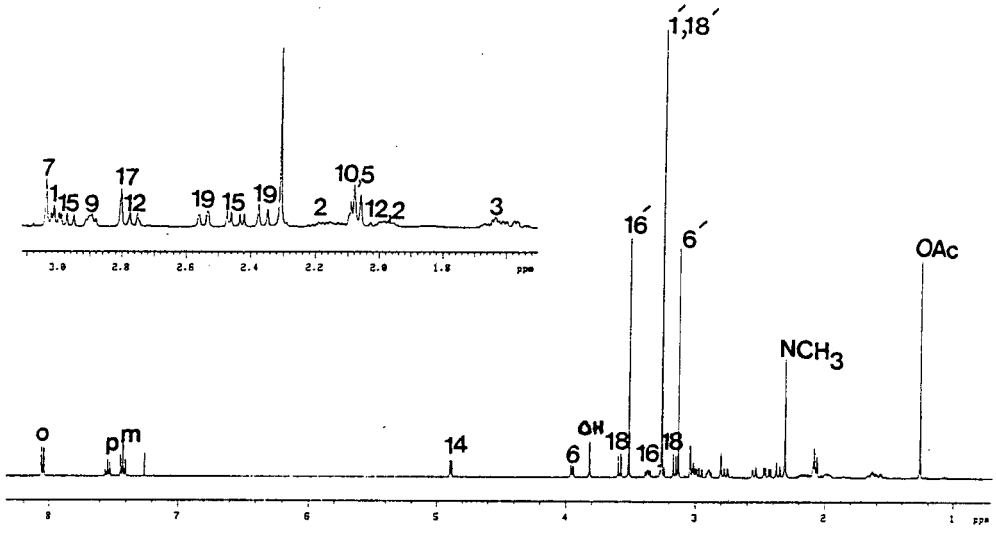

Figure 19 ^{1}H spectrum of delphinine

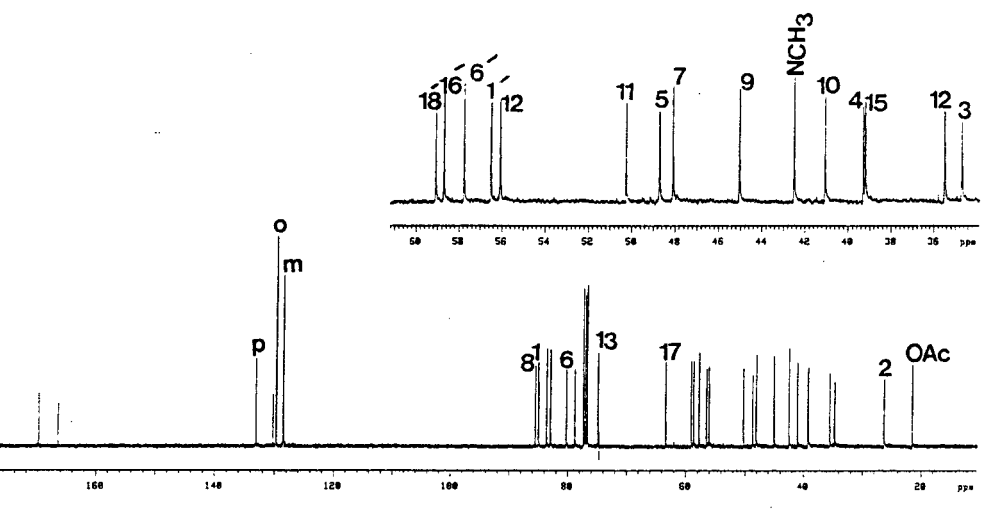

Figure 20 ^{13}C spectrum of delphinine

In the long range HETCOR spectrum the OH group (δ 3.18) correlates with a quaternary carbon signal which is undoubtedly C_{13}. This C_{13} group also shows three bond correlation to H_{10} in this spectrum. In the ROESY spectrum H_{14} correlates through space with the multiplet signal (δ 3.37) which undoubtedly is H_{16}. A H_{14}-H_{10} correlation is also observed in the ROESY spectrum thus indicating the nature of the stereochemistry of H_{10}, H_{14} and H_{16}. H_{16} shows long range coupling to C_{16}' in the long range HETCOR. A C_{16}'-H_{16}' coupling is also observed in this spectrum. Therefore the H_{16}' methyl proton chemical shift is δ 3.51. In the COSY spectrum H_{16} correlates to $H_{15\alpha\beta}$.

The methines of the phenyl group have been assigned considering their splitting patterns and correlation. The meta protons are at ~ δ 7.5(triplet). The ortho protons (multiplet) appear further downfield ~ δ 8.3 and show coupling to the para carbon atom (3 bond) and the para proton (triplet of triplets) shows coupling to the ortho carbons (3 bond). Also evident in the long range HETCOR is the correlation of the quaternary phenyl carbon (130.22ppm) to the meta proton (3 bond).

The H_{18} methylene is the most deshielded relative to the other methylene protons present due to the inductive effect of the methoxy group. The $H_{18\alpha\beta}$ protons are observed as doublets (δ 3.57 and 3.14ppm) and are correlated in the COSY spectrum. These protons also correlate with C_{18} at δ 80.25 in the HMQC spectrum. C_{18} shows long range coupling to H_{18}' methyl protons in the long range HETCOR (δ 3.258). Also observable in this spectrum is the correlation of C_{18}' to H_{18}' and H_{18}.

The correlation of the H_{19} methylene protons (δ 2.55 and 2.37ppm) is evident in the COSY spectrum. They are expected to be deshielded due to the influence of the nitrogen atom. These protons were assigned by analysis of the HMQC spectrum.

The doublet at δ 3.96 is assigned to H_6 since it is deshielded by the oxygen atom of the methoxy group but yet further evidence to confirm this argument is noted in the ROESY spectrum where a dipolar correlation of H_9 to H_6 is observed. In the COSY spectrum a

cross peak between H_6 and a multiplet is observed which presumably is H_5, its nearest neighbour. Apart from this scalar correlation a dipolar correlation is observed in the ROESY spectrum between H_6 and H_5 as well as a H_6 and H_7 correlation. The H_7 assignment is confirmed using the long range HETCOR which reveals a C_9-H_7 correlation. H_7 correlates to a quaternary carbon signal in the long range HETCOR which is assigned to C_8. Analysis of the long range HETCOR reveals a C_1-H_{17} correlation which implies that the ^{13}C resonance of δ 84.98 is that of C_1. The HETCOR spectrum assigns H_1 to the doublet at 2.96. The long range HETCOR assigns the singlet at δ 3.26 as H_1'. The quaternary carbon atom C_{11} shows long range coupling to H_{17} and H_1 in the long range HETCOR spectrum. Thus the quaternary carbon atom at δ 39.31ppm must be that of C_4. The -C(=O)-CH_3 methyl protons were assigned to the singlet at δ 1.27 and the long range HETCOR confirms this by the presence of a C=0 to CH_3 correlation.

The ^{13}C resonance of the N-CH_3 methyl is δ 42.51ppm obtained via HETCOR analysis since it is more shielded than the methoxy groups.

The final assignments were that of the methylene groups C_2 and C_3 carbons. The HETCOR analysis (Figure 21) was not conclusive in the assignment of these resonances but the increased sensitivity of the HMQC experiment was of assistance in their assignments. (Figure 22)

H_2 (δ 2.17 and 1.98 ppm) and H_3 (δ 1.63) correlation is observed in COSY spectrum with H_3 being more shielded. The multiplets at δ 1.88 and at δ 2.76 were assigned to H_{12}. The H_2 and H_{12} assignment is only made possible by the HMQC spectrum (Figure 22) which reveals two cross peaks in the F_1 dimension for each proton. The final set of assignments appear in Table 5 and Table 6.

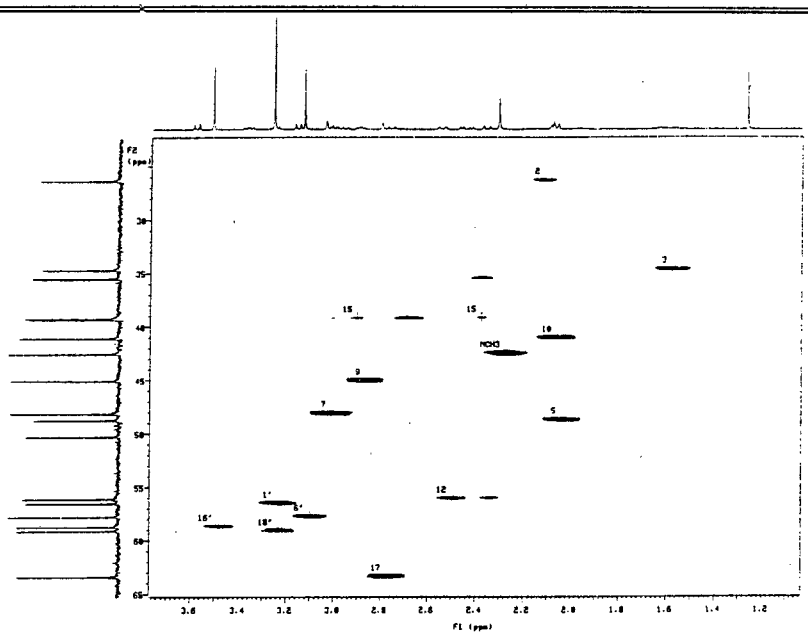

Figure 21 HETCOR spectrum of delphinine

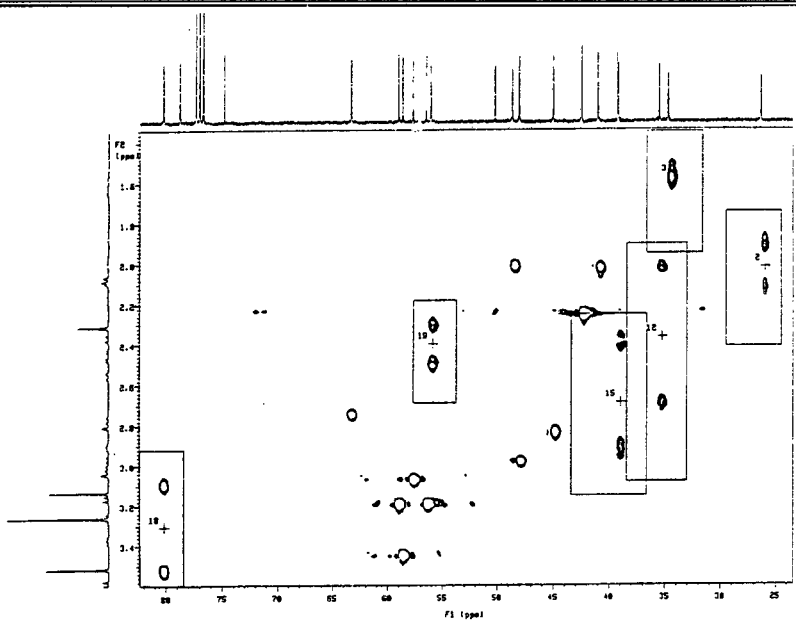

Figure 22 HMQC spectrum of delphinine

3.1.3 The assignment of Aconitine

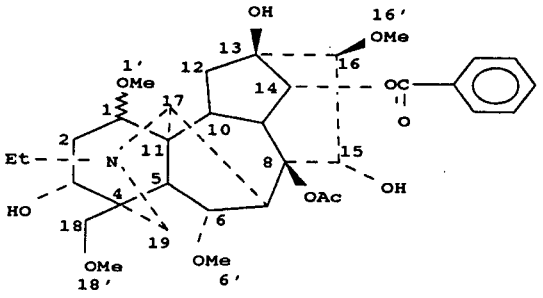

Structure [IV] Aconitine

The assignments of the ^{13}C spectrum of Aconitine (Figure 23) was made possible by considering the ^{13}C substituent effect and the assignments of delphinine. The aconitine molecular structure differs from delphinine by the additional presence of two hydroxy groups at C_3 and C_{15} and the presence of the ethyl substituent on the bridging nitrogen atom. There is also an inversion of stereochemistry of the ring A methoxy[61] where the methoxy group of aconitine is in an axial position.

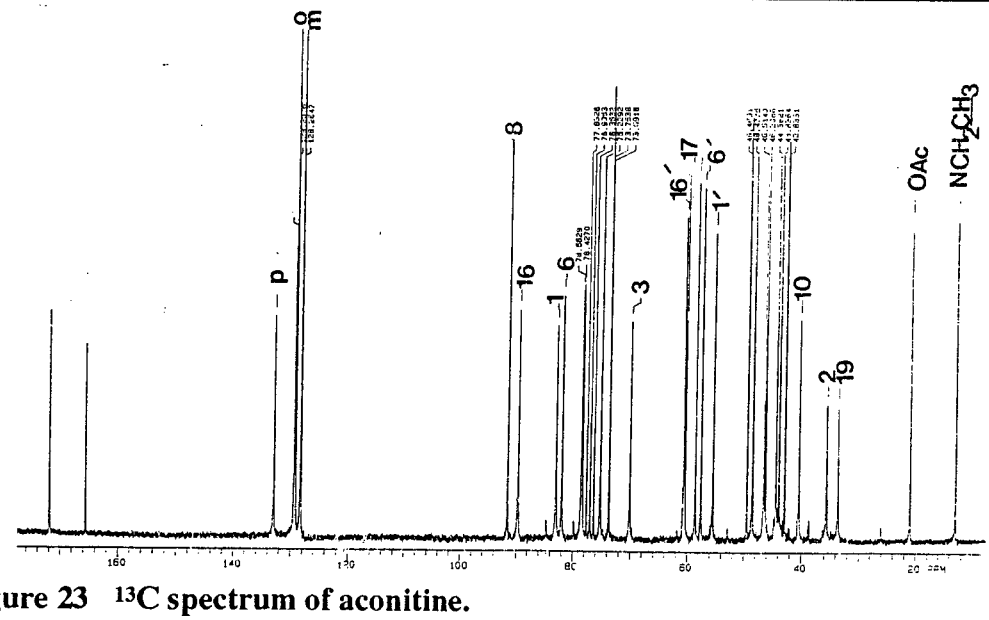

Figure 23 ^{13}C spectrum of aconitine.

The presence of hydroxy substituents on C_3 and C_{15} imply that the resonances of these carbon atoms will be deshielded. The upfield β shift of the C_2 methylene group and C_4 quaternary carbon atom in aconitine relative to delphinine occurs due to the presence of the hydroxy group at C_3.[62] Similar effects are evident for C_8 and C_{16} in aconitine due to the β hydroxy effect. The C_{17} chemical shift appears slightly shielded relative to delphinine possibly due to the ^{13}C substituent influence of the ethyl group attached to the nitrogen atom. The position of the resonances of C_7,C_{12},C_{18} of aconitine also appear slightly shielded relative to that of delphinine. The final set of ^{13}C assignments of aconitine are given in Table7.

3.1.4 Tabulation

Table 5 ^{1}H chemical shifts and assignments of Delphinine

Atom	δ_H	Multiplicity
1	2.96	d
2	2.17,1.98	m,m
5	2.07	m
6	3.96	d
7	3.04	s
9	2.90	m
10	2.09	m
12	2.55,2.36	dd,d
14	4.89	d
15	3.01,2.45	dd,dd
16	3.37	m
17	2.80	s
18	3.58,3.16	d,d
19	2.02,2.76	m,d
1'	3.26	s
6'	3.13	s
16'	3.51	s
18'	3.26	s
N-CH3	2.30	s
$-O(C=O)CH_3$	1.27	s
Phenyl	8.05 (*o*)	m
	7.42 (*m*)	m
	7.54 (*p*)	m

Table 6 ^{13}C **chemical shifts and assignments of delphinine**

Atom	δ_C	δ_C Lit.[62]
1	84.98	84.9
2	26.35	26.3
3	34.69	34.7
4	39.31	39.3
5	48.72	48.8
6	82.93	83.0#
7	48.10	48.2
8	85.51	85.4
9	45.05	45.1
10	41.07	41.0
11	50.26	50.2
12	35.50	35.7
13	74.86	74.8
14	78.80	78.9
15	39.21	39.3
16	83.59	83.7#
17	63.38	63.3
18	80.25	80.2
19	56.09	56.1
N-CH3	42.51	42.3
1'	56.52	56.1
6'	57.77	57.6
16'	58.71	58.6
18'	59.10	58.9
C=O-CH3	169.82	169.4
	21.56	21.4
C=O-C_6H_5	166.36	166.0
	130.22(q)	130.4
	133.06(p)	132.8
	129.69(o)	129.6
	128.50(m)	128.4.8

Interchangeable literature assignments

Table 7 ^{13}C chemical shifts and assignments of Aconitine

Atom	δ_C	δ_C(ppm) Lit.[62*]
1	83.03	83.4
2	35.60	36.0
3	70.09	70.4
4	42.83	43.2
5	46.21	46.6
6	81.95	82.3
7	44.38	44.8
8	91.58	92.0
9	43.84	44.2
10	40.38	40.8
11	49.47	49.8
12	33.57	34.0
13	73.69	74.0
14	78.56	78.9
15	78.43	78.9
16	89.69	90.1
17	60.42	61.0
18	75.23	75.6
19	48.48	48.8
N-***CH***$_2$-CH_3	46.51	46.9
N-CH_2-***CH***$_3$	12.97	13.3
1′	55.47	55.7
6′	57.60	57.9
16′	60.68	60.7
18′	58.60	58.9
-O-***C***-CH_3***(=O)***	171.91	172.2
-O-C-***CH***$_3$(=O)	20.97	21.3
-Ph-***C=O***	165.57	165.9
-***Ph***-C=O	129.21(*o*)	129.8
	128.26(*m*)	128.6
	132.90(*p*)	133.2
	129.43(*q*)	129.6

3.1.5 Comparison with literature assignments

The assignments of delphinine via the 2D methods are in essential agreement with that present in the literature.

Pelletier and Djarmati[62] obtained the ^{13}C NMR spectra of aconitum and delphinium species which included the diterpenoid alkaloids delphinine and aconitine. They based their assignments on the substituent effect which implied the sole use of chemical shift data since the signals of these alkaloids were affected by changes in its steric and electronic environment. The technique SFORD (single frequency off resonance decoupling) was used to distinguish between methyl, methylene and methine groups. The authors chose ^{13}C NMR rather than ^{1}H NMR since they observed that most of the carbon atoms in diterpenoid alkaloids gave rise to separate signals. The authors established the degree of substitution for the individual carbon resonances and assignments were made on the basis of chemical shifts calculated using additivity relationships and confirmed where possible by comparing the effects of specific structural changes. For instance, the oxygen substitution of the quaternary C_8 and C_{13} differentiated those quaternary carbons from C_4 and C_{11}. The absence of the C_{15} oxygen function in delphinine had the expected field shift of the C_8 carbon resonance. Since the C_6 and C_{16} resonances in delphinine were separated by only 0.7ppm the proposed assignments were only tentative. The signal at 39.3ppm of delphinine was assigned to C_{15} since it was characterized as a methylene group and was new compared to spectra of related compounds. The methine resonances were separated into high field and low field resonances with the latter believed to consist of hydroxy and methoxy substituted methine resonances. The β effect was mainly considered in these assignments. The methyl carbons were separated into four different types of carbons viz acyl,O-methyl,N-methyl and N-ethyl. The highly constant chemical shifts despite large structural changes enabled them to easily assign the methyl carbons. The assignments for the aromatic

carbons of the benzoxy group attached at C_{14} were determined by comparison with methyl benzoate.

The authors used selective comparison of many aconitium and delphinium species to effect their arguments. It does seem however that 2D NMR methods provide similar results but through direct correlation.

3.1.6 Some aspects of the stereochemistry of delphinine and aconitine

There has been considerable controversy over the location of the ring A methoxy substituents in delphinine and aconitine. Wiesner, Jay and Jay[61] have reported on the basic uncertainty about the conformation of ring A in alkaloids of the delphinine type. Their conclusion was that the configuration of the ring A methoxy in delphinine and aconitine had to be reversed and the ring A methoxy in delphinine is equatorial and axial in aconitine.

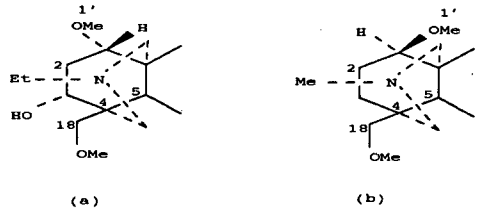

Figure 24 Stereochemical conformation of the ring A methoxyl of Aconitine and Delphinine

Using x-ray structure determination they concluded that ring A in delphinine occurs in a chair conformation and that the methoxy group at C_1 is equatorial. Ring B is also a chair, the five membered ring C occurs in the envelope conformation and ring D is a distorted half chair.

Pelletier *et al*[63] have also reported on the X-ray crystallographic analysis of delphinine and pyrodelphinine. Delphinine is a compound with the same ring system as pyrodelphinine and, except at C_8, has the same pattern of substitution. Rings A, C, E and F have the same conformation in both molecules whilst the conformation of rings B and D is different due to the C_8-C_{15} double bond effect in pyrodelphinine. The D ring of delphinine is in a bent chair conformation with atoms C_8, C_9, C_{13}, C_{15}, C_{16} nearly coplanar and C_{14} forming the flap.

The confirmation of some aspects of the stereochemistry of ring A of delphinine was attempted via 2D dipolar correlation. The interaction of spin magnetic moments of spins through space is an indirect means of determining internuclear distances and molecular motion. The ROESY experiment provides transverse nuclear Overhauser effect and the dynamics of the experiment result in positive noe values for all correlation times. The 2D NOESY experiment for delphinine yielded no constructive noe enhancements probably since the motional correlation times are such that noe values close to zero are obtained.

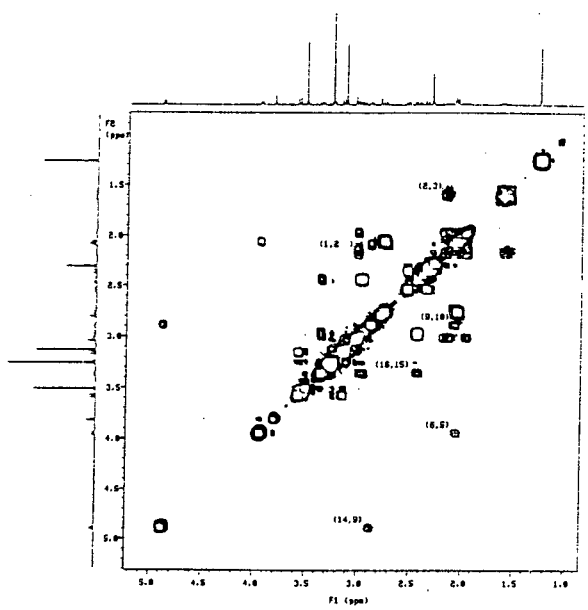

Figure 25 2D ROESY dipolar correlation

The following information is obtained from the ROESY experiment (Figure 25) to assist in stereochemical determination of ring A of delphinine.

H_1 proton correlates through space with H_2 and H_{10}. H_{10} is located on ring B. Since constructive evidence has been presented elsewhere on the stereochemistry of ring B, this provides vital clues in the confirmation of the stereochemistry of ring A.

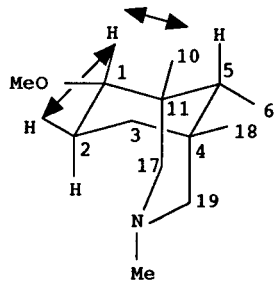

Figure 26 Stereochemical conformation of ring A of delphinine

(Arrows indicate sites of dipolar correlation]

Ring B has a chair conformation (this is confirmed in the ROESY spectrum by the interaction of H_5 and H_6 as well as H_6 and H_9.) which implies that the position of the methoxy group on C_1 atom of ring A must be equatorial and the H_1 atom axial. Since H_2 also interacts with H_{10} then ring A must be in a chair conformation.

CHAPTER FOUR

4.1 THE TRITERPENOID ALKALOIDS OF *Cucurbitaceae.*

4.1.1 INTRODUCTION TO CUCURBITACINS

The cucurbitacins are a group of triterpenoid *bitter principles* that have been isolated from various *cucurbitaceae*. They are a group of highly oxygenated species with an αβ unsaturated keto group. Much interest has been shown in these alkaloids and their derivatives as they compounds have been shown to possess antifertility,[64] cytostatic[65] and toxic[66] properties. Steyn[66] has reported on the toxicity of bitter tasting cucurbitaceous vegetables. It was suggested that the edible cucurbits may have cross fertilized with poisonous species of *cucumis* and its bitter and toxic properties were transferred to the edible cucurbits. Gitter *et al*[65] report on studies of antitumour effects of cucurbitacins. Moderate tumour growth inhibition was observed using three cucurbitacins i.e elatericin A, elatericin B and elaterin. Antifertility tests on the female mouse was reported by Shohat *et al.*[64] Cucurbitacin D which is a naturally occurring tetracyclic triterpine obtained from *Ecballium elaterium* was investigated for antifertility properties and it was concluded that the compound interfered with the endocrine mechanisms of the female reproductive system.

The ^{1}H and ^{13}C spectra of acetylated cucurbitacin derivatives were analyzed using various 2D NMR spectroscopic techniques.

4.1.2 Assignment of Cucurbitacin A 2,6,19 triacetate

The ^{1}H (Figure 27) and ^{13}C (Figure 28) spectra of **Cucurbitacin A 2,6,19 triacetate**[V] was fully assigned using 2D NMR spectroscopy and the ^{1}H and ^{13}C assignments were then compared to that of **Cucurbitacin B 2,16 diacetate**[VI] and **Cucurbitacin C 3,6,19 triacetate** [VII] .

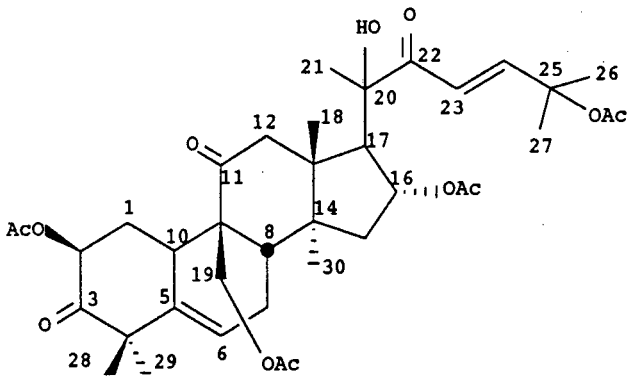

Structure [v] Cucurbitacin A 2,16,19 Triacetate

Cucurbitacin A 2,16,19 triacetate has a total of 38 carbon atoms and the analysis of the DEPT spectrum confirms that 11 protonated carbons correspond to methyl groups, 5 methylene groups and eight methine groups are present. Thus 16 quaternary groups are present.

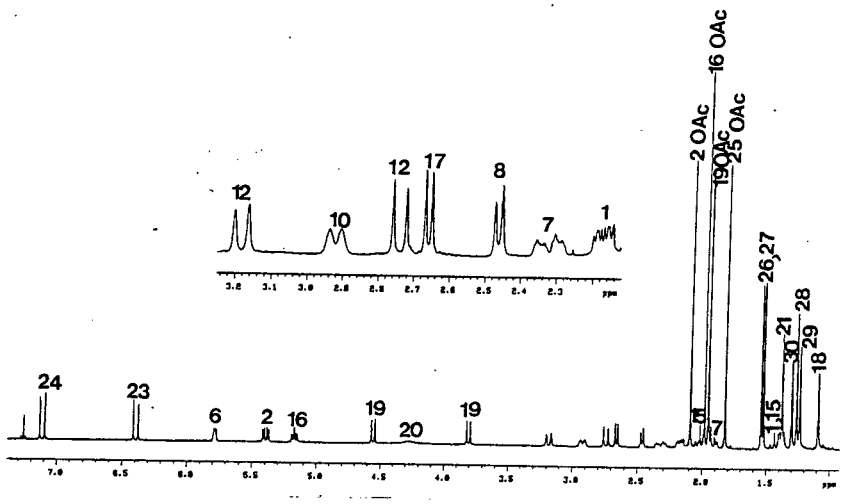

Figure 27 ^{1}H **spectrum of [V]**

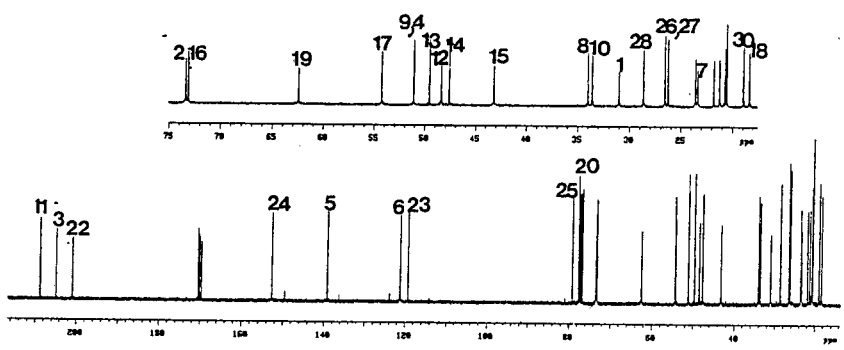

Figure 28 ^{13}C **spectrum of [V]**

The most easily assigned group is the **side chain** double bond of H_{23} and H_{24} since they are the most deshielded and doublets are observed in the ^{1}H spectrum. Homonuclear correlation is observed in the COSY spectrum indicative of the two bond coupling between the ethylenic pair. The long range HMBC shows coupling of both H_{23} and H_{24}

to a quaternary carbonyl at δ 200.89 and thus the position of the C_{22} carbonyl was confirmed. The C_{25} quaternary carbon coupling to the H_{23} and H_{24} ethylenic proton in the long range HMBC is also observed. In the long range HETCOR C_{25} correlation to methyls H_{26} and H_{27} was observed. The C_{22} carbonyl showed long range coupling to the methyl group at δ 1.38 in the long range HETCOR which presumably is three bond coupling to the H_{21} methyl group. In the long range HETCOR the H_{21} methyl group also shows correlation to a quaternary carbon which is assigned to C_{20}. The -OH group is observed in the ^1H spectrum as a broad singlet at δ 4.27.

The assignments of **Ring B and C** are as follows: the most obvious assignment is that of the methine proton of the olefenic group H_6. Therefore, the deshielded multiplet at δ 5.75 is assigned to the olefenic proton H_6. The observed splitting pattern is due to coupling to the $H_{7\alpha\beta}$ methylene protons. The COSY spectrum indicates a correlation between H_6 and one of the H_7 methylene protons. The $H_{7\alpha\beta}$ methylene protons show correlation in the COSY spectrum and correlation of $H_{7\alpha\beta}$ to H_8 methine proton is also observed. The long range HMBC reveals H_8 coupling to a quaternary carbon atom at δ 51.12 which was assigned to C_9. Noticeable in the long range HETCOR was a C_9-H_{10} coupling and a correlation of C_9 to one of the $H_{19\alpha\beta}$ methylene protons. The $H_{19\alpha\beta}$ proton correlation is observed in the COSY spectrum as well as the presence of two cross peaks in the HETCOR spectrum. It is the only methylene group which is linked to an acetoxy group and is therefore deshielded.

The $H_{19\alpha\beta}$ protons show long range coupling to the C_{11} carbonyl carbon in the HMBC spectrum. The C_{11} carbonyl coupling to $H_{12\alpha\beta}$ is observed in the long range HETCOR. The HETCOR spectrum confirms this proposal with the presence of two cross peaks in the F1 dimension for ^{13}C signal δ 48.43ppm.

The **ring A** assignments proceeds with the presence of the methylene group H_1 being confirmed by analysis of the COSY spectrum which indicates scalar coupling between

H_{10} and H_1. The presence of the H_1 methylene group is once again confirmed on analysis of the HETCOR spectrum. In the long range HETCOR, H_1 correlates with a methine group which is undoubtedly C_2. The remaining carbonyl group in the ^{13}C spectrum must be assigned to C_3 i.e at δ 204.86ppm. C_3 correlates with H_{28} and H_{29} methyl groups in the long range HETCOR spectrum. The H_{28} and H_{29} methyls in turn show correlation to C_4 (δ 51.09) and C_5 (d 139.15).

Finally **Ring D** can be assigned as outlined. The multiplet at δ 5.18 is undoubtedly the methine group H_{16} which is slightly deshielded due to the acetoxy group. Its chemical shift is similar to H_2 which is also a methine proton coupled to an acetoxy group but H_2 is more deshielded due to the presence of the C_3 carbonyl. Further correlation of H_{16} to H_{17} and H_{15} is noted in the COSY spectrum. The HETCOR spectrum confirms the presence of $H_{15\alpha\beta}$ protons. H_{17} shows correlation to a methyl group in the long range HMBC . This was assigned to the C_{18} methyl group. In the long range HETCOR the presence of H_{30} methyl groups is confirmed by observable coupling to two quaternary groups i.e C_{13} and C_{14}. C_{14} was assigned to δ 47.63 and C_{13} to the resonance at δ 49.57 by analysis of the HMBC spectrum which revealed a C_{13}-H_{12} and C_{14}-H_{12} correlation. The final sets of assignments are given in Tables 8 and 9.

4.1.3 The assignment of related compounds

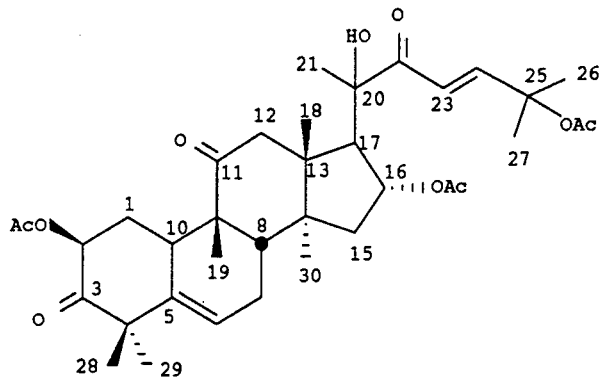

Structure [VI] Cucurbitacin B 2,16 Diacetate

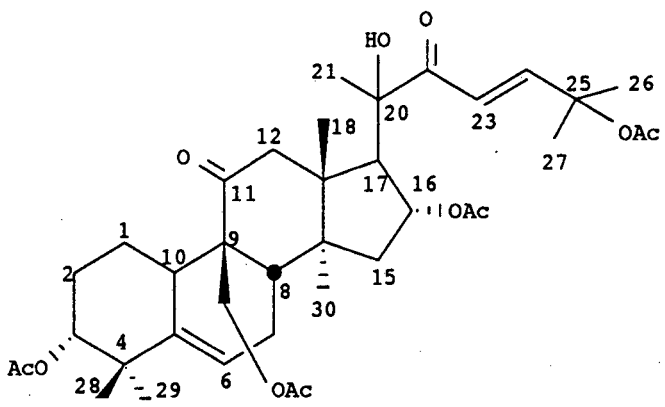

Structure [VII] Cucurbitacin C 3,16,19 Triacetate

a) The assignments of Cucurbitacin B 2,16 diacetate and Cucurbitacin C 2,16,19 triacetate

Two compounds that are related to [V] are Cucurbitacin B 2,16 diacetate [VI] and Cucurbitacin C 2,16,19 triacetate [VII]. The ^{1}H and ^{13}C spectra of these two additional derivatives can be assigned considering the ^{1}H and ^{13}C substituent effect.

[VI] differs from [V] at location C_{19}. The absence of an acetoxyl group at C_{19} of [VI] implies an influence on the chemical shifts of neighbouring atoms of ring B and C. The following trends were observed in the ^{13}C spectrum of [VI]. αC_9 is slightly shielded at δ 49.89 as can be expected. The C_{19} methyl group has a deshielding influence on the β atoms C_8,C_{10} and C_{11} and a similar effect is observed for the γ atoms C_1,C_5,C_7.

The following trends were noted in the ^1H spectrum for [VI]:

Noticeable is the influence of H_{19} on the multiplicity and shifts of γ protons H_8 and H_{10}. H_{10} of [V] appears at δ 2.93 (doublet) and H_8 at δ 2.47 as a doublet. For [VI] H_8 is a singlet which is deshielded at δ 2.55. H_{10} of [VI] produces a doublet at δ 2.70 i.e slightly shielded relative to H_{10} of [V]. The Δ protons of H_{19} are also influenced by the absence of the methoxy group in [VI] where H_1 is shielded relative to that of [V] whilst H_{12} and H_7 are deshielded.

[VII] differs from [V] at position 2 and 3 on ring A. The following trends are noted in the ^{13}C spectrum of [VII]. The absence of the methoxy group at position 2 of [VII] produces a shielding effect on the chemical shift of C_1 i.e at δ 23.95. The quaternary carbon atom C_4 (δ 47.6) is shielded due to the presence of the acetoxy substituent at C_3 as compared to the presence of the carbonyl substituent at C_3 of [V]. The position of C_5 quaternary carbon atom however appears at slightly lower field. An interesting observation is the deshielding influence of the C_3 acetoxy on the C_{28}, C_{29} methyl groups. The position of C_{29} is only slightly influenced whilst C_{28} is reasonably shielded at δ 24.35. This reveals the nature of the stereochemistry around C_4 and that C_{28} must be in the same plane as the acetoxy group.

The following trends were noted in the ^1H spectrum of [VII].

The Δ proton, H_{10}, is shielded at 2.27ppm and the γ H_1 protons exhibit a similar influence compared to [V] as a result of the absence of the C_2 acetoxy on [VII]. The H_{28} and H_{29} methyl groups are shielded in the ^1H spectrum relative to that of [V].

b) **Assignment of the acetoxy groups for the Cucurbitacin derivatives**

The acetoxy groups could be assigned by deduction and selective comparison taking into consideration the results of Velde and Lavie.[68] All three compounds have in common the acetoxy group of the side chain i.e C_{25}-OAc. Velde and Lavie have assigned Cucurbitacin D 2,16 diacetate which is similar to [VI] except for the absence of the C_{25}-OAc group. The authors assign C_{16} and C_2 acetoxy methyl groups at δ 20.7ppm and the carbonyl of both acetoxy groups to the resonance at δ 170.1 ppm in the ^{13}C spectrum. Considering these results the acetoxy groups at positions C_2 and C_{16} of [VI] was assigned and thus it was deduced that the C_{25} acetoxy methyl shift must be at δ 21.84 ppm and the carbonyl group must be that at δ 169.59 (See Table 11). The C_{19} acetoxy group common to both [V] and [VII] was assigned by comparison of the ^{13}C results which appear in Table 9 and Table 13. ^1H data for the acetoxy groups of [V], [VI], [VII] was assigned similarly.

4.1.4 Tabulation of results

Table 8 ^1H CHEMICAL SHIFTS AND ASSIGNMENTS OF CUCURBITACIN A 2,16,19 TRIACETATE

ASSIGNMENT	δ(ppm)	MULTIPLICITY
H_1	1.46,2.16	s,m
H_2	5.40	dd
H_6	5.76	m
H_7	1.90,2.31	m,m
H_8	2.47	d
H_{10}	2.93	d
H_{12}	2.75,3.20	d,d
H_{15}	1.45,2.02	s,m
H_{16}	5.17	m
H_{17}	2.66	d
H_{18}	1.09	s
H_{19}	3.82,4.56	d,d
H_{21}	1.38	s
H_{23}	7.13	d
H_{24}	6.41	d
H_{26}	1.53	s
H_{27}	1.54	s
H_{28}	1.23	s
H_{29}	1.26	s
H_{30}	1.30	s
2-OAc	2.09	s
16-OAc	1.95	s
19-OAc	1.98	s
25-OAc	1.83	s

Table 9 ^{13}C CHEMICAL SHIFTS AND ASSIGNMENTS OF CUCURBITACIN A 2,16 TRIACETATE

ATOM	δ(PPM)	LIT [67] δ(PPM)
C_1	31.03	31.2
C_2	73.42	73.5
C_3	204.86	204.4
C_4	51.09	51.2
C_5	139.15	139.9
C_6	121.22	121.5
C_7	23.38	23.8
C_8	34.04	34.7
C_9	51.12	51.6
C_{10}	33.62	34.3
C_{11}	208.77	208.4
C_{12}	48.43	48.8
C_{13}	49.57	49.9
C_{14}	47.63	47.9
C_{15}	43.23	43.7
C_{16}	73.18	73.7
C_{17}	54.30	54.9
C_{18}	18.36	18.5
C_{19}	62.45	62.9
C_{20}	77.67	78.1
C_{21}	23.61	24.1
C_{22}	200.89	201.2
C_{23}	119.24	120.1
C_{24}	152.64	152.3
C_{25}	79.13	79.4
C_{26}	26.61	26.8
C_{27}	26.29	26.6
C_{28}	28.64	21.7
C_{29}	21.28	19.2
C_{30}	18.95	29.0

C_2-OC=O-**Me**	20.59
C_{16}-OC=O-**Me**	20.76
C_{19}-OC=O-**Me**	20.28
C_{25}-OC=O-**Me**	21.82
C_2-O**C=O**-Me	170.02
C_{16}-O**C=O**-Me	170.29
C_{19}-O**C=O**-Me	170.44
C_{25}-O**C=O**-Me	169.61

Table 10 ^1H CHEMICAL SHIFTS AND ASSIGNMENTS OF CUCURBITACIN B 2,16 DIACETATE

ASSIGNMENT	δ(ppm)	MULTIPLICITY
H_1	2.04,1.47	m,m
H_2	5.43	dd
H_6	5.72	m
H_7	1.33,1.87	m,m
H_8	2.35	s
H_{10}	2.70	m
H_{12}	2.3	m
H_{15}	2.6,3.2	m,d
H_{16}	5.15	t
H_{17}	1.94	m
H_{18}	0.99	s
H_{19}	1.06	s
H_{20}	4.27	s
H_{21}	1.38	s
H_{23}	6.4	d
H_{24}	7.1	d
H_{26}	1.53	s
H_{27}	1.55	s
H_{28}	1.28	s
H_{29}	1.27	s
H_{30}	1.25	s
2-OAc	2.10	s
16-OAc	1.99	s
19-OAc	1.99	s
25-OAc	1.83	s

TABLE 11 ^{13}C CHEMICAL SHIFTS AND ASSIGNMENTS OF CUCURBITACIN B 2,16 DIACETATE

ATOM	δ (PPM)	LIT [67] δ (PPM)
C_1	31.93	32.1
C_2	73.30	73.6
C_3	205.69	205.1
C_4	51.20	51.3
C_5	139.69	140.4
C_6	120.42	120.6
C_7	23.72	24.0
C_8	42.06	42.6
C_9	49.89	48.8
C_{10}	34.21	34.9
C_{11}	211.90	212.5
C_{12}	48.43	48.9
C_{13}	48.38	50.2
C_{14}	47.95	48.2
C_{15}	43.05	43.5
C_{16}	73.54	73.5
C_{17}	54.10	54.7
C_{18}	19.72	18.7
C_{19}	19.91	20.0
C_{20}	77.67	78.1
C_{21}	23.61	24.0
C_{22}	200.89	201.1
C_{23}	119.26	120.1
C_{24}	152.57	152.2
C_{25}	79.13	79.4
C_{26}	26.59	26.8
C_{27}	26.33	26.6
C_{28}	28.75	28.9
C_{29}	21.27	21.4
C_{30}	18.68	19.7

C_2-OC=O-**Me**	20.63
C_{16}-OC=O-**Me**	20.60
C_{25}-OC=O-**Me**	21.84
C_2-O**C=O**-Me	170.32
C_{16}-OC=O-Me	170.07
C_{25}-OC=O-Me	169.59

Table 12 ^1H CHEMICAL SHIFTS AND ASSIGNMENTS OF CUCURBITACIN C 3,16,19 DIACETATE

ASSIGNMENT	δ(ppm)	MULTIPLICITY
H_1	1.00,1.74	s,m
H_2	1.33,1.78	m,m
H_3	4.41	dd
H_6	5.72	d
H_7	1,94,2.28	s,m
H_8	2.38	d
H_{10}	2.27	m
H_{12}	2.68,3.14	d,d
H_{15}	1.44,1.90	m,s
H_{16}	5.14	t
H_{17}	2.65	d
H_{18}	1.22	s
H_{19}	3.86,4.60	d,d
H_{20}	4.3	s
H_{21}	1.36	s
H_{23}	6.4	d
H_{24}	7.1	d
H_{26}	1.54	s
H_{27}	1.53	s
H_{28}	0.973	s
H_{29}	1.01	s
H_{30}	1.06	s
3-OAc	2.00	s
16-OAc	1.9	s
19-OAc	1.98	s
25-OAc	1.82	s

TABLE 13 ^{13}C CHEMICAL SHIFTS AND ASSIGNMENTS OF CUCURBITACIN C 3,16,19 TRIACETATE

ATOM	δ (PPM)	LIT [67] δ (PPM)
C_1	23.95	24,5
C_2	27.14	27.4
C_3	77.72	78.0
C_4	47.60	41.3
C_5	140.48	140.5
C_6	119.82	120.0
C_7	23.29	23.6
C_8	34.00	34.4
C_9	51.30	51.6
C_{10}	34.96	35.4
C_{11}	209.37	209.2
C_{12}	48.38	48.7
C_{13}	49.67	49.9
C_{14}	40.99	47.3
C_{15}	43.25	43.6
C_{16}	73.57	73.8
C_{17}	54.25	54.7
C_{18}	19.18	18.3
C_{19}	62.89	63.2
C_{20}	77.72	78.0
C_{21}	23.59	24.0
C_{22}	200.96	201.2
C_{23}	119.30	120.0
C_{24}	152.52	152.2
C_{25}	79.12	79.3
C_{26}	26.59	26.7
C_{27}	26.34	26.5
C_{28}	24.35	20.6
C_{29}	21.45	24.5
C_{30}	18.23	19.3

C_2-OC=O-**Me**	20.61
C_{16}-OC=O-**Me**	20.81
C_{19}-OC=O-**Me**	21.8
C_{25}-OC=O-**Me**	21.8
C_2-O**C=O**-Me	170.29
C_{16}-O**C=O**-Me	170.41
C_{19}-O**C=O**-Me	170.57
C_{25}-O**C=O**-Me	169.58

4.1.5 Comparison with literature assignments

Bull et al[67] have reported on the ^{13}C NMR of Cucurbitacin A,B,C and E , their peracetylated derivatives and degradation products. The authors used SFORD multiplicities to assign these compounds. The use of structural modifications enabled the correlation of shift responses and the use of general shielding rules was an aid in their assignments. Their report reflects the assignment procedures applied prior to the advent of 2D NMR spectroscopy. The results obtained via 2D NMR spectroscopy are generally in good agreement with that proposed by Bull et al. The use of 2D NMR spectroscopy however is superior in certain respects since assignments were possible without the need for comparison with related products.

Bull *et al* note that the assignment of C_8 and C_{10} was not trivial since only one of the resonances was shifted to a significant extent when an oxygen function was introduced at C_{19}. This was also evident in the comparison of [V] and [VI]. The C_{20} signal was assigned by noting a "small but consistent shift" in response to the acetylation of C_{16}. Some difficulties were experienced in the assignment of C_{13} and C_{14} compared to the use of long range correlation (HMBC and HETCOR) which easily solved this problem. The geminal pair C_{26} and C_{27} were assigned by comparison of shifts with that of their degraded products. The acetoxy signals were not resolved since resolution and differentiation of methyl groups in the SFORD spectra did not make this possible.

Velde and Lavie[68] have assigned the ^{1}H and ^{13}C spectra of nine representative cucurbitacins using deduction and selective comparison of these compounds. The authors used SFORD to assign these spectra. The compounds [V], [VI] and [VII] differ from those reported by Velde and Lavie but many similarities in the structures of these related compounds allow for a comparison of the assignments. The authors were able to

assign their derivatives by choosing different compounds with characteristic differences at specific sites. The assignments for C_{26}, C_{27} were reported to be interchangeable. The three methine carbons C_8, C_{10}, C_{17} were noted to be under the influence of the γ effect and this enabled the assignments of the methyl groups C_{18}, C_{28} and C_{30}. They also noted that C_7 was a characteristic attribute of the cucurbitane skeleton since its position was usually under the influence of the C_{19} methyl and this was evident in [2]. The geminal pair C_{28} and C_{29} will each have a different resonance due to the π orbitals of the C_3-CO and the Δ^5 functions and thus the authors noted that they were easy to differentiate. C_{18} and C_{30} were independent of any modification of ring A or the side chain.

4.1.6 Discussion of the stereochemistry of Cucurbitacin A 2,16,19 triacetate.

The Cucurbitacin derivatives possess a cucurbitane skeleton characterized by a 19(10→9β) *abeo*-10α-lanostane which implies that they are steroidal molecules with the angular methyl group C_{19} located on C_{10} rather than C_9 and in the α position with the nature of the side chain at position 17 determining the base name of the compound. It is a 5α series derivative which implies that ring A is trans. The angular methyl group C_{18} also assists in stereochemical designation. The groups that lie on the same general side of the molecule as the angular methyl groups are designated as β substituents.
In order to confirm some of the stereochemical characteristics of [V] a ROESY analysis was performed. The highly flexible side chain reveals interesting dipolar correlations especially of H_{23} which correlates with the H_{27} methyl group, the H_{17} methine proton and the H_{21} methyl group. The H_{21} methyl also correlates with H_{12}, H_{17} and H_{21} and a more interesting correlation is that of the C_{25} acetoxy with the H_{21} methyl group indicating the extent of flexibility of the side chain. Velde *et al*[68] noted that the side chain flexibility extends in such a manner that the C_{25} group may come in contact with the C_{11} ketone.

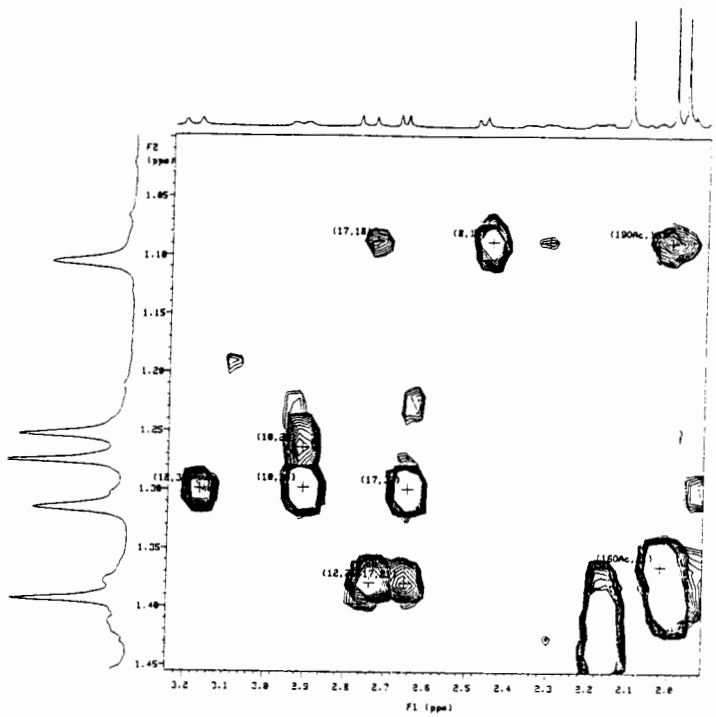

Figure 29 ROESY spectrum of Cucurbitacin A 2,16,19 triacetate

Confirmation of the stereochemistry about the H_{10} and H_{19} protons was achieved as follows: The dipolar correlation H_{10} to H_{29} and H_{10} to H_{30} confirms that the stereochemistry of H_{10} is α. The β position of the 19-OAc group is confirmed by correlation with H_{18}, the angular methyl group. Other interesting ring A ring B correlations important for the confirmation of stereochemistry about the H_{28}, H_{29} methyl groups include the $H_{2\alpha}$ correlation to H_{29} and H_6 to H_{28}. For ring B H_6 to $H_{7\alpha\beta}$ correlation is noted. Interesting correlations of ring C and D worth mentioning include that of $H_{12\alpha}$ to H_{30} and H_{17}. The correlation of H_8 to H_{18} reveals that H_8 must be in the β position. H_{17} correlation with H_{30} indicating that the conformation of H_{17} should be α. Considering the above stereochemical assignments the conclusion is that the side chain is flexible, ring A is in a chair conformation, ring B is in a half chair conformation whilst ring C is chair and ring D is in an envelope conformation.

CHAPTER FIVE

5.1 EXPERIMENTAL

5.1.1 Data Acquisition

The compounds codeine, papaverine, delphinine and aconitine were kindly donated by E. Merck (SA) to Mr Campbell of the Department of Chemistry. The cucurbitacin derivatives were prepared by Professor Bull and his research team at the CSIR.

All NMR experiments were performed in $CDCl_3$ solution using a 5mm inverse detection probe on a Varian Unity400 MHz NMR spectrometer. The ^{13}C spectrum of aconitine was recorded on the Varian VXR 200 MHz spectrometer using a 5mm switchable probe All spectra were recorded at 25°C and referenced with respect to $CDCl_3$ i.e 7.25ppm in the ^{1}H spectrum and 77.0ppm in the ^{13}C spectrum.

5.1.2 Data Processing

The following **weighting functions** were applied to absolute value and phase sensitive 2D spectra before fourier transformation whenever necessary.

i) **Sinebell constant (sb)**

The value of ***sb*** applied is given in seconds were a positive value implies a sinebell of the form $sin(t*\pi/(2*sb))$ whilst a negative value implies a squared sinebell function of the form $sin^2(t*\pi/(2*sb))$

ii) **Sinebell shift constant (sbs)**

The value of sbs applied is given in seconds where a positive value implies shifting of the origin of the sinebell function of the form $sin((t-sbs)*\pi/(2*sb))$ and the square of this function is applied if sb is negative viz $sin^2((t-sbs)*\pi/(2*sb))$.

iii) **Gaussian Time Constant (gf)**

Defined in seconds and applied for a Lorenztian to Gaussian type transformation and its value defines a Gaussian function of the form $exp(-(t/gf)^2)$.

iv) **Gaussian Shift Time Constant (gfs)**

The values applied shifts the centre of the Gaussian function $exp(-((t-gfs)/gf)^2)$. Gaussian apodisation with *gfs* set to unused leads to Gaussian lineshapes.

v) **Line Broadening (lb)**

The application of this weighting function results in exponential weighting where a positive value gives a line broadening and a negative value gives a resolution enhancement. *lb* greater than zero produces gaussian lineshapes.

In each 2D Fourier transformation the number of data points transformed i.e. fn is the first power of two (i.e 16K,32K etc) greater or equal to the number of points used to acquire the data (np). If fn was greater than np then this resulted in the remaining points in the transformation process being filled with values of zero i.e *zero filling.*

The processing and transformation of phase sensitive 2D data sets was accomplished as follows. Usually the Fourier transformation of F2 was preceded by correction of the first point of the fid using a first point multiplier in order to eliminate t_2 ridges. Also the F2 dimension was weighted by equating the value of sb and sbs to the aquisition time (at). After transformation of F2 , F1 was weighted using the appropriate weighting functions. Finally a full transformation of both the real and imaginary parts of F1 and F2 with baseline correction in F2 was applied to yield a 2D contour plot.
Phasing of the diagonal peaks (absorption mode) relative to the cross peaks in homonuclear phase sensitive spectra was essential to achieve optimum sensitivity.

CONCLUSION

The structural chemistry of natural products has presented an effective means for the demonstration of the versatility of modern multipulse NMR techniques. The rapidly developing field of multipulse NMR has offered the natural product chemist an array of choices of multipulse NMR techniques for structural elucidation depending on the special attributes of the compound being investigated. Prior to the advent of the modern 2D NMR techniques, natural product chemists had to be content with the use of one dimensional NMR spectroscopy which merely presented chemical shift data and coupling constant values. The natural product chemist was thus highly dependent on prior research publications and the selective use of multiple compounds in order to comparatively assign the various derivatives.

With the advent of two dimensional NMR spectroscopy the scope for complete unambiguous structural assignment has considerably extended knowledge of previously "unknown" compounds. In keeping with the demand for faster and less time consuming acquisition as well as the quest for the deriving adequate information from a single pulse sequence NMR spectroscopists have developed a vast array of multipulse techniques. The process of assigning the ^{1}H and ^{13}C spectrum of natural products demonstrates the necessity of the application certain multipulse techniques over others. It was therefore imperative to compare the techniques based on the information they provided, their application to the specified compounds and the complexity of the spectral acquisition.

In the structural assignment of the opium alkaloids the use of the COSY experiment for homonuclear scalar correlation was adequate and the application of the HMQC experiment offered a heteronuclear direct correlation with the need for only a limited amount of sample and reduced spectrometer time. However, most interesting was the long range heteronuclear correlation from which the HMBC experiment offered

conclusive evidence for the assignment of the quaternary groups but weaker cross peaks for other two to three bond correlations. The reverse was noticeable in the long range HETCOR experiment.

In the structural assignment of the diterpenoid alkaloid, delphinine the COSY experiment was again adequate for homonuclear scalar correlation. The necessity for use of the HMQC experiment for complete analysis of the methylene groups as compared to the use of the short range HETCOR experiment demonstrated that the HMQC pulse sequence is superior for limited sample quantity as well as offering spectra of greater sensitivity. The application of the ROESY experiment as opposed to the NOESY experiment to confirm some aspects of stereochemistry of the molecule revealed that a choice of techniques exists for dipolar correlation of the molecule depending on the motional correlation time in solution. Furthermore the application of these multipulse techniques was of tremendous assistance in assigning the ^{13}C spectrum of aconitine.

In the structural assignment of the cucurbitacin derivatives technical difficulties with the inverse detection probe at that stage prevented the application of the HMQC experiment and thus the use of the conventional short range HETCOR spectrum was necessary. However, it was possible to apply the HMBC experiment to the analysis to effect a comparison with the long range HETCOR experiment. The results reveal that certain correlations which are observable in the long range HETCOR may not be present in the HMBC experiment and vice versa. For instance, both $H_{19\alpha\beta}$ protons show correlation to the C_{11} group in the HMBC experiment whilst only a single correlation is observed in the long range HETCOR. For the $H_{12\alpha\beta}$ protons both correlations are observed in the long range HETCOR but this is not the case in the HMBC experiment.
The ROESY experiment demonstrated a significant number of dipolar correlations and allowed for confirmation of the stereochemical position of $H_{10\alpha}$ and thus provided some

indication of the conformation of ring A, B, C, D as well as demonstrating the flexibility of side chain.

Evidence of extensive dipolar correlation in the ROESY experiment proves that this technique is highly applicable for compounds of this nature.

The results thus demonstrate that the COSY experiment is usually adequate for scalar correlation whilst for heteronuclear correlation a choice exists for application of the short range HETCOR or HMQC experiment depending on sample quantity, spectrometer time available and the sensitivity required. The complexity of the structures of some natural products make the use of the long range heteronuclear experiments imperative for the structural assignment of quaternary groups. Most interesting was the application of the long range HMBC and HETCOR techniques. It seems that the application of both or either techniques is highly dependent on the sample quantity and structural conformation. Also the HMBC experiment may be a more sensitive alternative to the long range HETCOR experiment if there is a highly limited sample volume. However, the application of the inverse experiments calls for a highly stable environment and the use of the HMBC spectrum does not allow for the application of the BIRD pulse sequence for cancellation of protons attached to ^{12}C since this hampers suppression of protons that do not have long range couplings to ^{13}C. Also in the HMBC experiment there is no refocussing at the end of the pulse sequence so a coupled spectrum is obtained.

The ROESY experiment seems to be the favoured alternative for dipolar correlation of the medium sized molecule as these molecules motional correlation times are such that nOe enhancements close to zero may be observed only in this experiment as compared to the NOESY experiment.

REFERENCES

1. Bell, J.D.; Sadler, P.J., ***Chemistry in Britain***, 1993, 29, 597.
2. Feeney, J., ***Chemistry in Britain***, 1993, 29, 605.
3. Allerhand, A.; Maple, S.R., ***Analytical Chemistry***, 1987, 59, 441A
4. Derome, A.E., ***Modern NMR Techniques for Chemistry Research***, Pergamon Press, 1987.
5. Benn, R.; Gunther, H., ***Angew. Chem. Int. Engl,*** 1983, 22, 350.
6. Mullen, K.; Pregosin, P.S., ***Fourier Transform NMR techniques: A practical Approach***, Academic Press (London), 1976, Chapter 1.
7. Bax, A., ***Two Dimensional Nuclear Magnetic Resonance in Liquids***, 1984.
8. Schraml, J.; Bellama, J.M., ***Two Dimensional NMR Spectroscopy***, Wiley, 1988.
9. Kessler, H.; Gehrke, M.; Griesinger, C., ***Angew. Chem. Int. Ed. Engl.***, 1988, 27, 490
10. Schraml, J.; Bellama, J.M., ***Two Dimensional NMR Spectroscopy***, Wiley, 1988, 189
11 States, D.J.; Haberkorn, R.A.; Ruben, D.J., ***J. Magn. Reson,*** 1982, 48, 286.
12. Keeler, J.; Neuhaus, D., ***J. Magn. Reson***, 1985, 454.
13. Aue, W.P.; Bartholdi, E.; Ernst, R.R., ***J. Chem. Phys***, 1976, 64, 2229.
14. Bax, A; Freeman, R., ***J. Magn. Reson.***, 1981, 44, 542.
15. Bax, A., ***Two Dimensional Nuclear Magnetic Resonance in Liquids***, 1984, 69
16. Schraml, J.; Bellama, J.M., ***Two Dimensional NMR Spectroscopy***, Wiley, 1988, 97

17. Derome, A.E., ***Modern NMR Techniques for Chemistry Research***, Pergamon Press, 1987, 227

18. Derome, A.E., *ibid*, 232

19. Derome, A.E., *ibid*, 230

20. Bax, A.; Davis, D.G., ***J. Magn. Reson.***, 1985, 65, 355.

21. Bircher, H.; Muller, C.; Bigler, P., ***Magn. Reson. Chem.***, 1991, 29, 726.

22. Muller, L., ***J. Am. Chem. Soc.***, 1979, 101, 4481.

23. Bruwiller, D.; Wagner,G., ***J. Magn. Reson.***, 1986, 69, 546.

24. Bax, A.; Subramanian, S., ***J. Magn. Reson.***, 1986, 67, 565.

25. Lerner, L.; Bax, A., ***J. Magn. Reson.***, 1986, 69, 375.

26. Summers, M.F.; Marzilli, L.G.; Bax, A., ***J. Am. Chem. Soc.***, 1986, 108, 4285.

27. Bax, A.; Summers, M.F., ***J. Am. Chem. Soc.***,1986, 108, 2093.

28. Kaiser, R., ***J. Chem. Phys.***, 1965, 42, 1838.

29. Campbell, I.D.;Freeman, R., ***J. Magn. Reson.***, 1973, 11, 143.

30. Kessler H; Bermel, W; Friedrich A.; Krack, G.; Hull, W.E., ***J. Am. Chem. Soc.***, 1982, 104, 6297.

31. Kumar A.; Wagner, G.; Ernst R.R.; Wuthrich K., ***J. Am. Chem. Soc.***, 1981, 103, 3654.

32. Jeener, J.; Meir, B.H.; Bachmann, P.; Ernst, R.R., ***J. Chem. Phys***, 1979, 71, 4546.

33. Meier, B.H.; Ernst, R.R., ***J. Am. Chem. Soc*** , 1979, 101, 6441

34. Balaram, P.; Bothner-By, A.A.; Dadok, J., ***J. Am. Chem. Soc.***, 1972, 94, 4015.

35. Richarz, R.; Wuthrich, K., ***J. Magn. Reson.***, 1978, 30, 147.

36. Bystov, V.F.; Arseniev, A.S.; Gavrilov, Y.D., ***J. Magn. Reson,*** 1978, 30, 151.

37. Dobson, C. M; Olejniczak, E.T.; Poulsen, F.M.; Ratcliffe, R.G., ***J. Magn. Reson.***, 1982, 48, 97

38. Bax, A.; Davis, D.G., ***J. Magn. Reson.***, 1985, 63, 207.

39. Neuhaus, D; Keeler, J., ***J. Magn Reson.***, 1986, 68, 568.

40. Cavanagh, J.; Keller, J., ***J. Magn. Reson.***, 1988, 80, 186.

41. ***Blacks Medical Dictionary*** , A and C London, 37edn , 425.

42. Henry, T.A., ***The Plant Alkaloids***, Churchill, 1949, 196.

43. Henry, T.A., *ibid*, 265

44. Malek-Ahmadi, P.; Ramsey, M., ***Neurobehavioral Toxicology and Teratology*** 1985, 7, 193. Abstracted in ***American Journal of Nursing***, 1986, 86, 62.

45. ***Blacks Medical Dictionary*** , A and C London, 37edn, 126.

46. Stermitz, F.R.; Rapoport, H., ***Nature.***, 1961, 189, 310.

47. Stermitz, F.R.; Rapoport, ***J. Am. Chem. Soc.***, 1961, 83, 4045.

48. Battersby, A,R; Harper, J.T., ***J. Chem. Soc.***, 1962, 3526.

49. Batterham, T.J; Bell, K.H.; Weiss, U., ***Aust. J. Chem.***, 1965, 18, 1799.

50. Wehrli, F.W., ***J. C. S. Chem. Comm.***, 1973, 379.

51. Terrui, Y.; Tori, K.; Maeda, S.; Sawa, Y.K., ***Tett. Lett.***, 1975, 33, 2853.

52. Chazin, W.J.; Colebrook, L.D., ***J. Org. Chem.***, 1986, 51, 1243.

53. Carroll, F.I.; Moreland, C.G.; Brine, G.A.; Kepler,J.A., ***J. Org. Chem.***, 1976, 41, 6.

54. Marsoili, A.J.; Ruveda, E.A.; Reis, F.de A.M., ***Phytochemistry***, 1978, 17,1655.

55. Rae, I.D.; Simmonds, P.M., ***Aust. J. Chem.***, 1987, 40, 915.

56. Janssen, R.H.A.M.; Lousberg, R.J.J.Ch.; Wijkens, P.; Kruk, C.; Theuns, H.G., ***Phytochemistry***, 1989, 28, 2833.

57. Henry, T.A., ***The Plant Alkaloids***, Churchill, 1949, 697.

58. Henry, T.A., ***ibid***, 700.

59. Henry, T.A., ***ibid***, 674.

60. Henry, T.A., ***ibid***, 690.

61. Birnbaum, K.B.; Wiesner, K.; Jay, E.W.K.; Jay, L. ***Tetrahedron Lett.***, 1971, 13, 867.

62. Pelletier, S.W.; Djarmati, Z., ***J. Am. Chem. Soc.***, 1976, 98, 2626.

63. Pelletier, W.S.; Finer-Moore, J.; Desai, R.C.; Mody, N.V.; Desai, H.K., ***J. Org. Chem.***, 1982, 47, 5290.

64 Steyn, D.G., ***S. A. Medical Journal***, 1950, 24, 713.

65. Gitter, S.; Gallily, R.; Shohat, B.; Lavie, D., ***Cancer Research***, 1961, 21, 516.

66. Shohat, B.; Beemer, A.M.; Gitter, S.; Lavie, D., ***Experientia***, 1972, 28, 1203

67. Bull, J.R.; Chalmers, A.A.; Coleman, P.C., ***S. Afr. J. Chem.***,1979, 1, 32.

68. Velde, V.V.; Lavie, D., ***Tetrahedron***, 1983, 2, 317.

APPENDIX A

ADEPT SPECTRUM ANALYSIS

index		frequency	ppm	intensity
1	D	13420.0	133.430	24.407
2	D	12896.2	128.222	20.729
3	D	12017.2	119.483	26.218
4	D	11358.3	112.931	25.246
5	D	9198.5	91.457	23.686
6	D	6685.1	66.467	31.456
7	D	5919.2	58.853	26.185
8	Q	5664.8	56.323	13.443
9	T	4668.6	46.419	25.333
10	Q	4328.9	43.041	17.920
11	D	4092.5	40.690	25.432
12	T	3593.4	35.728	23.890
13	T	2057.0	20.452	25.598

Number of protonated carbons: 13

CH : 8

CH2: 3

CH3: 2

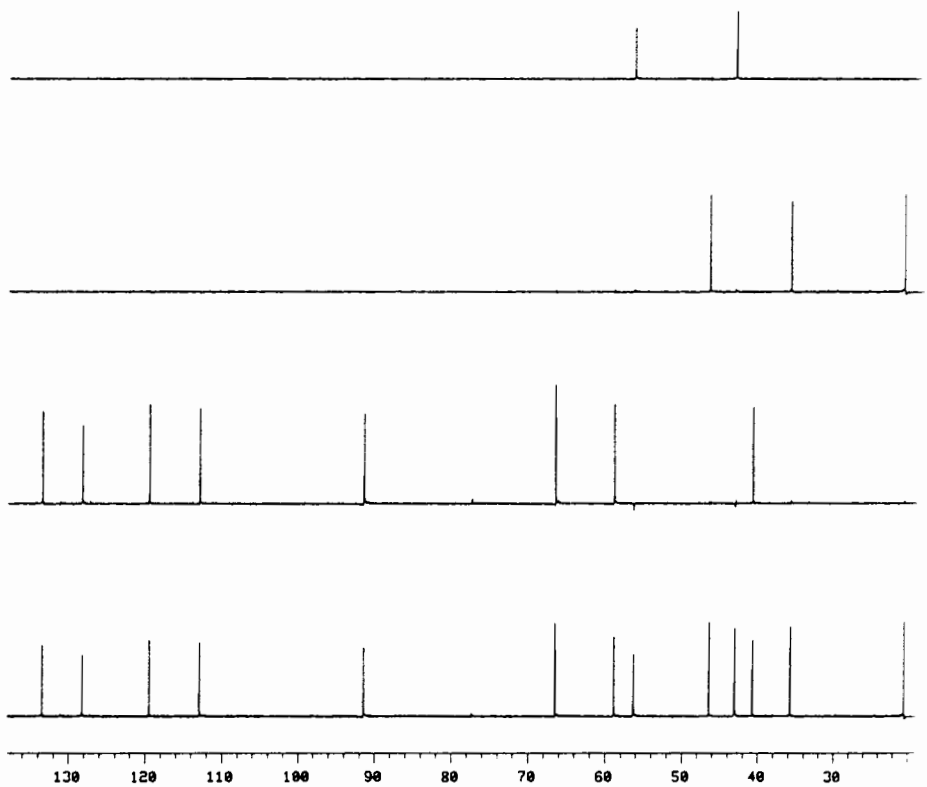

A:1 DEPT SPECTRUM OF CODEINE

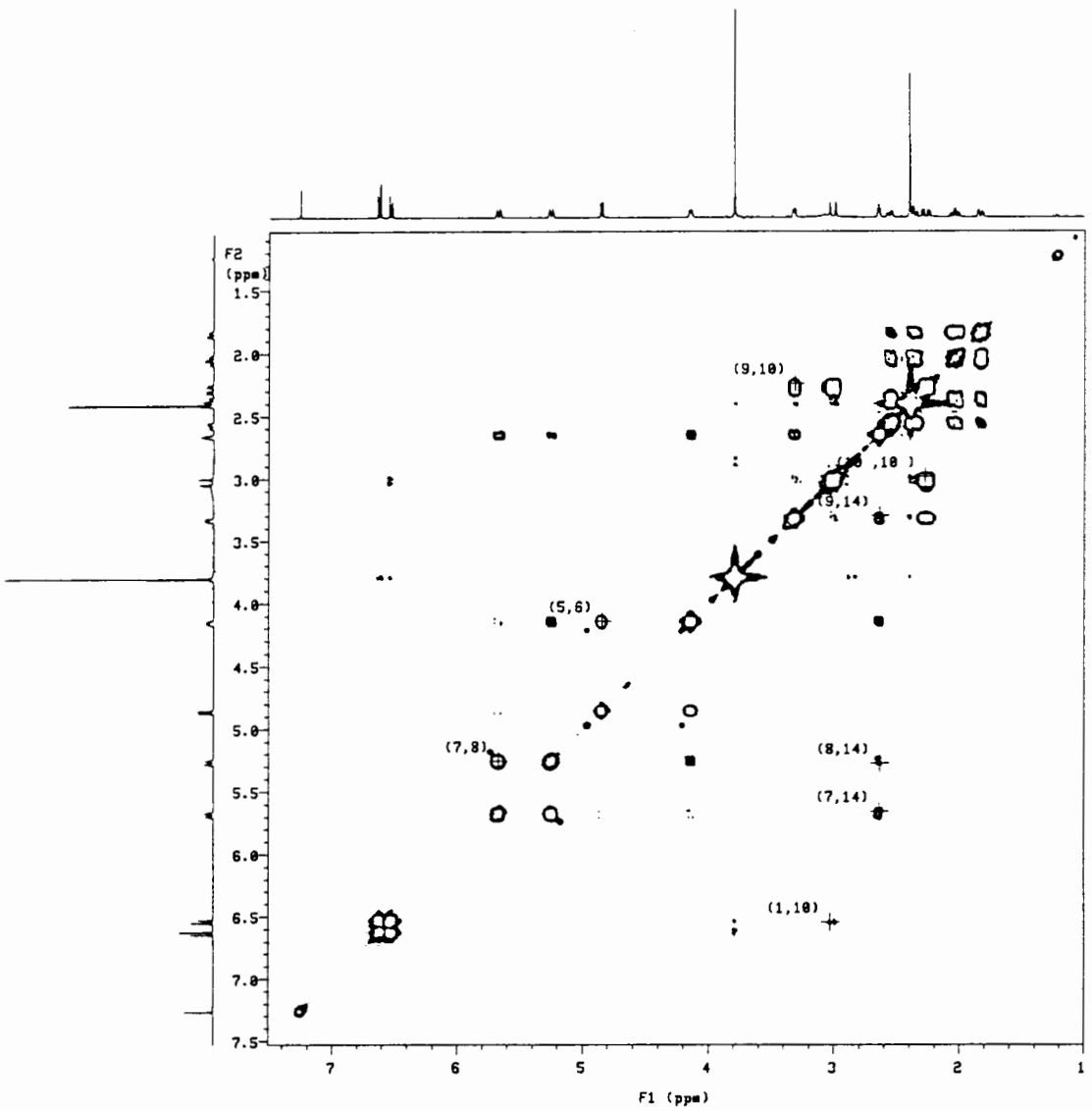

A:2 COSY SPECTRUM OF CODEINE

Data was recorded at 400MHz using a 90° observe pulse with an acquisition time of 0.147s and 16 transients and 256 increments as well as a relaxation delay of 1s. Data was processed as a 1024×1024 matrix using the sinebell function of 0.074s in F1 and 0.038s in F2.

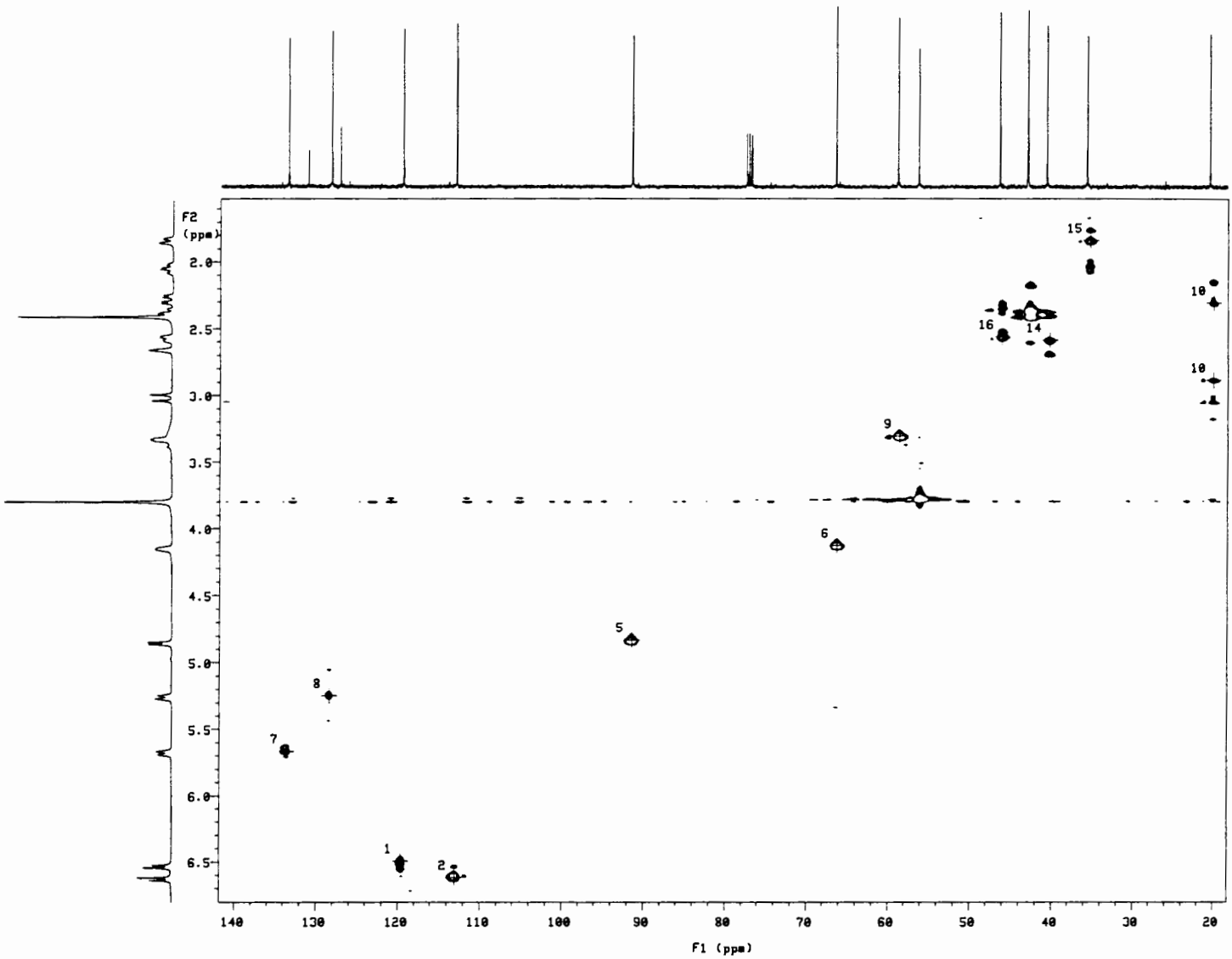

A:3 HMQC SPECTRUM OF CODEINE

4 transients were recorded for each of the 256 increments at 400MHz using an acquisition time of 0.184s. A relaxation delay of 2s was applied and the data was processed as a 1024×2048 matrix using a sinebell and shifted sinebell function in F1 of -0.184s and in F2 a sinebell of 0.008s, a shifted sinebell of -0.006s and a gaussian function of 0.007s.

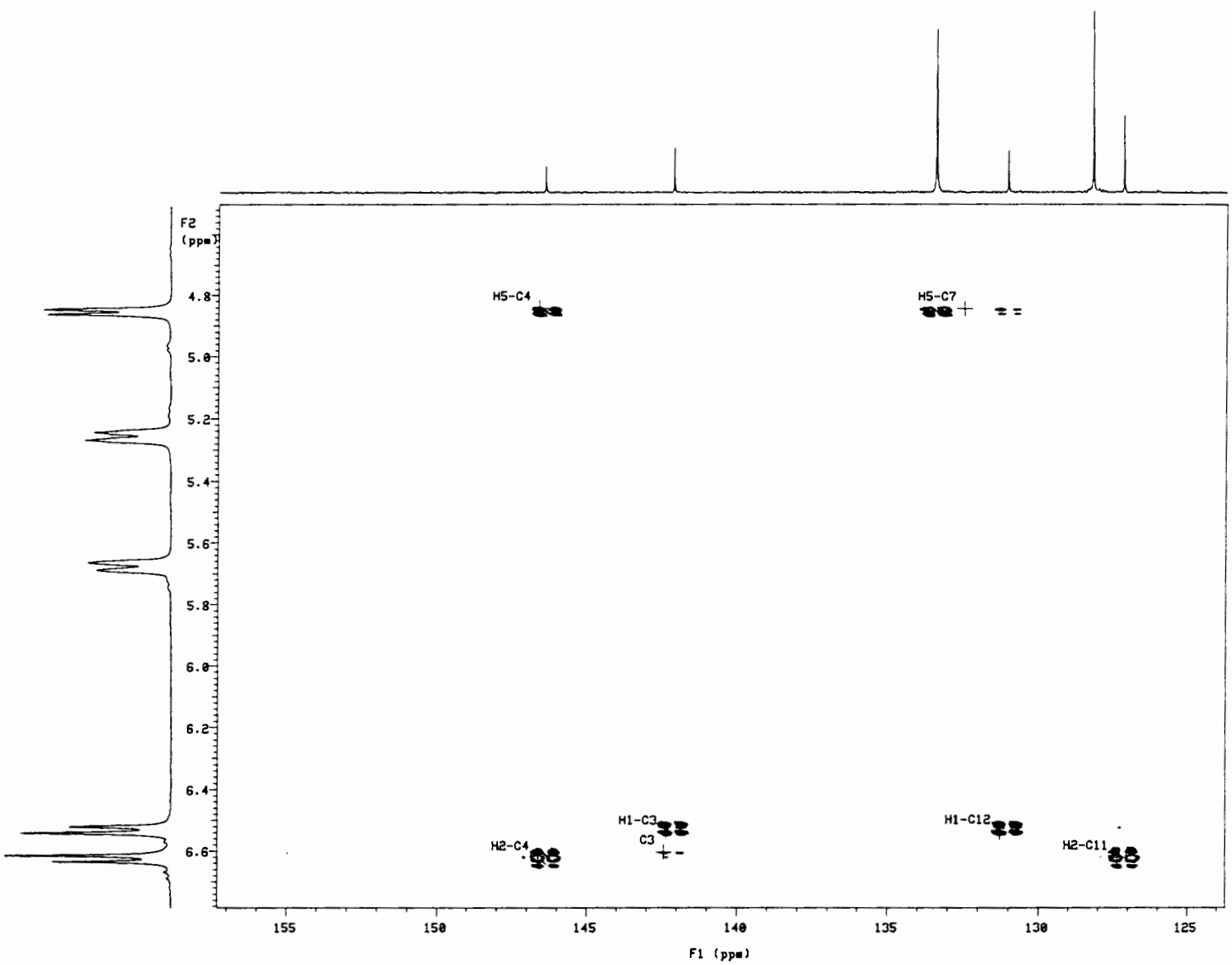

A:4 HMBC SPECTRUM OF CODEINE

4 transients were recorded for each of the 256 increments with an acquistion time of 0.184s and a relaxation delay of 2s. Data was processed as a 1024×2048 matrix with sinebell and shifted sinebell functions at -0.184s in F1 and sinebell of 0.008s and shifted sinbell of 0.001s in F2 .

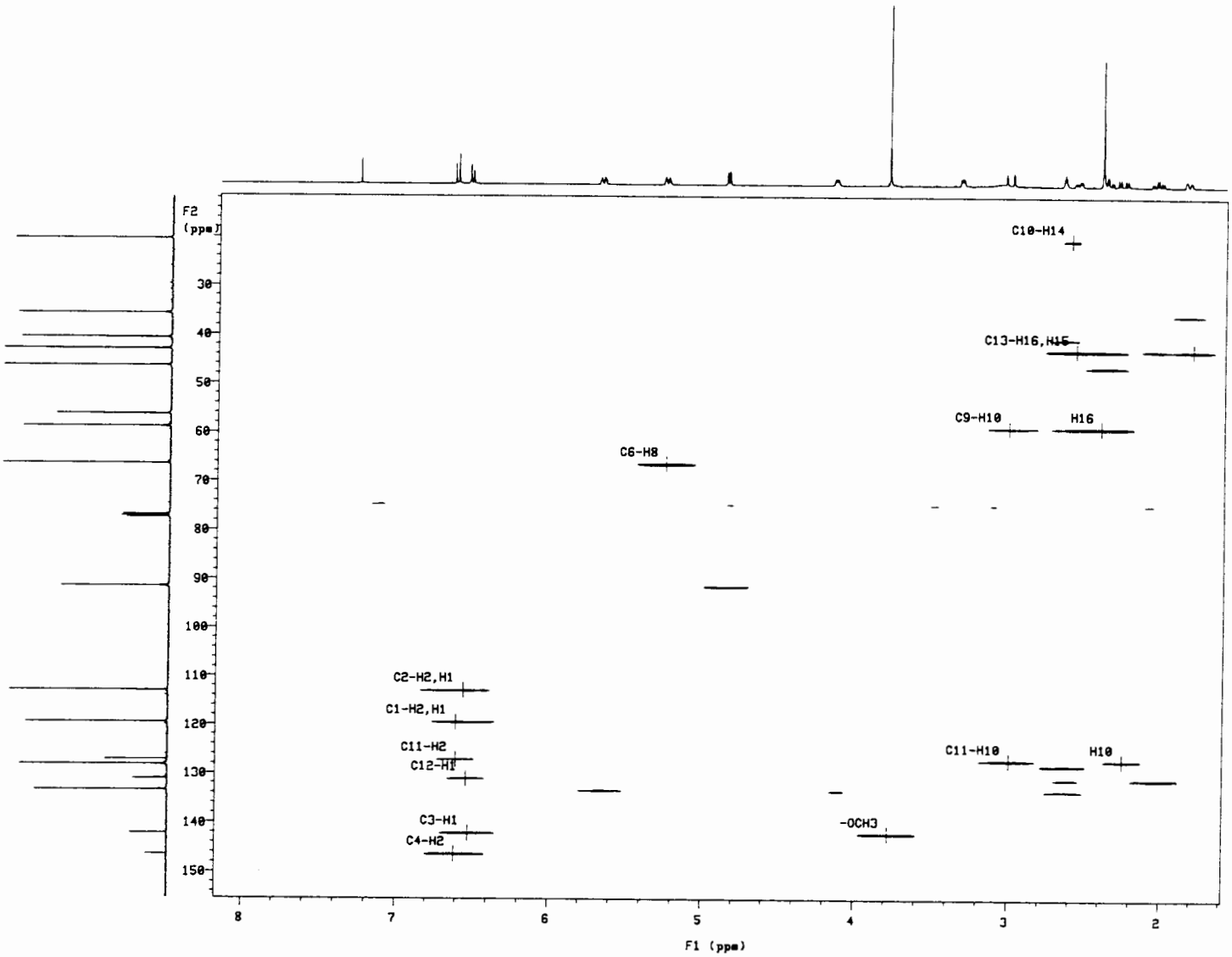

A:5 LONG RANGE HETCOR OF CODEINE

256 increments and 64 transients were recorded using an acquisition time of 0.081s and a relaxation delay of 1s. Data was processed as a 4096×512 matrix with the application of a sinebell function of 0.040s in F1 and 0.009s in F2.

ADEPT SPECTRUM ANALYSIS

index		frequency	ppm	intensity
1	D	14163.9	140.826	9.074
2	D	12117.2	120.477	13.781
3	D	11931.5	118.630	12.413
4	D	11251.5	111.870	14.411
5	D	11183.9	111.197	14.057
6	D	10580.1	105.194	13.001
7	D	10468.7	104.087	12.267
8	Q	5615.3	55.831	9.188
9	Q	5603.9	55.718	16.123
10	T	4232.1	42.078	11.656

Number of protonated carbons: 10
CH : 7
CH2: 1
CH3: 2

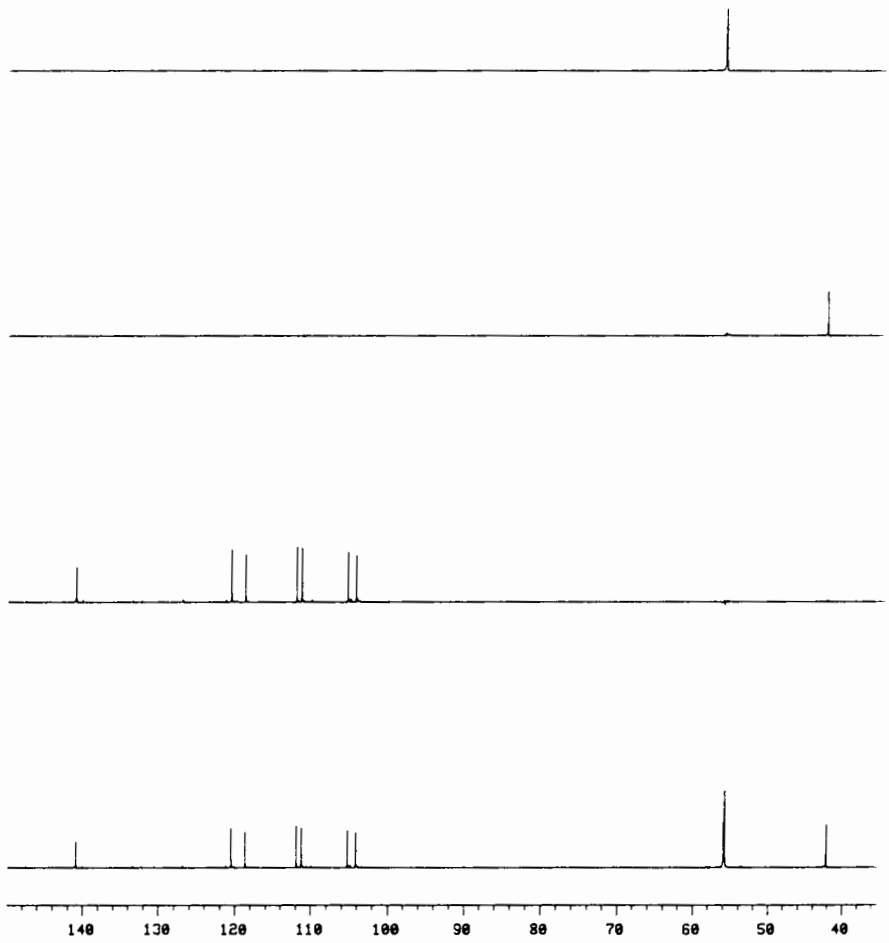

A:6 DEPT SPECTRUM OF PAPAVERINE

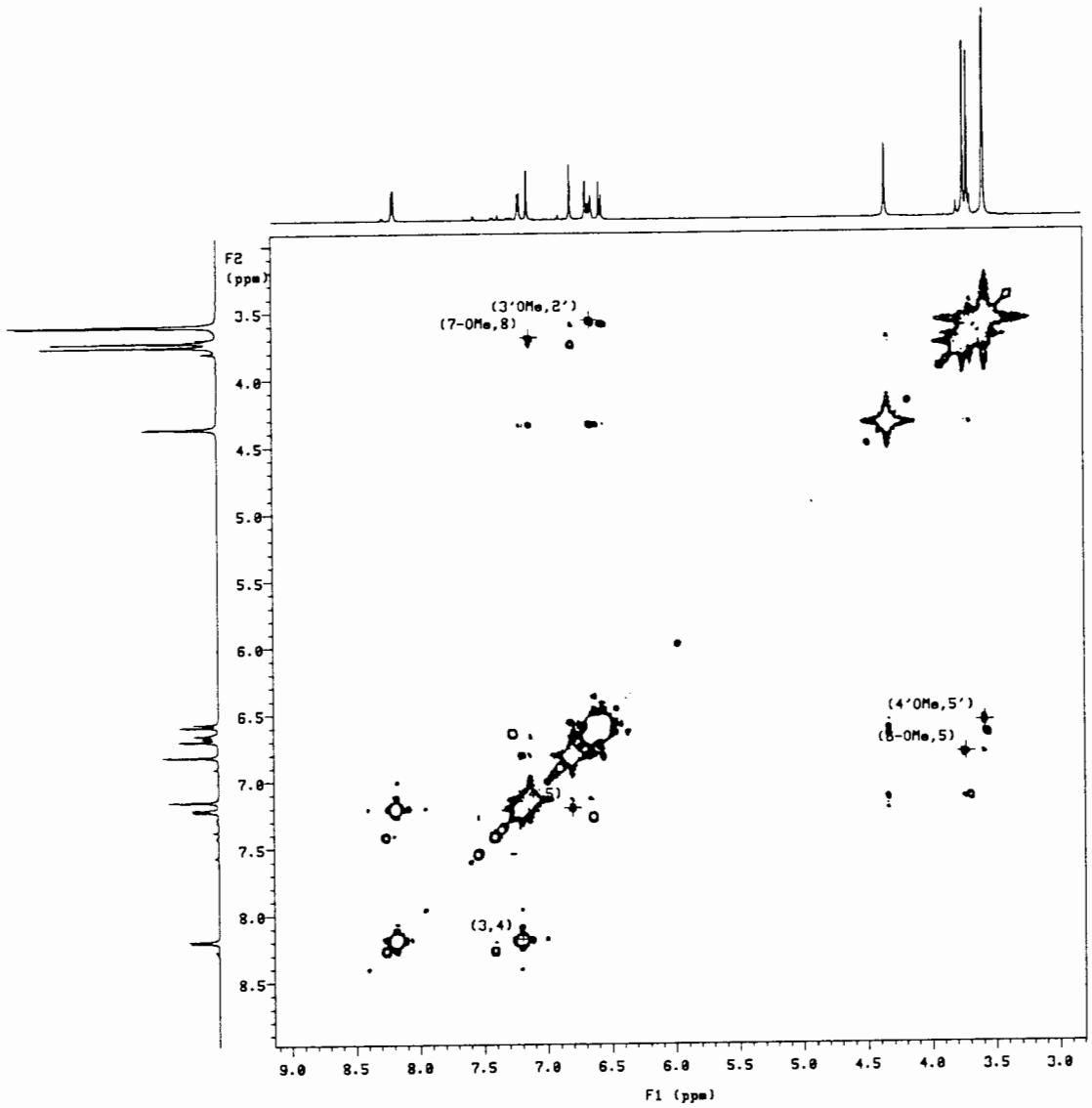

A:7 COSY SPECTRUM OF PAPAVERINE

Data was recorded at 400MHz with a 90° observe pulse, an acquistion time of 0.147s using 16 transients for each of the 256 increments and a relaxation delay of 1s. Data was processed as a 1024×1024 matrix with folding and the application of a sinebell function of 0.036s in F2 and 0.074s in F1.

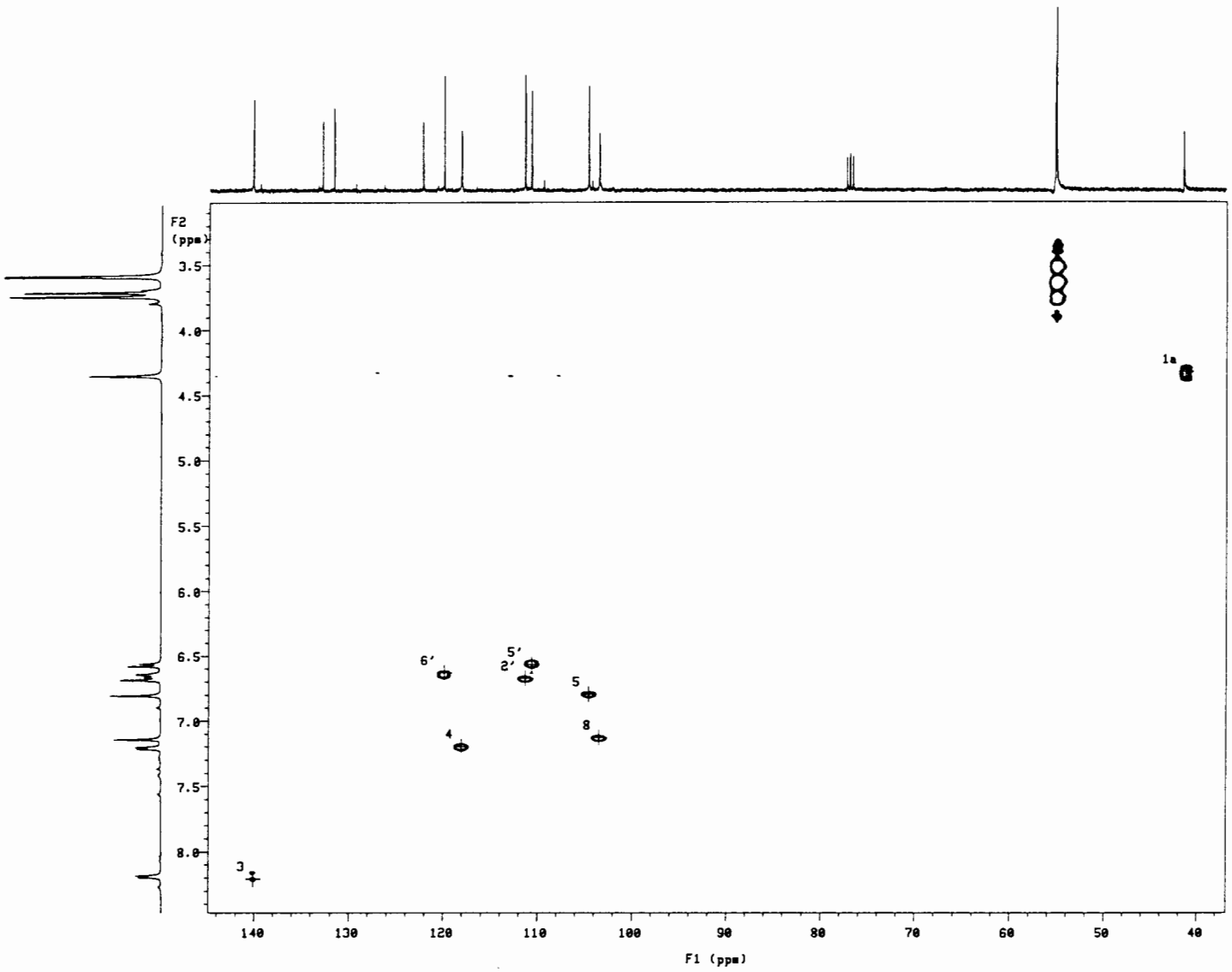

A:8 HMQC SPECTRUM OF PAPAVERINE

4 transients were recorded for each of the 256 increments using an acquisition time of 0.222s and a relaxation delay of 1s. Data was processed as a 1024×2048 matrix with sinebell and sinebell shifted in F1 at -0.222s whilst in F2 a sinebell of 0.009s, a sinebell shifted of -0.007s and a gaussian function of 0.007s was applied.

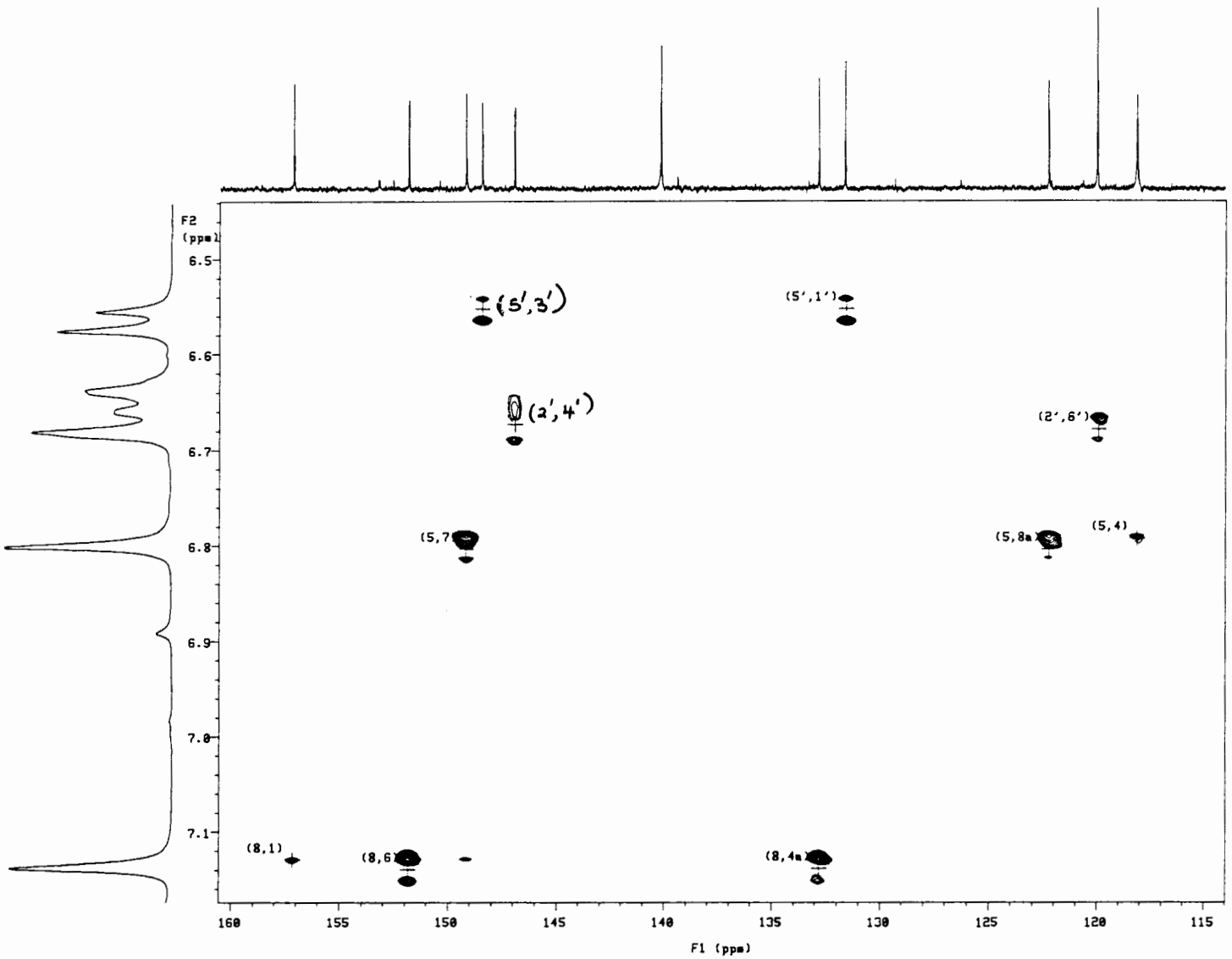

A:9 PART OF HMBC SPECTRUM OF PAPAVERINE

4 transients were recorded for each of the 256 increments using an acquisition time of 0.222s and a relaxation delay of 1s. Data was processed as a 1024×2048 matrix with sinebell and sinebell shifted in F1 at -0.222s and gaussian function at 0.103s whilst in F2 a sinebell value of 0.009s, a sinebell shifted of -0.009s and a gaussian function of 0.014s was applied.

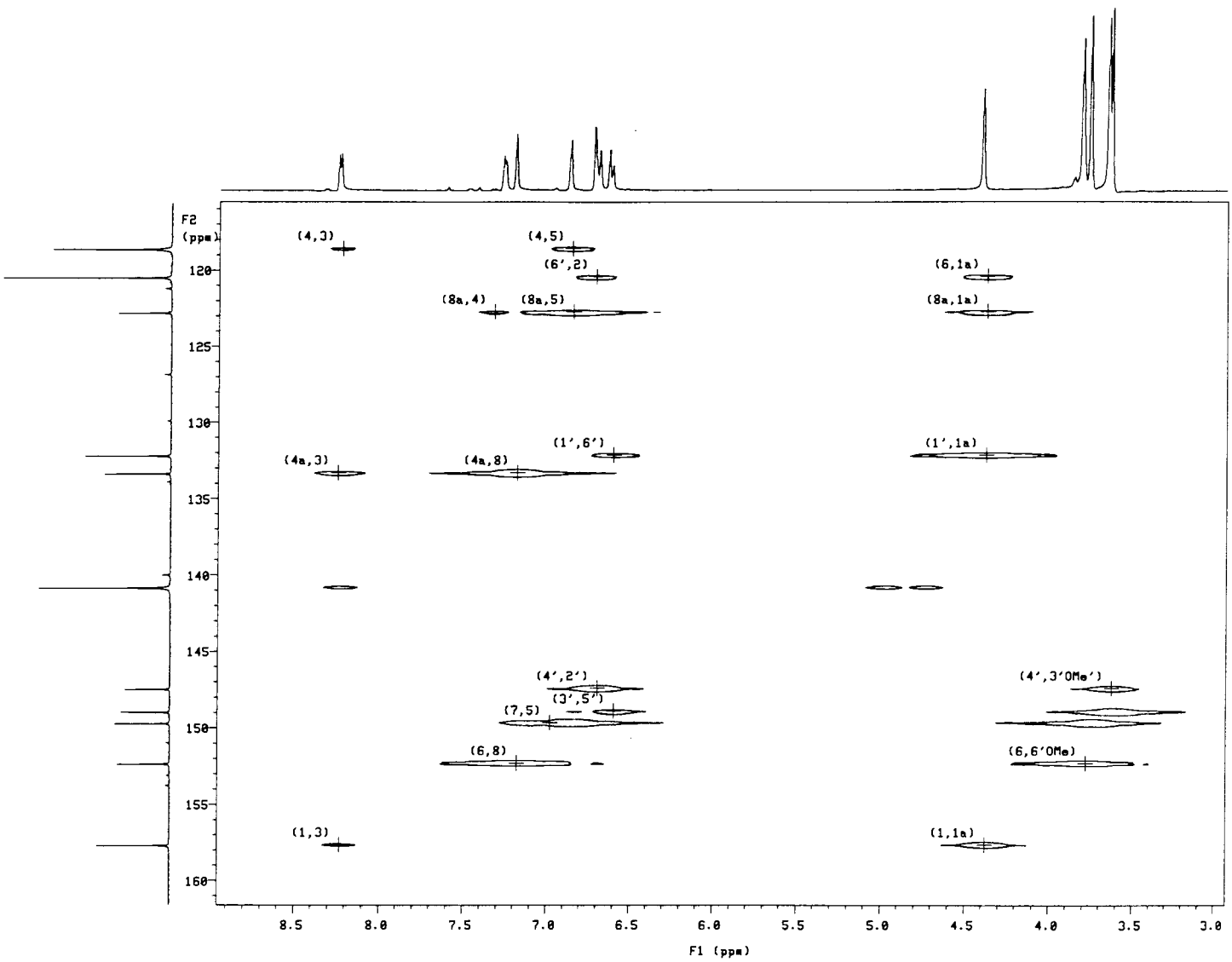

A:10 LONG RANGE HETCOR OF PAPAVERINE

Data was acquired at an acquisition time of 0.081s with 256 transients for each of the 64 increments at a relaxation delay of 1s. Data was processed as a 4096×512 matrix with the application of a sinebell function of 0.041s in F1 and 0.020s in F2.,

APPENDIX B

ADEPT SPECTRUM ANALYSIS

index		frequency	ppm	intensity
1	D	13382.7	133.059	27.201
2	D	13043.4	129.685	59.733
3	D	12924.3	128.501	58.153
4	D	8546.3	84.973	23.887
5	D	8407.1	83.589	26.698
6	D	8348.9	82.931	28.021
7	T	8071.5	80.252	22.894
8	D	7924.8	78.794	27.743
9	D	6374.3	63.377	25.533
10	Q	5943.4	59.093	37.197
11	Q	5904.7	58.709	35.635
12	Q	5810.5	57.772	36.165
13	Q	5684.5	56.519	32.875
14	T	5641.6	56.093	19.280
15	D	4899.5	48.714	19.699
16	D	4838.8	48.103	27.866
17	D	4530.5	45.045	27.188
18	Q	4275.9	42.513	29.656
19	D	4130.3	41.066	23.796
20	T	3943.9	39.213	18.264
21	T	3570.7	35.502	17.983
22	T	3489.2	34.692	15.718
23	T	2650.7	26.355	13.893
24	Q	2167.9	21.554	32.765

Number of protonated carbons: 24
CH : 12
CH2: 6
CH3: 6

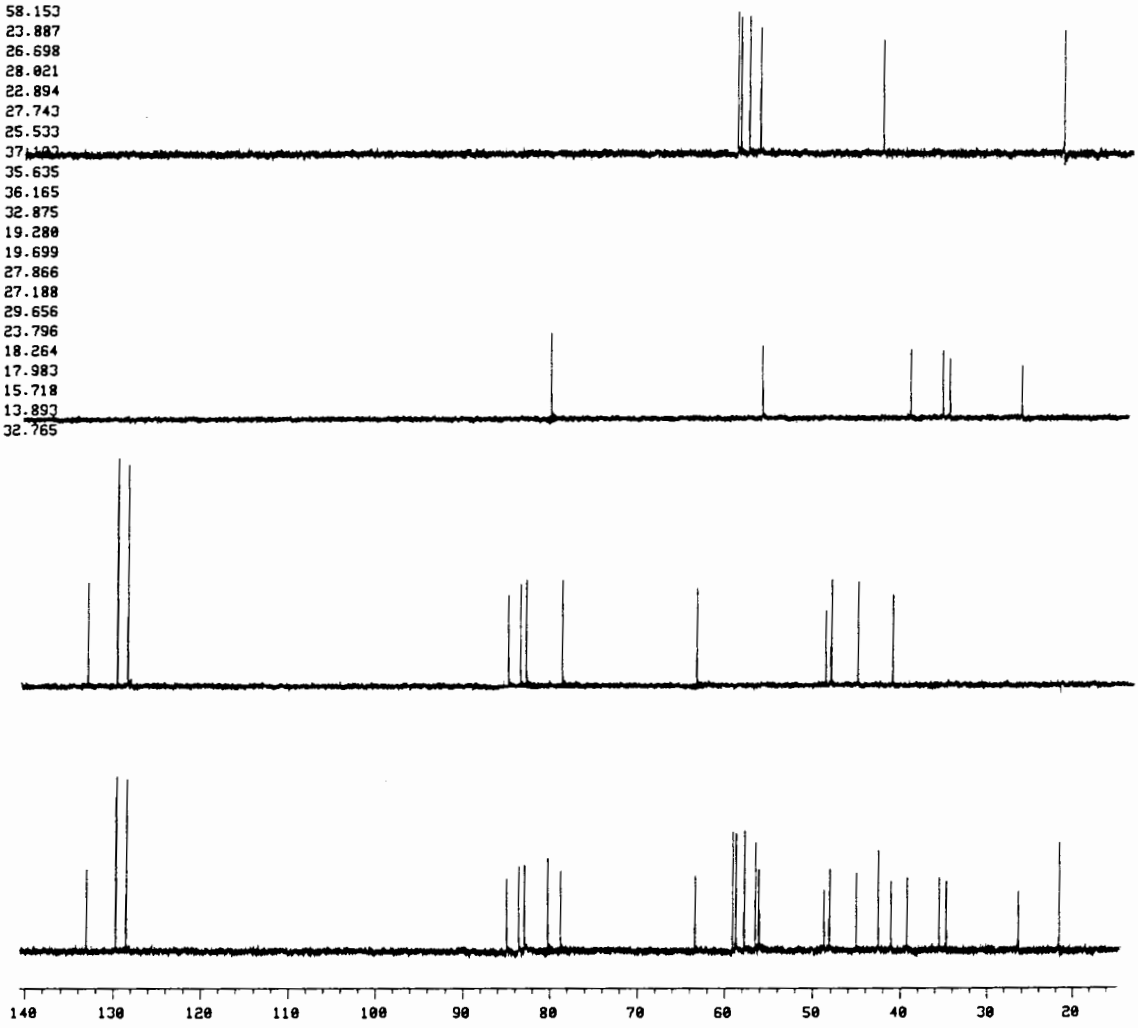

B:1 DEPT SPECTRUM OF DELPHININE

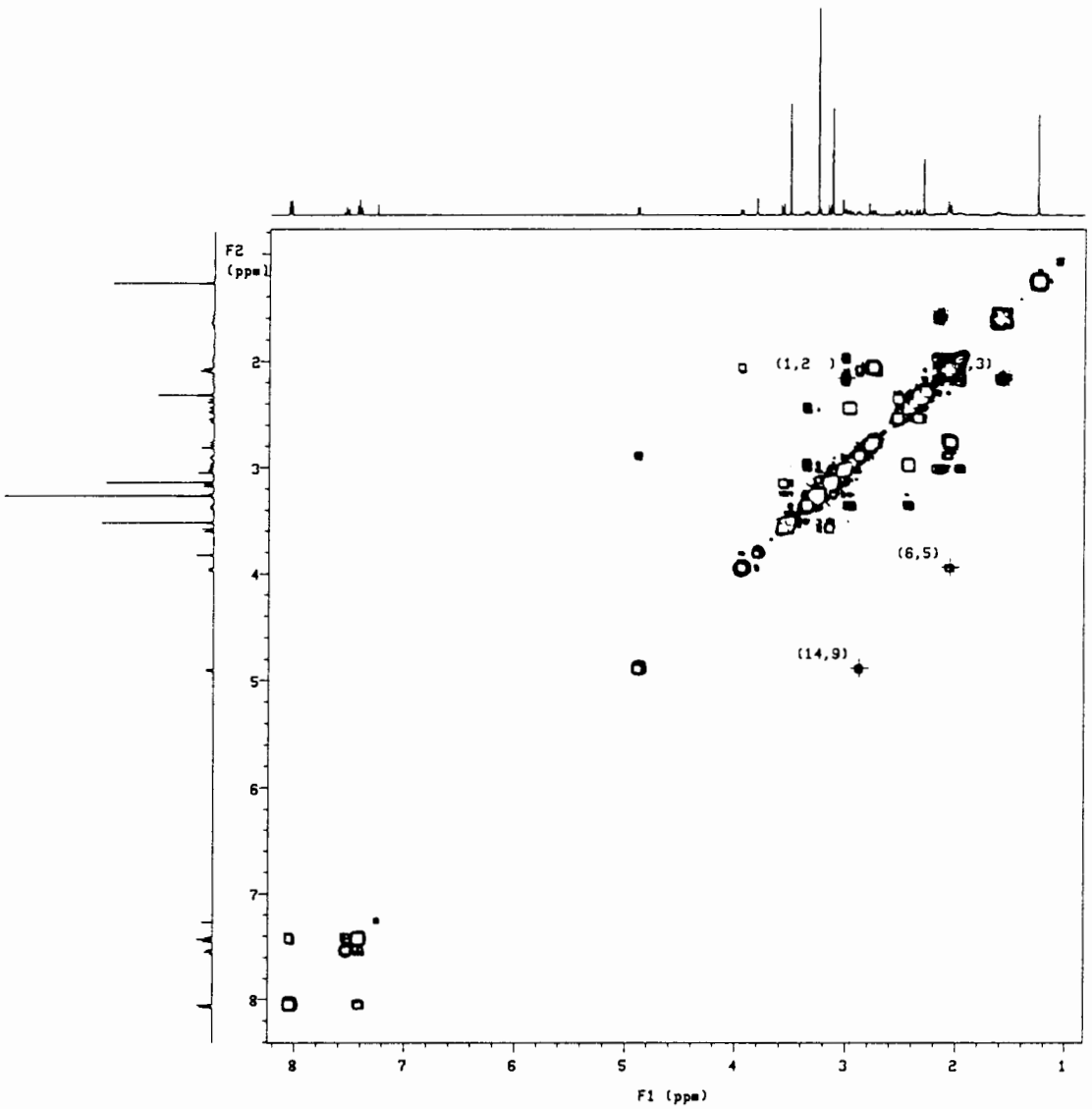

B:2 COSY SPECTRUM OF DELPHININE

Data was recorded at 400MHz using a 90° observe pulse with an acquisition time of 0.138s and 32 transients and 128 increments as well as a relaxation delay of 1s. Data was processed as a 1024×1024 matrix using the sinebell function of 0.064s in F1 and 0.017s in F2.

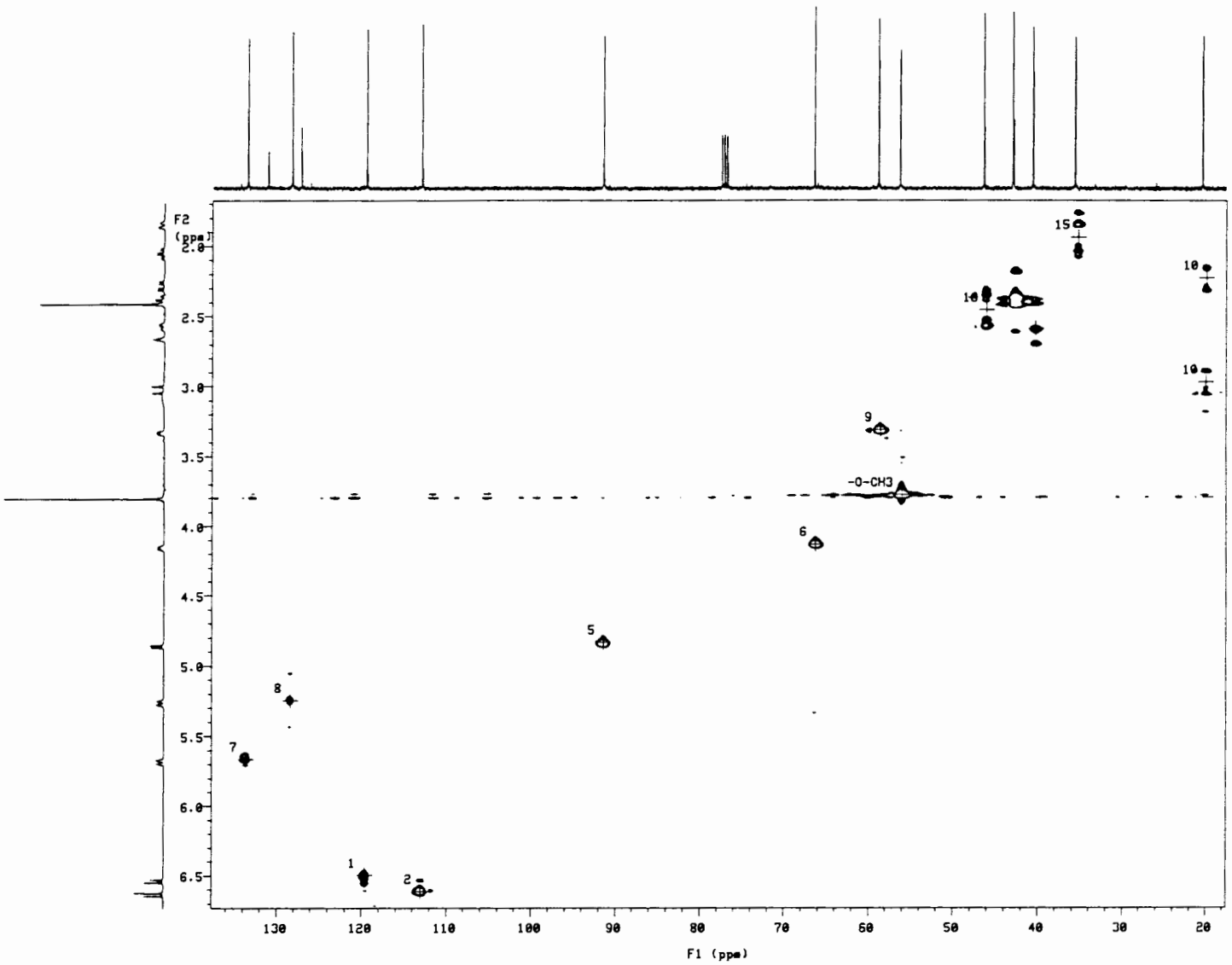

B:3 HMQC SPECTRUM OF DELPHININE

4 transients were recorded for each of the 512 increments at 400MHz using an acquisition time of 0.138s. A relaxation delay of 2s was applied and data was processed as a 1024x2048 matrix using a sinebell and shifted sinebell function in F1 of -0.138s and in F2 a sinebell of 0.016s, and a shifted sinebell of -0.014s.

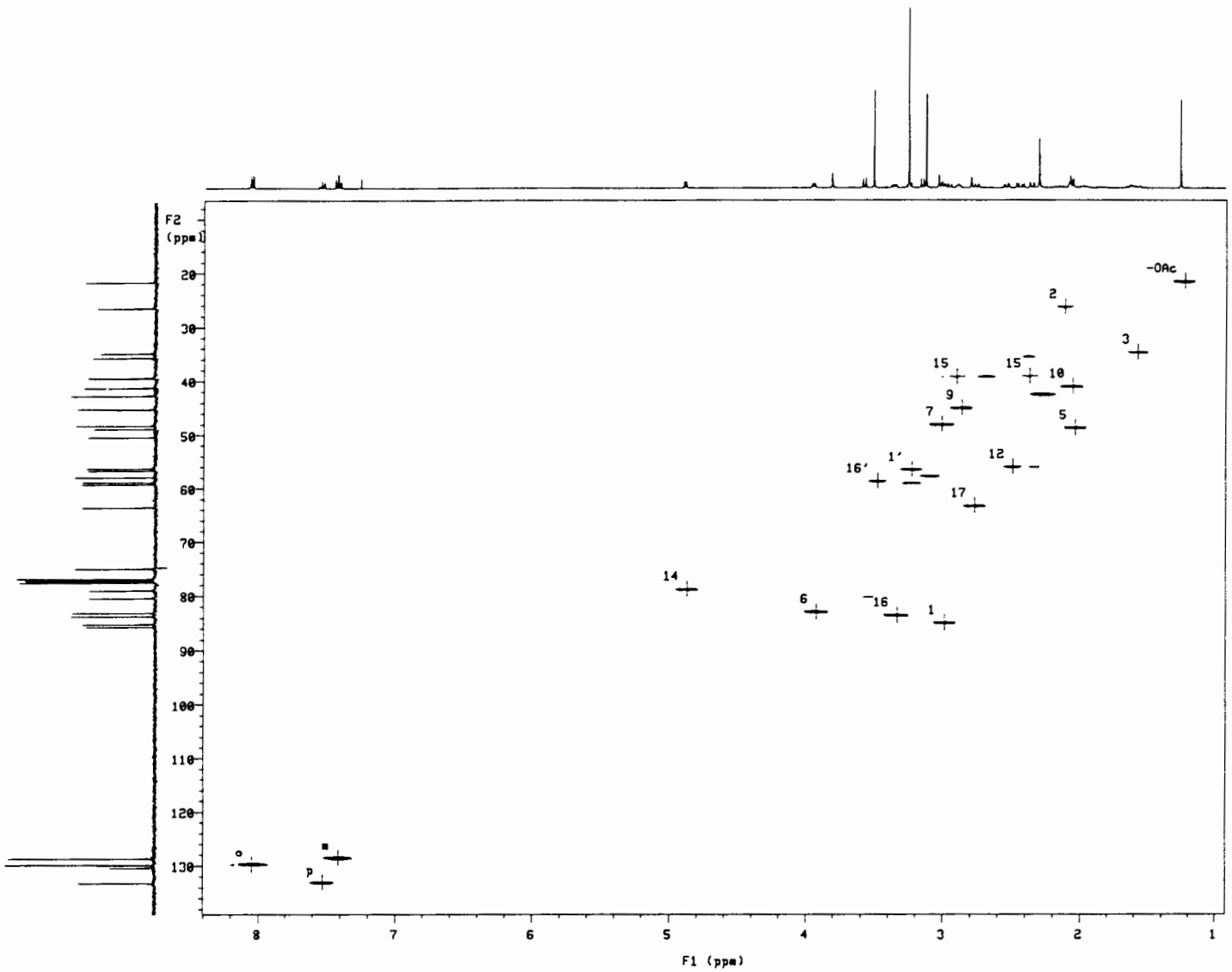

B:4 HETCOR OF DELPHININE

128 increments and 128 transients were recorded using an acquisition time of 0.081s and a relaxation delay of 1s. Data was processed as a 4096×512 matrix with the application of a sinebell function of 0.031s in F1 and 0.020s in F2.

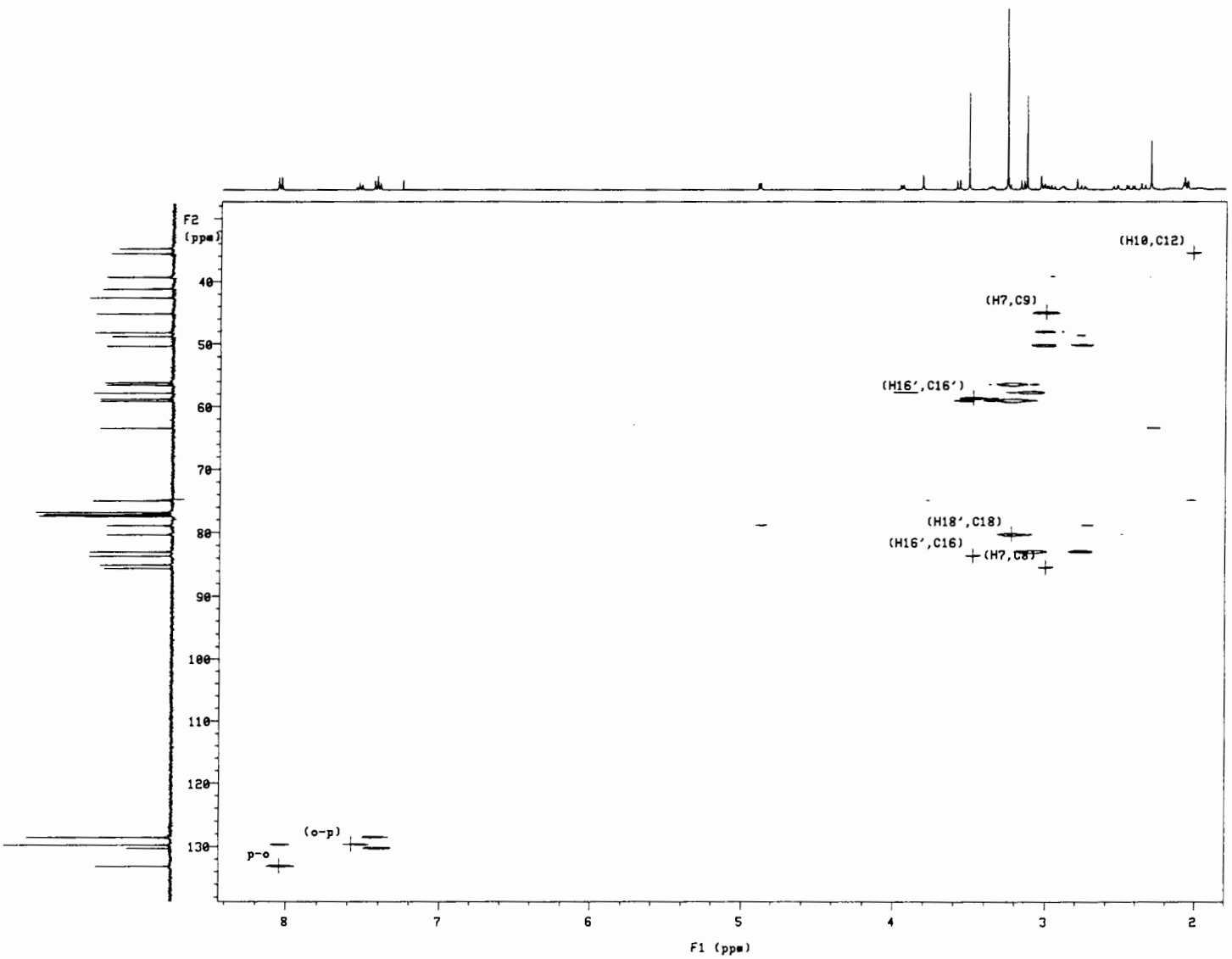

B:5 LONG RANGE HETCOR OF DELPHININE

256 increments and 128 transients were recorded using an acquisition time of 0.081s and a relaxation delay of 1s. Data was processed as a 4096×512 matrix with the application of a sinebell function of 0.041s in F1 and 0.020s in F2.

APPENDIX C

ADEPT SPECTRUM ANALYSIS

index		frequency	ppm	intensity
1	D	15353.8	152.657	7.955
2	D	12192.1	121.221	10.109
3	D	11993.5	119.247	10.020
4	D	7383.9	73.416	9.047
5	D	7359.4	73.172	10.809
6	T	6280.8	62.448	8.832
7	D	5461.3	54.299	9.929
8	T	4870.4	48.425	7.851
9	T	4348.4	43.234	7.897
10	D	3423.7	34.040	9.572
11	D	3381.7	33.623	9.664
12	T	3122.1	31.041	7.530
13	Q	2885.1	28.686	11.457
14	Q	2676.5	26.612	13.274
15	Q	2645.5	26.303	12.880
16	Q	2375.8	23.622	10.004
17	T	2352.2	23.387	6.216
18	Q	2196.2	21.836	12.224
19	Q	2140.3	21.281	10.071
20	Q	2088.3	20.764	13.196
21	Q	2071.8	20.599	22.964
22	Q	1907.2	18.963	10.445
23	Q	1847.3	18.367	9.433

Number of protonated carbons: 23
CH : 8
CH2: 5
CH3: 10

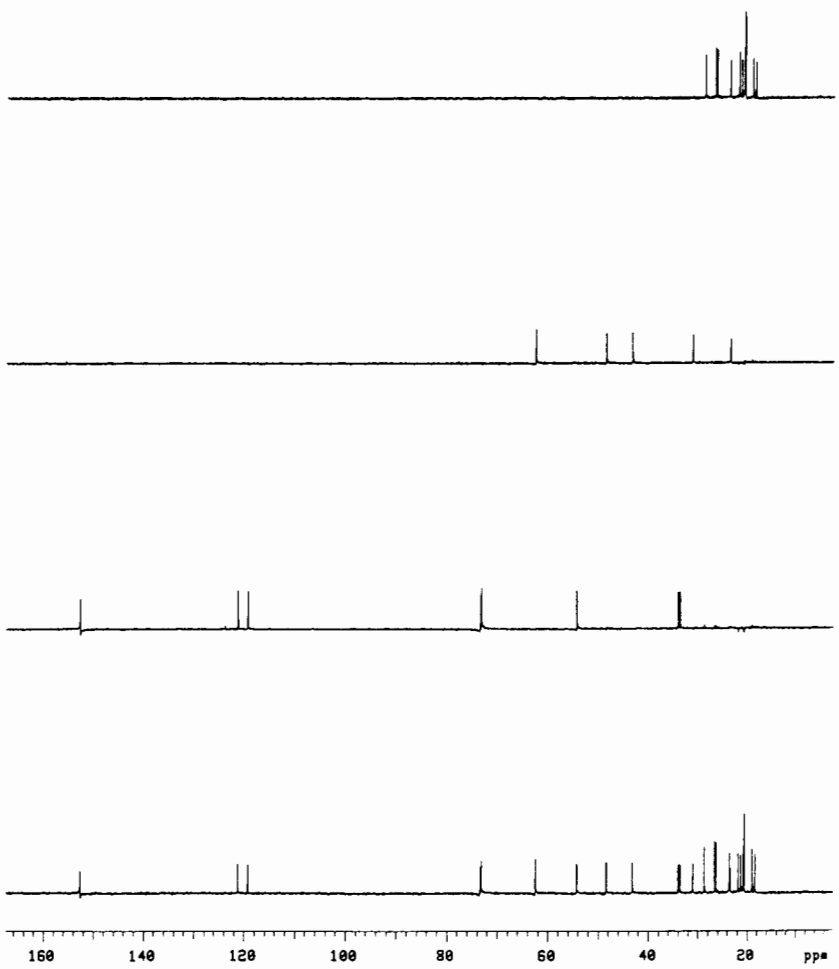

C:1 DEPT SPECTRUM OF CUCURBITACIN A 2,16,19 TRIACETATE

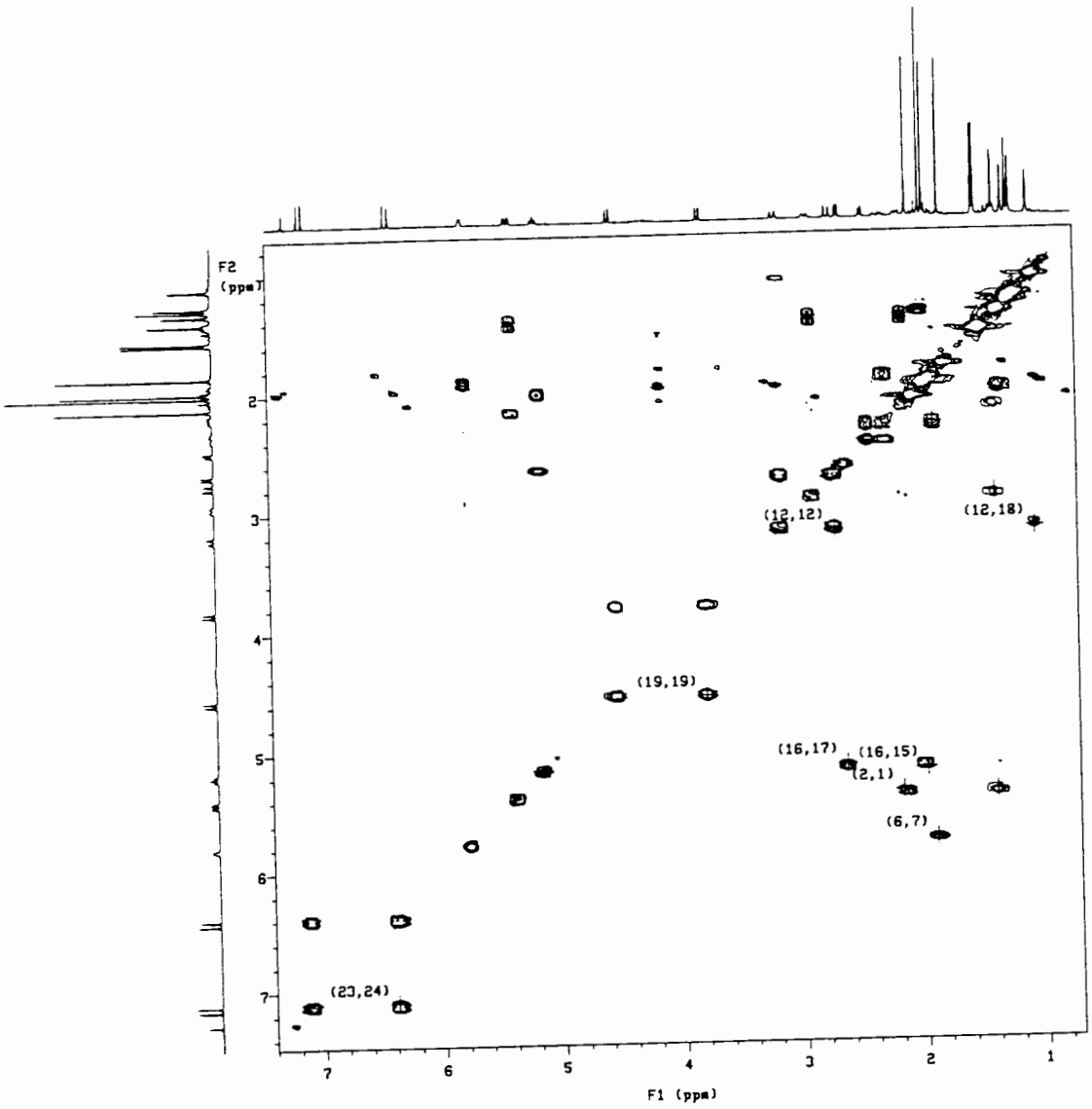

C:2 COSY SPECTRUM OF CUCURBITACIN A 2,16,19 TRIACETATE.

Data was recorded at 400MHz using a 90° observe pulse with an acquisition time of 0.053s and 256 transients and 128 increments as well as a relaxation delay of 1s. Data was processed without folding as a 1024×1024 matrix using the sinebell function of 0.027s in F1 and 0.020s in F2.

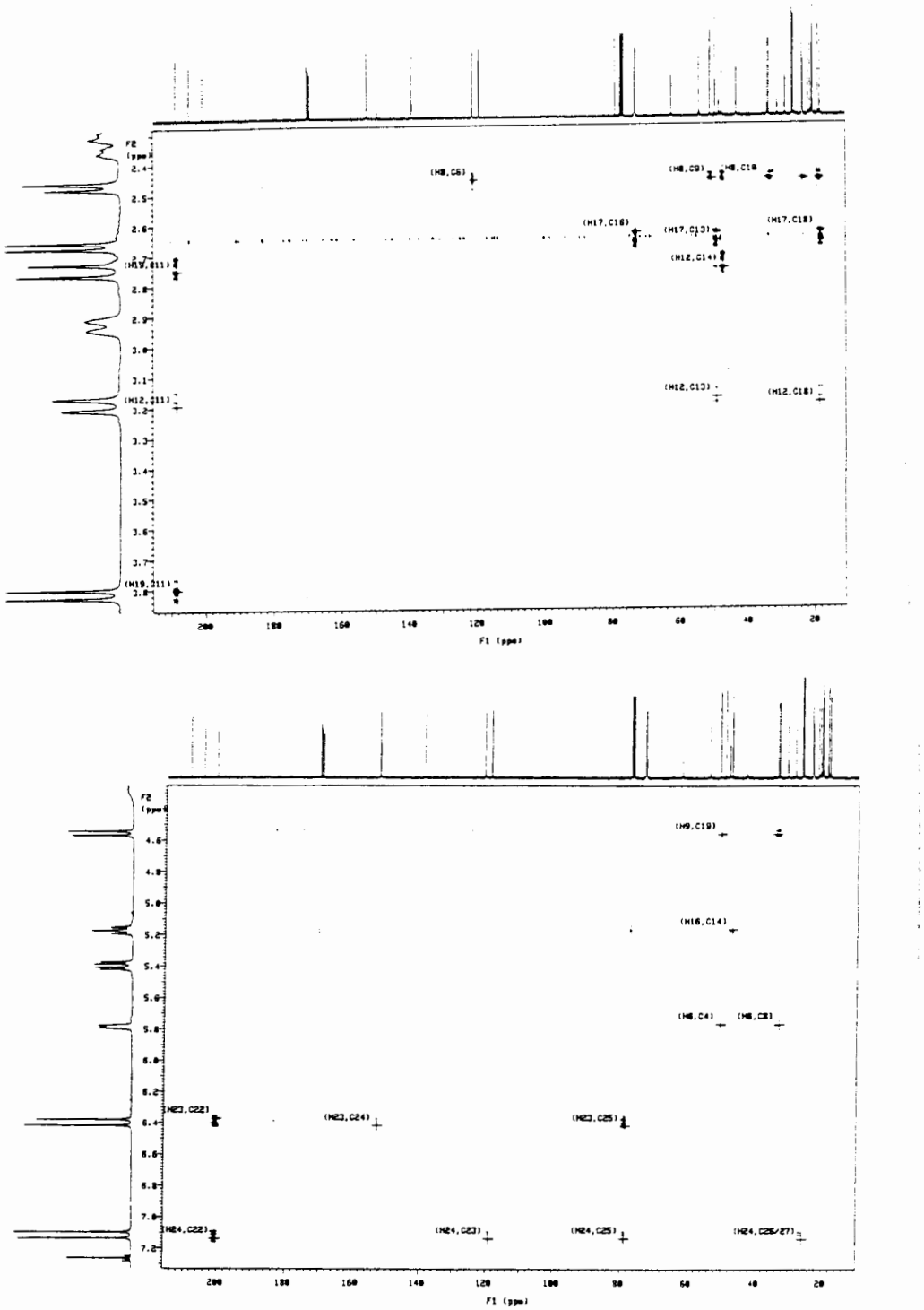

C:3 HMBC SPECTRUM OF CUCURBITACIN A 2,16,19 TRIACETATE

8 transients were recorded for each of the 512 increments at 400MHz using an acquisition time of 0.170s. A relaxation delay of 2s was applied and data was processed as a 1024×2048 matrix using a sinebell and shifted sinbell function in F1 of -0.170s and in F2 a sinebell of 0.010s, a shifted sinebell of -0.006s and a gaussian function of 0.018s..

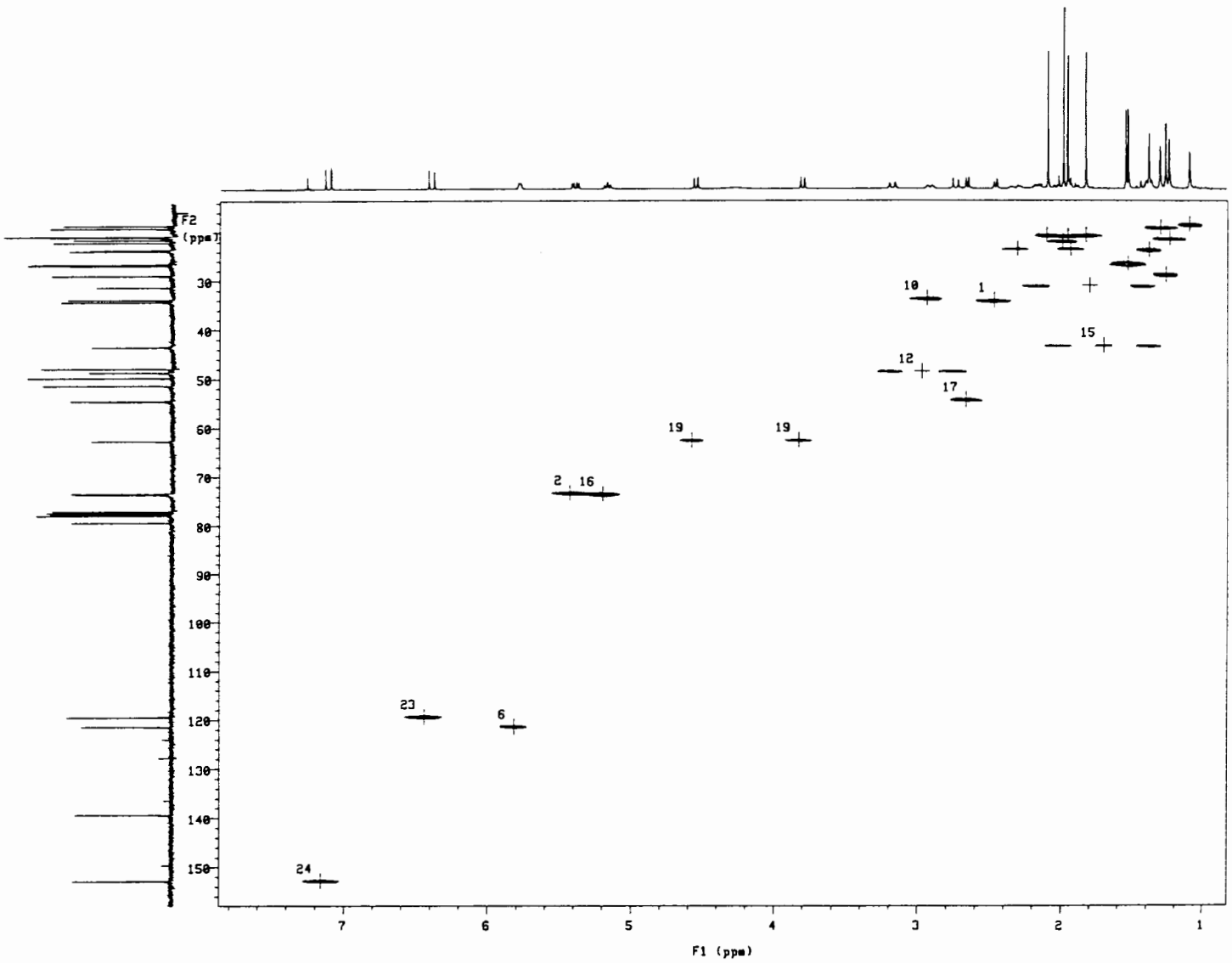

C:4 HETCOR OF CUCURBITACIN A 2,16,19 TRIACETATE

128 increments and 256 transients were recorded using an acquisition time of 0.053s and a relaxation delay of 1s. Data was processed as a 2048×256 matrix with the application of a sinebell function of 0.027s in F1 and 0.020s in F2.

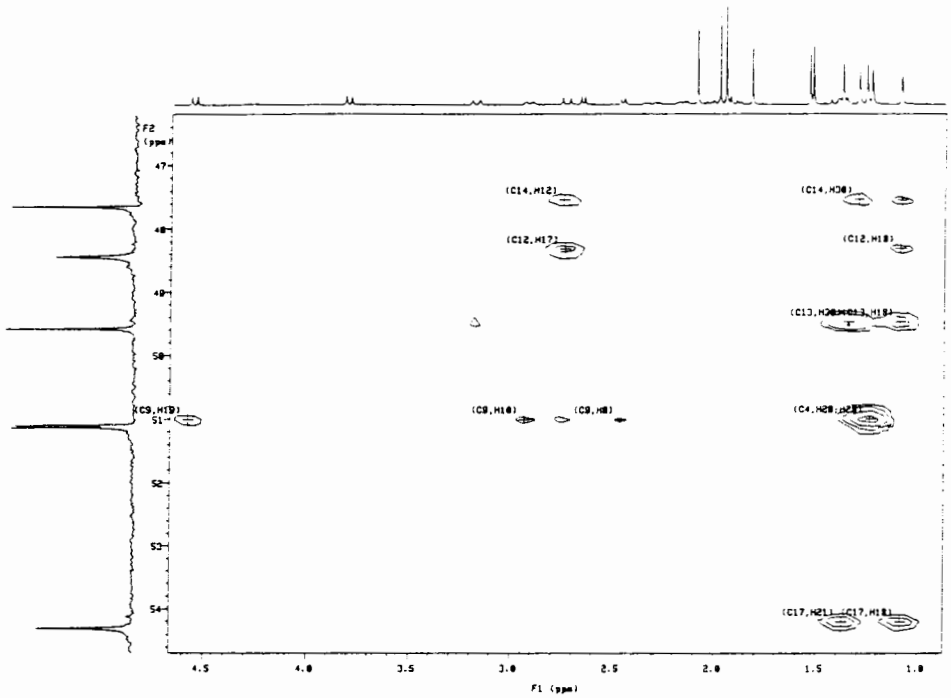

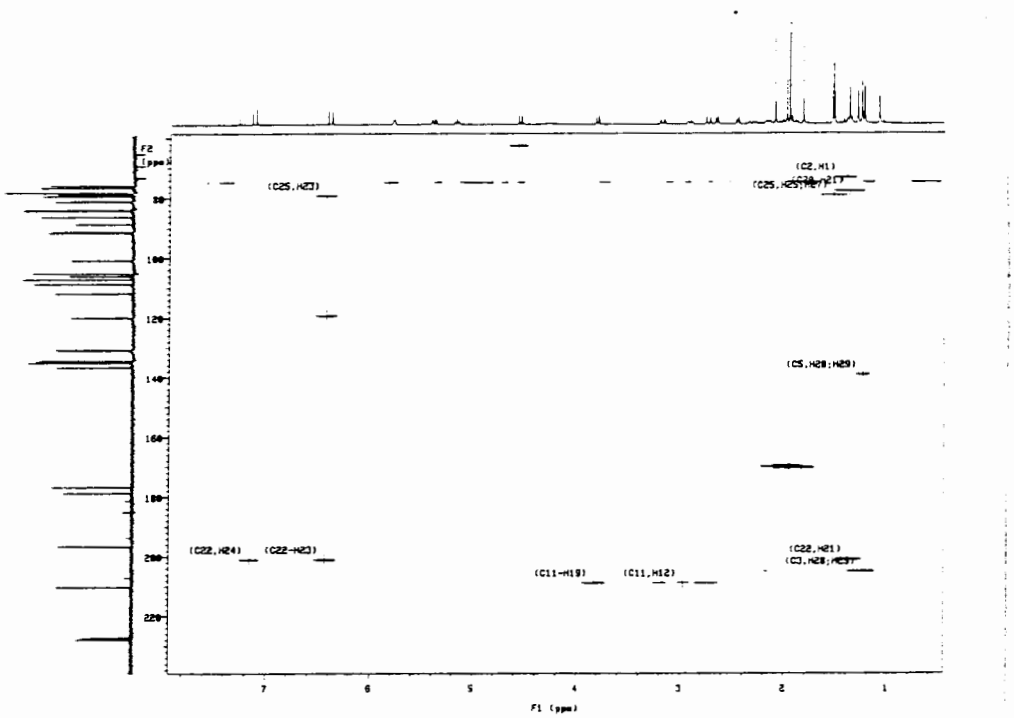

C:5 LONG RANGE HETCOR OF CUCURBITACIN A 2,16,19 TRIACETATE

128 increments and 87 transients were recorded using an acquisition time of 0.081s and a relaxation delay of 1s. Data was processed as a 4096×256 matrix with the application of a sinebell function of 0.041s in F1 and 0.014s in F2.

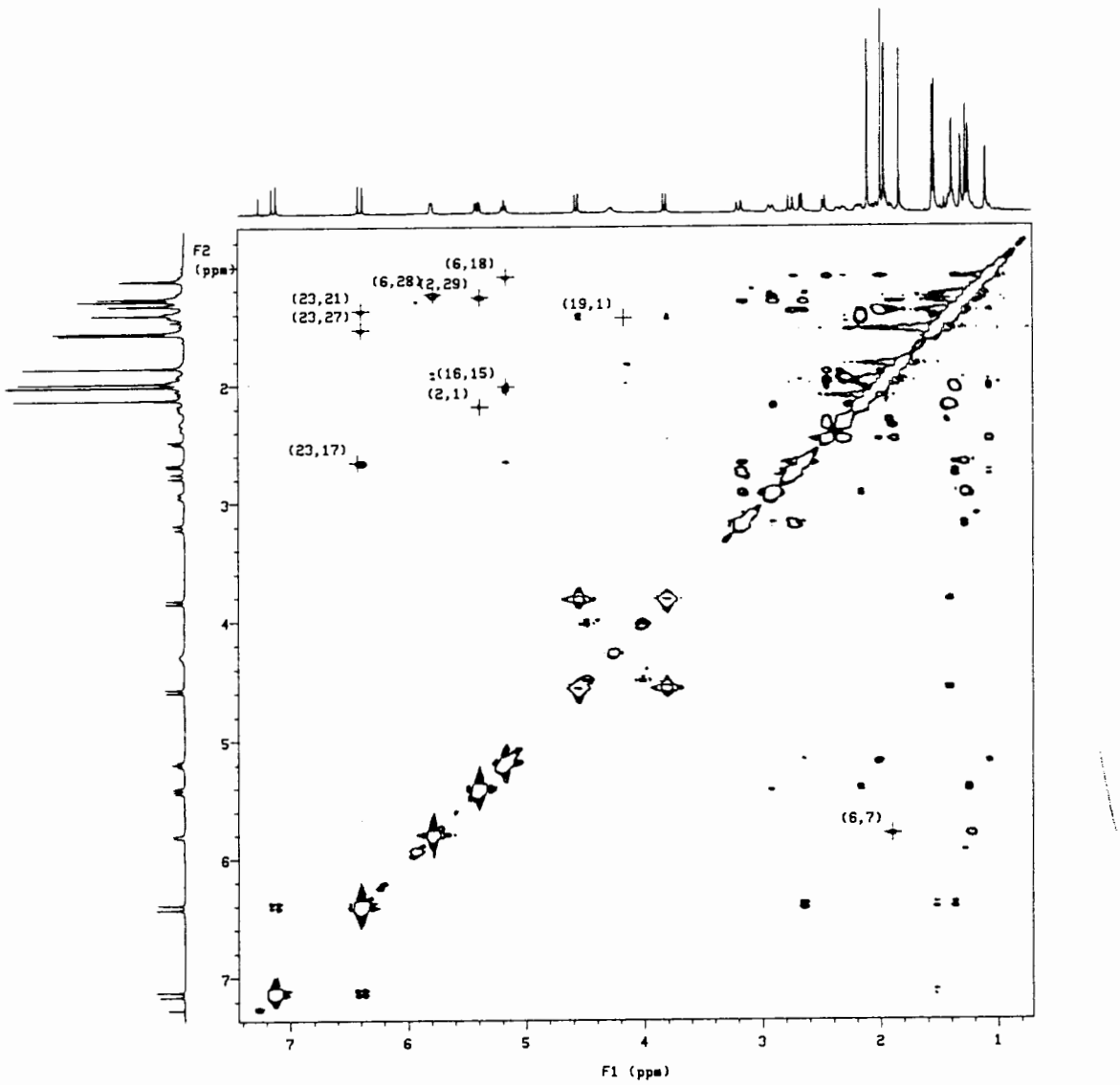

C:6 ROESY SPECTRUM OF CUCURBITACIN A 2,16,19 TRIACETATE

Data was recorded at 400MHz with an acquisition time of 0.170s and mixing time of 200ms with 4 transients and 256 increments as well as a relaxation delay of 1s. Data was processed without folding as a 1024×512 matrix using the sinebell and sinebell shifted function of -0.017s in F1 and a sinebell function of 0.030s with a sinebell shifted function of -0.018s and gaussian function of 0.047s in F2.

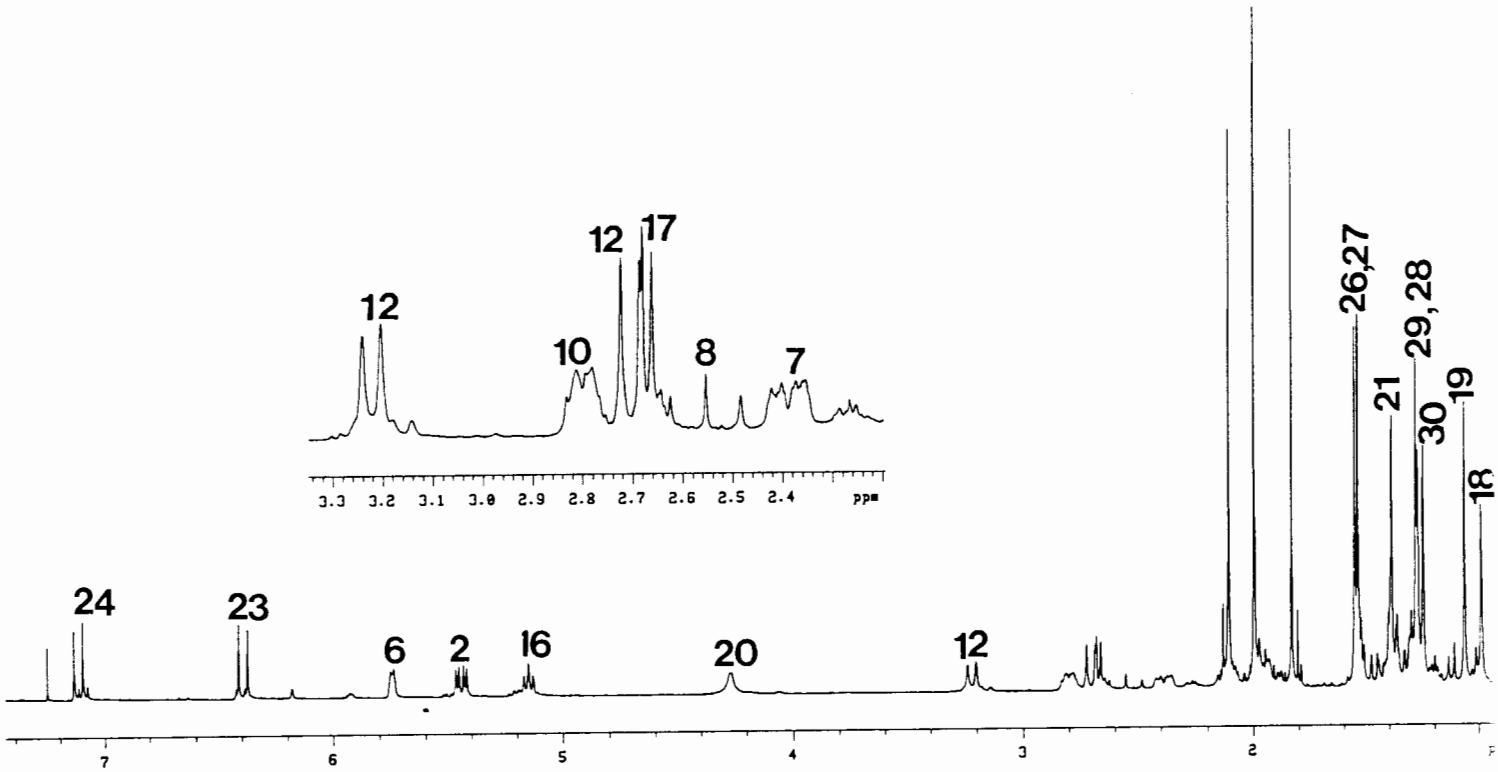

C:7 ^{1}H SPECTRUM OF CUCURBITACIN B 2,16 DIACETATE.

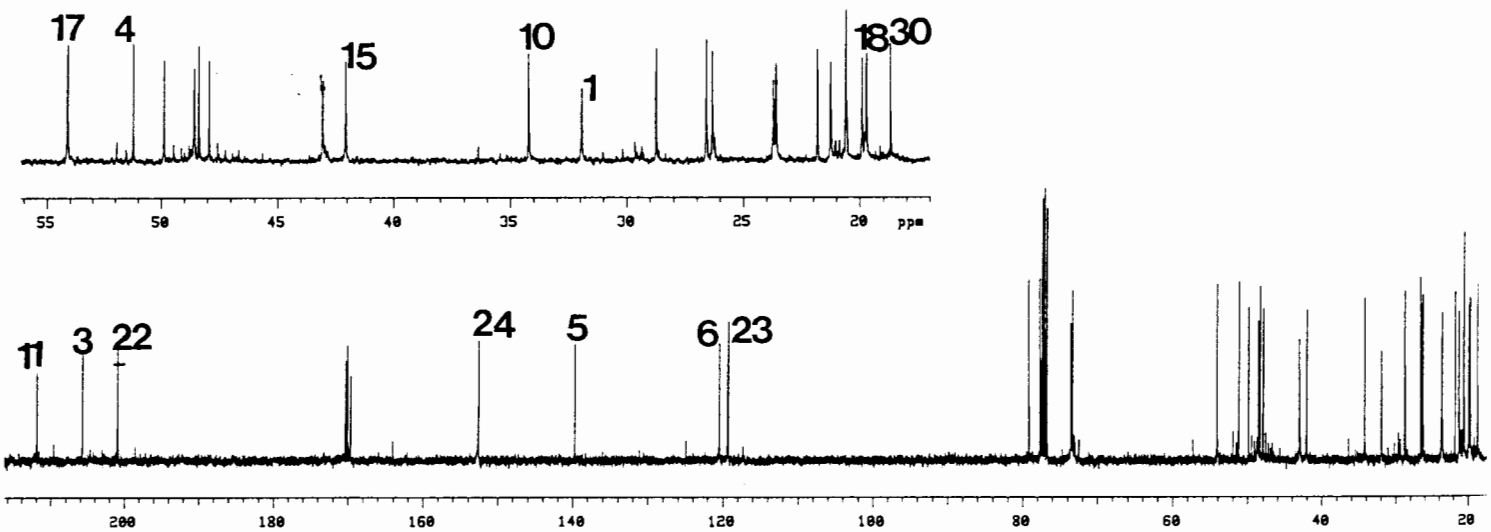

C8: ^{13}C SPECTRUM OF CUCURBITACIN B 2,16 DIACETATE

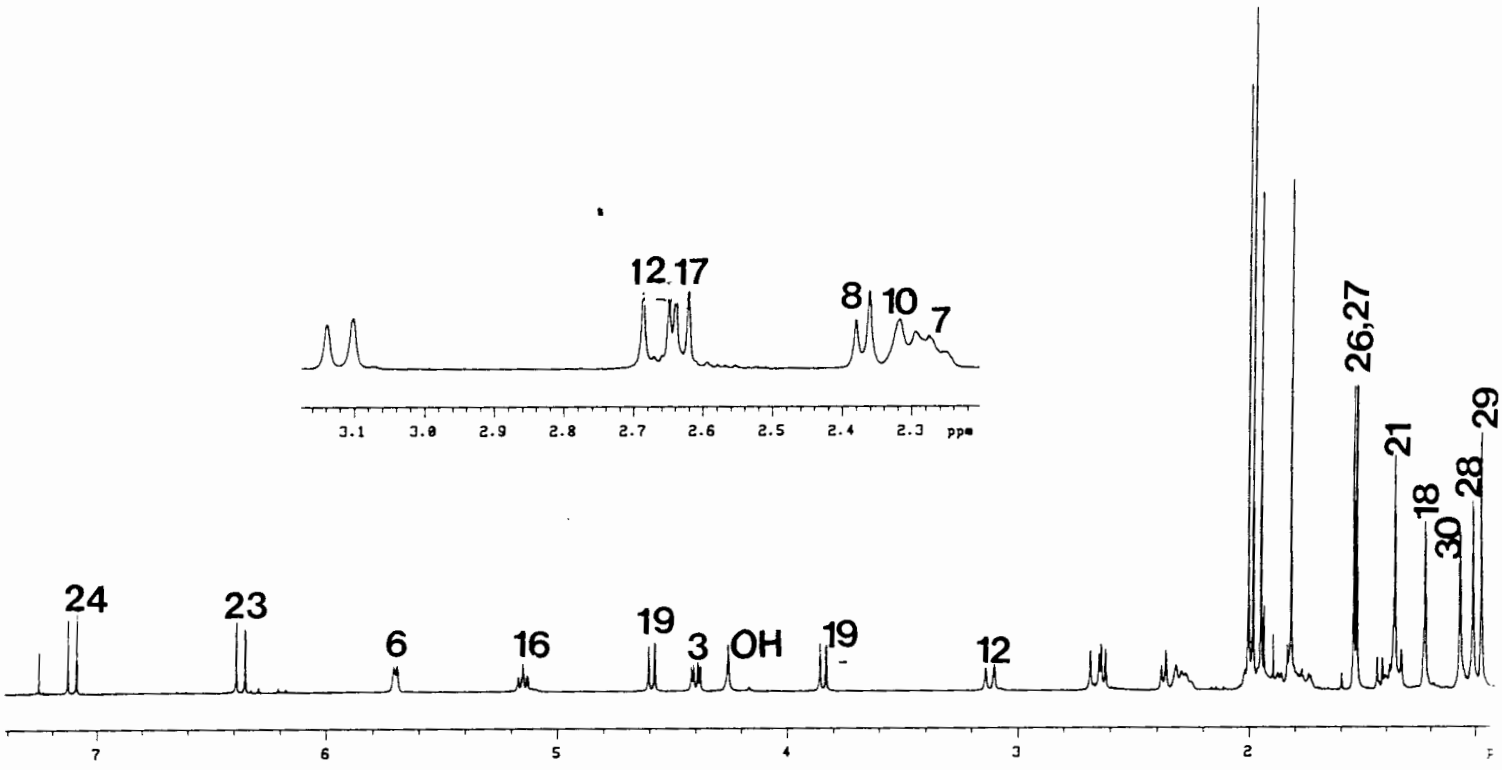

C:9 ^{1}H SPECTRUM OF CUCURBITACIN C 3,16,19 TRIACETATE

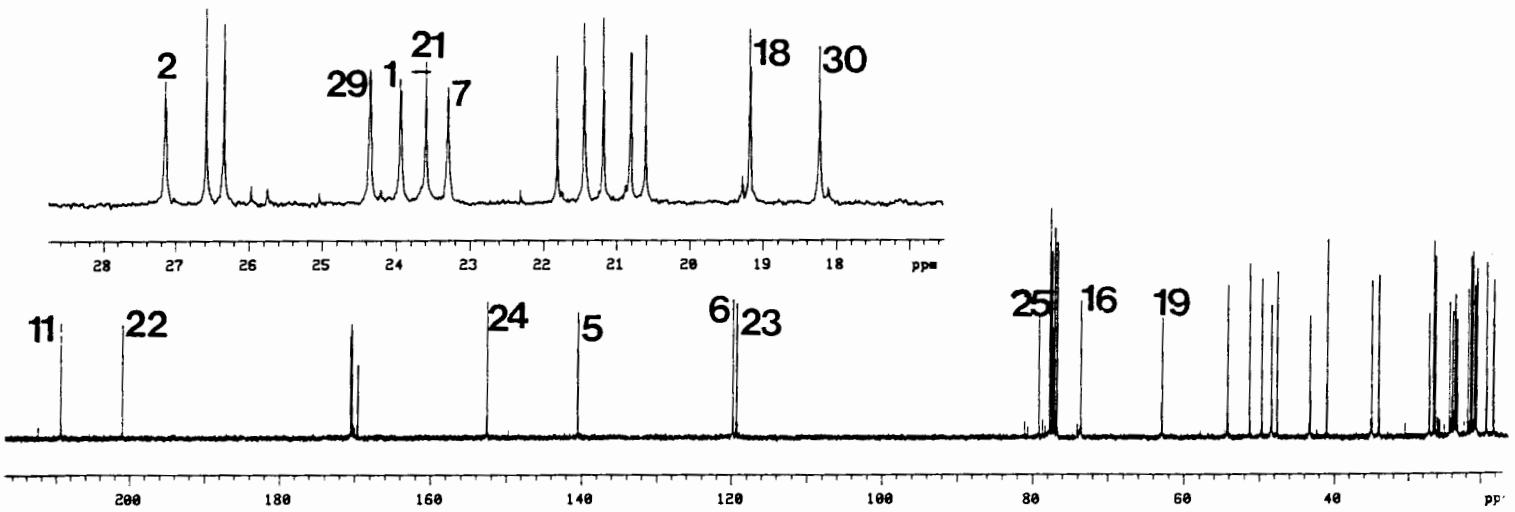

C:10 ^{13}C SPECTRUM OF CUCURBITACIN 3,16,19 TRIACETATE.